

Electronic Thesis and Dissertation Repository

8-17-2023 11:00 AM

Examining the Emergence of Mood and Anxiety Molecular Phenotypes Resulting from Chronic Prenatal Nicotine Exposure in Cerebral Organoids

Emma K. Proud, *Western University*

Supervisor: Laviolette, Steven R., *The University of Western Ontario*

A thesis submitted in partial fulfillment of the requirements for the Master of Science degree in Neuroscience

© Emma K. Proud 2023

Follow this and additional works at: <https://ir.lib.uwo.ca/etd>



Part of the [Molecular and Cellular Neuroscience Commons](#)

Recommended Citation

Proud, Emma K., "Examining the Emergence of Mood and Anxiety Molecular Phenotypes Resulting from Chronic Prenatal Nicotine Exposure in Cerebral Organoids" (2023). *Electronic Thesis and Dissertation Repository*. 9572.

<https://ir.lib.uwo.ca/etd/9572>

This Dissertation/Thesis is brought to you for free and open access by Scholarship@Western. It has been accepted for inclusion in Electronic Thesis and Dissertation Repository by an authorized administrator of Scholarship@Western. For more information, please contact wlsadmin@uwo.ca.

Abstract

Prenatal nicotine exposure (PNE) from maternal smoking disrupts regulatory processes vital to fetal development. These changes result in long-term behavioural impairments, including mood and anxiety disorders, that manifest later in life. However the relationship underlying PNE, and the underpinnings of mood/anxiety molecular phenotypes remains elusive. To model nicotine exposure during prenatal development, our study used human cerebral organoids that were chronically exposed to nicotine and collected for molecular analyses. Short-term, nicotine altered molecular markers of neural identity, mood/anxiety disorders and those involved in maintaining the excitatory/inhibitory (E/I) balance in the cortex. RNA sequencing further revealed transcriptomic changes in genes pertaining to embryonic development, neurogenesis, and DNA binding. Collectively, our results demonstrated that nicotine altered E/I balance, dopamine receptor expression and changes in neural identity markers that persist into later stages of development. These findings validate an *in vitro* model of PNE to better comprehend the emergence of neuropsychiatric molecular phenotypes resulting from gestational nicotine exposure.

Keywords

Prenatal development, prenatal nicotine exposure, anxiety, depression, human cerebral organoids.

Summary for Lay Audience

In recent years, there has been a rise in nicotine vaping among women of reproductive age due to the misconception that vaping is safer than smoking traditional cigarettes. Yet, vapes contain higher doses of nicotine that pass through the placental barrier and affect the brain of the developing fetus. Previous research suggests that prenatal nicotine exposure (PNE) can negatively impact many important processes vital to fetal development and can cause long-lasting changes in brain regions associated with mood and anxiety control. Clinical studies indicate that the children of mothers who smoke nicotine during pregnancy have a much higher likelihood of developing anxiety and depression later in life. However, the mechanism underlying PNE, and the emergence of these neuropsychiatric disorders is not well understood. To overcome the limitations of other human and animal-based models, our project uses human cerebral organoids to further investigate this relationship. Cerebral organoids are tiny, lab-grown, brains created from reprogrammed human skin cells. They contain similar structures and cell types found in the prenatal human brain and are a great model to study the effect of gestational drug exposure, such as PNE, on the developing brain. Cerebral organoids were treated with one of three doses of nicotine or no nicotine, for 14 days, and collected immediately following nicotine exposure and at 6 months. The collected organoids underwent various molecular experiments to examine nicotine-induced changes in cortical development, markers linked to mood and anxiety disorders and changes in gene expression. We found that immediately following nicotine exposure, there are changes in markers of neural identity, mood/anxiety disorders (nicotinic acetylcholine and dopamine receptors) and markers associated with maintaining the excitatory/inhibitory (E/I) balance in the cortex. RNA sequencing also revealed transcriptomic changes in genes pertaining to embryonic development, neurogenesis, and DNA binding. Mature organoids show similar disruptions in E/I balance, decreased neural identity markers and altered dopamine receptor expression. Altogether, these findings validate an *in vitro* model of PNE to better comprehend the emergence of neuropsychiatric molecular phenotypes later in development resulting from chronic nicotine exposure.

Acknowledgments

First and foremost, I would like to thank my supervisor Dr. Steve Laviolette for granting me the opportunity to work under his guidance and be a part of his amazing team of neuroscientists. I have learned so much more than I could have imagined starting this journey and I am so thankful for the support and encouragement I have received.

I would like to express my gratitude to the members of my advisory committee Dr. Walter Rushlow, Dr. Dan Hardy and Dr. Sean Cregan. Your expertise and advice provided in these meetings were integral to my growth as a student and the success of my thesis.

I would like to thank all the members of the addiction research group: Dr. Marieka DeVuono, Dr. Hanna Szkudlarek, Dr. Marta De Felice, Dr. Taguan Uzuneser, Dr. Enzo Perez Valenzuela, Mohammed Sarikahya, Matt Jones, and Jason Ng. I appreciate everyone's willingness to help and answer any questions I had. Thank you for being so friendly and I will miss you all so much.

I want to give special thanks to Dr. Mar Rodriguez and Dana Gummerson. We were the best team of three and I loved working with you both every day. Mar, you are the organoid queen, and I would not be where I am today without you. You were an incredible teacher, so patient and encouraging. Because of you, I am a better scientist, and I am so appreciative of everything you taught me. Dana, I am so happy to have met you and I enjoyed all the time we spent together both inside and outside of the lab, we did everything together and I wouldn't have had it any other way. Thank you for always being there to help me, for all the laughs and jokes to get us through the day and weekly treat runs after a long week in the lab. I couldn't have done this without you.

I would like to thank my partner, Nick; I cannot tell you how much I appreciate your endless support throughout these past two years. Even though you were just as busy with your Master's, thank you for always reassuring me, for the home-cooked meals and always being there for me in any way you could. You are the best.

Finally, I would like to thank **all my amazing friends and family** for cheering me on throughout my academic journey. Mom and Dad, thank you for everything you have done for me, I am so incredibly thankful. Thank you for being my biggest fans, and always believing in me. I would not be here without you (or the kitties!).

Table of Contents

Abstract.....	ii
Summary for Lay Audience.....	iii
Acknowledgments.....	iv
Table of Contents.....	vi
List of Tables.....	x
List of Figures.....	xi
List of Appendices.....	xiii
List of Abbreviations.....	xiv
1 Introduction.....	1
1.1 Influence of Nicotine on Prenatal Health Outcomes and Development.....	2
1.2 Cortical Biomarkers of Mood and Anxiety Disorders.....	4
1.2.1 α_7 and $\alpha_4\beta_2$ nAChRs.....	4
1.2.2 Dopamine 1 and Dopamine 2 Receptors.....	6
1.2.3 E/I balance.....	7
1.2.4 ERK1-2 and GSK3 β Signaling.....	8
1.3 Transcriptomic Signatures of Mood and Anxiety Disorders.....	9
1.4 Clinical and Epidemiological Studies: Association Between PNE and Mood/Anxiety Disorders.....	10
1.5 Preclinical Models of Developmental Nicotine Exposure and Emergence of Mood and Anxiety Disorders.....	11
1.6 Introduction to Cerebral Organoids.....	12
1.7 Research Goal, Aims and Hypothesis.....	16
2 Methods.....	18
2.1 Maintenance of iPSCs.....	18

2.1.1	iPSC Thawing	18
2.1.2	iPCS Medium Changes and Passaging	19
2.2	Organoid Generation.....	20
2.2.1	EB Formation (Day 0-5).....	20
2.2.2	Induction (Day 5-7).....	20
2.2.3	Expansion (Day 7-10).....	21
2.2.4	Maturation (Day 10+).....	21
2.3	Antibiotic Treatment.....	22
2.4	Nicotine Preparation and Organoid Treatment.....	23
2.5	Sample Preparation for Immunofluorescence and Hematoxylin and Eosin Staining	24
2.5.1	Fixation	24
2.5.2	Cryopreservation.....	24
2.5.3	Embedding	25
2.5.4	Cryosectioning	25
2.6	Immunofluorescence.....	25
2.6.1	Blocking.....	25
2.6.2	Primary Antibodies	26
2.6.3	Secondary Antibodies	26
2.6.4	Coverslips	27
2.6.5	Confocal Microscopy.....	27
2.6.6	Image Analysis.....	28
2.7	Hematoxylin and Eosin Staining	28
2.8	Western Blot	29
2.8.1	Snap Freezing.....	29
2.8.2	Protein Extraction	29

2.8.3	Protein Quantification.....	29
2.8.4	Gel Electrophoresis, Blocking and Antibodies.....	30
2.8.5	Blot Analysis.....	31
2.9	qPCR.....	31
2.9.1	RNA Extraction	31
2.9.2	Complementary DNA (cDNA) Synthesis.....	32
2.9.3	qPCR.....	32
2.10	RNA Sequencing.....	35
2.11	Statistical Analyses	36
3	Results.....	37
3.1	Short-term Effects of PNE - D42 Results.....	37
3.1.1	PNE Model Characterization	37
3.1.2	Effect of Nicotine on Characterization Markers.....	39
3.1.3	Mood/Anxiety Molecular Biomarker Results.....	42
3.1.4	Transcriptomic Results	50
3.2	Long-term Effects of PNE- D180 Results	60
3.2.1	Mood/Anxiety Molecular Biomarker Results.....	60
3.2.2	Transcriptomic Results	62
4	Discussion	66
4.1	PNE Dysregulates Aspects of Neurogenesis and Alters the Expression of Neural Identity Markers in the Cortex	67
4.2	PNE Has Short-term Effects on α_4 and β_2 nAChR Subunit Expression, but not α_7	68
4.3	PNE Dysregulates Dopaminergic Signaling and Unremittingly Perturbs D1R Expression.....	70
4.4	PNE Has Short-term Effects on the Total Expression of Specific Kinases Implicated in Mood and Anxiety Disorders.....	70

4.5 PNE Persistently Disrupts GABA and Glutamate Markers Associated with Cortical E/I Balance	72
4.6 Nicotine Organoids Endure Significant Transcriptomic Changes in Genes Pertaining to Nervous System Development, Neurogenesis and Transcription Regulation	73
4.7 Limitations	74
4.8 Future Directions	76
4.9 Conclusions.....	77
References.....	78
Appendices.....	97
Curriculum Vitae	101

List of Tables

Table 1: Demographic Information of iPSC Lines from RUCDR Infinite Biologics	18
Table 2: Cell Confluency and Corresponding Split Ratios for iPSC Passaging.....	19
Table 3: Preparation of STEMdiff Cerebral Organoid Media	22
Table 4: Primary Antibodies Used in Immunofluorescence.....	26
Table 5: Secondary Antibodies Used in Immunofluorescence.....	27
Table 6: Primary Antibodies Used in Western Blots.....	31
Table 7: Secondary Antibodies Used in Western Blots.....	31
Table 8: qPCR Primer Sequences	34
Table 9: Nicotine Had No Effect on Expression of Select Characterization Markers.....	40
Table 10: Top 20 DE Genes in VEH and Nicotine Organoids	54
Table 11: Common Top 20 Ranked Genes Related to Nicotine, Anxiety and Depression Phenotypes	59

List of Figures

Figure 1: Overview of PNE's influence on behavioural outcomes	4
Figure 2: Presynaptic α_7 nAChRs mediate neurotransmitter release and maintenance of E/I balance in the cortex	6
Figure 3: Cerebral organoids replicate human cortical development	14
Figure 4: Process of the generation of iPSC-derived cerebral organoids to model PNE.	16
Figure 5: Description of cerebral organoid culture system and representative microscopic images.	22
Figure 6: Details of nicotine treatment and organoid collection.....	24
Figure 7: iPSC-derived cerebral organoids display cortical differentiation	38
Figure 8: iPSC-derived cerebral organoids express markers specific to early brain regionalization and vital to development.....	39
Figure 9: PNE significantly increases cell death and number of early-born neurons on D42.....	41
Figure 10: PNE selectively upregulates certain nAChR populations at D42	43
Figure 11: PNE induces significant alterations in dopaminergic receptors implicated in mood and anxiety disorders at D42	45
Figure 12: PNE induces significant deficits in markers vital to GABAergic synthesis, transport and signaling on D42	47
Figure 13: PNE trends towards the dysregulation of kinases implicated in mood/anxiety disorder pathology on D42.....	49
Figure 14: PNE elicits short-term changes in various neural identity markers on D42 ...	51

Figure 15: RNA-Seq differential expression in VEH and organoids exposed to 0.1 μ M nicotine.....	53
Figure 16: Functional enrichment analysis of VEH and nicotine-treated organoids.....	55
Figure 17: GO terms of overrepresented genes in VEH and nicotine organoids.....	58
Figure 18: PNE induces long-term alterations in neuronal differentiation, dopaminergic and glutamatergic markers.....	61
Figure 19: PNE elicits persistent, long-term changes in multiple neural identity markers.....	63
Figure 20: PNE elicits long-term changes in glutamatergic, GABAergic and dopaminergic markers implicated in mood and anxiety disorders	65

List of Appendices

Appendix 1: Supplemental Non-Significant D42 Western Blot Results.....	97
Appendix 2: Supplemental Non-Significant D180 Western Blot Results	98
Appendix 3: Supplemental Non-Significant D42 IF Results.....	99
Appendix 4: Supplemental Non-Significant D180 qPCR Results.....	100

List of Abbreviations

AC	Adenylate cyclase
ADHD	Attention-deficit hyperactivity disorder
Akt/PKB	Protein kinase B
ANOVA	Analysis of variance
BP	Biological process
BSA	Bovine serum albumin
CC	Cellular component
CDH13	Cadherin-13
CNS	Central Nervous system
CP	Cortical plate
CTIP2	COUP-TF-interacting protein 2
Cq	Cycle quantification
DAPI	4',6-diamidino-2-phenylindole
DE	Differentially expressed
dPBS	Dulbecco's phosphate buffered saline
D1R	Dopamine 1 receptor
D2R	Dopamine 2 receptor
EB	Embryoid body

E/I	Excitatory/inhibitory
EMX1	Empty spiracles homeobox 1
ENDS	Electronic nicotine delivery systems
EOMES/TBR2	Eomesodermin/T-box brain protein 2
FDR	False discovery rate
FGFR1	Fibroblast growth factor receptor 1
FOXG1	Forkhead-box G1
FZD9	Frizzled-9
GABA	γ -aminobutyric acid
GAD	Generalized anxiety disorder
GAD1	Glutamate decarboxylase 1
GAD67	Glutamic Acid Decarboxylase 67
GAT-1	GABA transporter type 1
GO	Gene ontology
GPCR	G-protein coupled receptor
GRM2	Metabotropic glutamate receptor 2
GRM3	Metabotropic glutamate receptor 2
GSK3 β	Glycogen synthase kinase 3 beta
H&E	Hematoxylin and eosin

HDAC	Histone deacetylase
HPA	Human protein atlas
IF	Immunofluorescence
IGF2	Insulin-like growth factor 2
iPSCs	Induced pluripotent stem cells
ISL1	ISL LIM homeobox 1
MAP2	Microtubule-associated protein 2
MAPK/ERK	Mitogen-activated protein kinase/extracellular signal-related kinase
MDD	Major depressive disorder
MDS	Multidimensional scale
MF	Molecular function
mGLUR2/3	Metabotropic glutamate receptor 2/3
mRNA	Messenger ribonucleic acid
nAchR	Nicotinic acetylcholine receptor
NGFR	Nerve growth factor receptor
NMDA	N-methyl-D-aspartate
NR2A	NMDA receptor subunit 2A
NR2B	NMDA receptor subunit 2B
PBS	Phosphate buffered saline

PBS-T	Phosphate buffered saline with Tween 20
pERK1-2	Phosphorylated ERK1-2
PFA	Paraformaldehyde
PFC	Prefrontal cortex
pGSK3 β	Phosphorylated GSK3 β
PKA	Protein kinase A
PNE	Prenatal nicotine exposure
PROX1	Prospero homeobox 1 protein
PV	Parvalbumin
qPCR	Real-time quantitative polymerase chain reaction
RIPA	Radioimmunoprecipitation assay
RNA-Seq	Ribonucleic acid sequencing/RNA sequencing
ROI	Region of interest
ROK	Rho-kinase
SEM	Standard error of mean
SLC6A3	Solute carrier family 6 member 3 / dopamine transporter
SPP1	Secreted phosphoprotein 1
SVZ	Subventricular zone
T-GSK3 β	Total GSK3 β

T-ERK1-2	Total ERK1-2
TF	Transfac
TBS	Tris buffered saline
TBS-T	Tris buffered saline with Tween 20
TBR1	T-box brain transcription factor 1
TWAS	Transcriptome-wide association study
VEH	Vehicle
VL	Ventricular-like
VZ	Ventricular zone
WP	WikiPathways
Wnt	Wingless/integrated

1 Introduction

Rates of cigarette smoking have declined in recent years. However, electronic nicotine delivery systems (ENDS) such as vapes and e-cigarettes, have gained considerable popularity among adolescents, young adults and as a result, women of reproductive age (Brooks & Henderson, 2021; Obisesan et al., 2020). Not only has nicotine, the primary psychoactive component in these devices, been demonstrated to harm the consuming individual, but when used during pregnancy, it disrupts several regulatory processes vital to fetal development (Dwyer et al., 2009). As a result, prenatal nicotine exposure (PNE) has been linked to numerous physical and emotional conditions that persist later into the life of the offspring (Blood-Siegfried & Rende, 2010; Dwyer et al., 2009). Specifically, nicotine modulates the release and signaling of several neurotransmitter systems within the central nervous system (CNS), such as glutamate, γ -aminobutyric acid (GABA) and dopamine (Mahar et al., 2012; Moylan et al., 2013; Sailer et al., 2019). This can lead to the future development of neuropsychiatric ailments, such as mood and anxiety disorders (Corrêa et al., 2022; Hudson et al., 2021; Jobson et al., 2019; Moylan et al., 2013, 2015). Thus, understanding how nicotine alters the immature CNS during gestation and the long-term consequences of these alterations is of great importance.

Despite the teratogenic nature of nicotine, smoking cessation is difficult to achieve for many pregnant women in part due to the addictive properties of nicotine (Wickström, 2007). Amid the current vaping epidemic, this is often accompanied by a wealth of misinformation regarding the safety of using ENDS during pregnancy (Obisesan et al., 2020; Regan & Pereira, 2021). These factors in tandem are detrimental to the developing fetal brain, which is extremely vulnerable to environmental toxins such as drug exposure. This gives rise to long-lasting structural and functional changes in regions implicated in mood and anxiety control such as the prefrontal cortex (PFC; Dwyer et al., 2009; Jobson et al., 2019; Laviolette, 2021). Due to the paucity of access to fetal brain tissue, most of our knowledge regarding PNE, and the emergence of mood and anxiety disorders comes from clinical populations and animal models (Blood-Siegfried & Rende, 2010; Corrêa et al., 2022; Dwyer et al., 2009; Ekblad et al., 2010; Mahar et al., 2012; Minatoya et al., 2019; Moylan et al., 2013; Niemelä et al., 2016; Sailer et al., 2019; A. M. Smith et al.,

2010). Although valuable, these models have a plethora of limitations due to confounding variables and species differences in brain development, respectively. To bridge the gap between animal and two-dimensional *in vitro* models, three-dimensional (3D) cerebral organoids are proposed as an effective preclinical platform to recapitulate aspects of the developing human brain, in this case, in conjunction with PNE (Centeno et al., 2018; Kim et al., 2020; Lancaster et al., 2013). Previous organoid studies investigating the effect of PNE on prenatal brain development exist but have not taken into consideration the emergence of mood and anxiety molecular phenotypes (Notaras et al., 2021; Y. Wang et al., 2018). The current project aims to use a human-derived 3D model to further elucidate the relationship between PNE, neurodevelopmental alterations and the advent of mood and anxiety biomarkers.

1.1 Influence of Nicotine on Prenatal Health Outcomes and Development

Regardless of the known risk factors and negative outcomes of PNE, roughly 20% of Canadian women continue to smoke during pregnancy (Andres & Day, 2000; Paterson et al., 2003). Each year, in Canada alone, this equates to approximately 75,000 babies born who were prenatally exposed to firsthand smoke (Andres & Day, 2000; Paterson et al., 2003). Despite 75% of these women wanting to quit, only 20-30% are successful (Tong et al., 2009; Ruggiero et al., 2000). In recent years, as the risks of smoking have become more evident, many women have turned to other forms of nicotine consumption such as ENDS (Wickström, 2007). Since the introduction of ENDS in 2007, nicotine consumption has increased in popularity with many ENDS users without a previous smoking history (Obisesan et al., 2020; Regan & Pereira, 2021). These systems of nicotine delivery are often perceived as safe alternatives to smoking traditional cigarettes or an aid to assist with smoking cessation, but they are highly addictive (Adkison et al., 2013; Breland et al., 2019; England et al., 2016; Huey & Granitto, 2020; Mark et al., 2015; McCubbin et al., 2017; Whittington et al., 2018). As a result, pregnant women have become vulnerable to this misinformation (England et al., 2016; Orzabal & Ramadoss, 2019; Whittington et al., 2018). Although they may be motivated to stop smoking, studies estimate around 7% of women use ENDS during pregnancy; 45% of them believed it was a safer method than non-electronic methods of nicotine smoking (Obisesan et al., 2020).

Due to the high and variable concentrations of nicotine present in ENDS (0-20 mg/mL in Canada), this is an alarming consensus (Government of Canada Justice Laws, 2023).

Smoking nicotine is one of the most avoidable causes of morbidity and mortality for both the health of the mother and fetus, with ENDS containing higher concentrations of nicotine compared to traditional cigarettes and posing a substantial risk to the unborn baby (Orzabal & Ramadoss, 2019; Whittington et al., 2018). Due to nicotine's lipophilic nature, it can easily cross the placental barrier and concentrate in fetal serum and brain tissue at much higher concentrations than what is reported in maternal blood (De Long et al., 2014). As a result, there are many possible pregnancy risks including hypoxic insults, fetal growth restriction, placental abruption, preterm birth, stillbirth, and low birth weight (Cardenas et al., 2019; Ekblad et al., 2015; England et al., 2016; Mark et al., 2015; Obisesan et al., 2020; Whittington et al., 2018). Babies exposed to nicotine are also susceptible to other serious physical health outcomes such as metabolic, respiratory, or cardiac conditions (Banderali et al., 2015; Obisesan et al., 2020; Wongtrakool et al., 2012). Indeed, PNE has been shown to alter several biological processes, however, nicotine impacts more than pregnancy and physical health outcomes. Prenatal neurogenesis is a precise series of synchronized events during which the brain is tremendously vulnerable to external environmental stimuli, like nicotine exposure (Ross et al., 2015). This produces perpetual alterations in neuronal cytoarchitecture and brain circuitry of the fetus in brain regions vital for emotional regulation, such as the PFC, with adverse neurobehavioral outcomes persisting into adulthood (Figure 1; Aoyama et al., 2016; Blood-Siegfried & Rende, 2010; Dwyer et al., 2019; Laviolette, 2021; Mahar et al., 2012; Minatoya et al., 2019; Moylan et al., 2015; Sailer et al., 2019; Smith et al., 2010). For example, there are many reports of PNE resulting in various externalizing behavioural outcomes in the offspring, such as attention-deficit hyperactivity disorder (ADHD), aggression, and other conduct issues (Brook et al., 2006; Moylan et al., 2015; Thapar et al., 2003). However, less research effort is directed toward investigating the association between PNE and internalizing behaviours (anxiety and depression; Moylan et al., 2015). Both anxiety and depressive disorders contribute substantially to global health-related burdens (Santomauro et al., 2021). Unlike other factors associated with

these disorders (e.g., genetics), the development of these behaviours resulting from PNE is potentially preventable (Moylan et al., 2015).

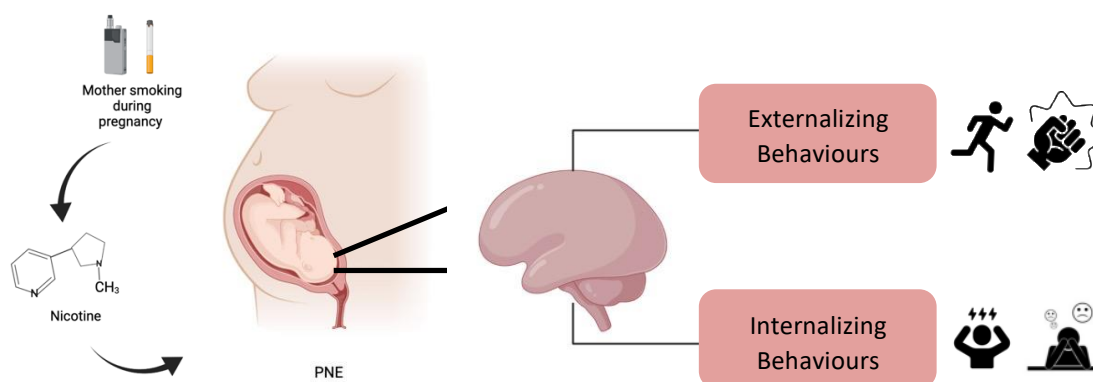


Figure 1: Overview of PNE's influence on behavioural outcomes. Nicotine crosses the placental barrier which underlies the emergence of externalizing behaviours, hyperactivity and aggression, and internalizing behaviours, anxiety, and depression. Figure made using BioRender.

1.2 Cortical Biomarkers of Mood and Anxiety Disorders

1.2.1 α_7 and $\alpha_4\beta_2$ nAChRs

Nicotine is an agonist at nicotinic acetylcholine receptors (nAChRs), which are pentameric ligand-gated ion channels permeable to sodium and calcium (Dwyer et al., 2009). They have three different receptor conformations: open, closed, and desensitized (Dwyer et al., 2009). When the channel is open, the receptor is permeable to ions and it is impermeable in the closed conformation (Dwyer et al., 2009). Desensitization occurs when ligand binding does not allow the channel to open, which occurs from prolonged exposure to agonists (Dwyer et al., 2009; Ekblad et al., 2015). These receptors can be heteromeric or homomeric in nature and are composed of a combination of α (α_2 - α_7) and/or β (β_2 - β_4) subunits, which determines their ion specificity, desensitization capacity and pharmacological characteristics (Dwyer et al., 2009; Falk et al., 2005). nAChRs are widely distributed in the brain and are expressed early during the development of the CNS, appearing as early as gestational week 5 (Falk et al., 2002, 2005). They are critical in facilitating key neurodevelopment aspects such as neurogenesis, cell survival, apoptosis, and axonal and synaptic growth (Ekblad et al., 2010; A. M. Smith et al., 2010). Cholinergic signaling plays a crucial role in coordinating brain maturation and premature

or chronic overactivation of nAChRs during this critical period of neurodevelopment interferes with these cholinergic regulatory processes (Dwyer et al., 2009; Moylan et al., 2013). This produces detrimental changes in nAChR distribution, sensitivity, and neurotransmitter functions, which lays a foundation for future mood and anxiety disorders. (Dwyer et al., 2009; Laviolette, 2021; Mahar et al., 2012; Sailer et al., 2019). The most abundant nAChRs in the cortex that are implicated in mood and anxiety disorders are the α_7 and $\alpha_4\beta_2$ receptors. $\alpha_4\beta_2$ nAChRs are located both pre- and postsynaptically to control cell excitability, neurotransmitter release and depolarization (Dwyer et al., 2009; Mcgrath-Morrow et al., 2020). These receptors have a high affinity for nicotine and tend to desensitize more slowly at lower nicotine concentrations than other nAChR subtypes (Dwyer et al., 2019; Fenster et al., 1999). Blockage or partial agonism of $\alpha_4\beta_2$ nAChRs in mouse models has been shown to provoke antidepressant-like responses and is a clinically relevant biological target for antidepressant development (Mineur et al., 2011; Philip et al., 2010). On the other hand, α_7 nAChRs bind to nicotine with a lower affinity but desensitize at a much higher rate (Dwyer et al., 2009; Mcgrath-Morrow et al., 2020). These receptors also play a major modulatory role in the induction of neurotransmitter release independent of depolarization (Dwyer et al., 2009; Livingstone et al., 2010). Specifically, α_7 nAChRs located presynaptically on glutamatergic neurons indirectly mediate the release of dopamine from neighbouring neurons, which alters dopamine signaling and excitatory/inhibitory (E/I) balance in the cortex (Figure 2; Livingstone et al., 2010). Thus, if nAChRs become dysregulated or experience changes in sensitivity resulting from PNE, variations in their expression may be indicative of changes in downstream cortical circuitry implicated in mood and anxiety-related pathophysiology.

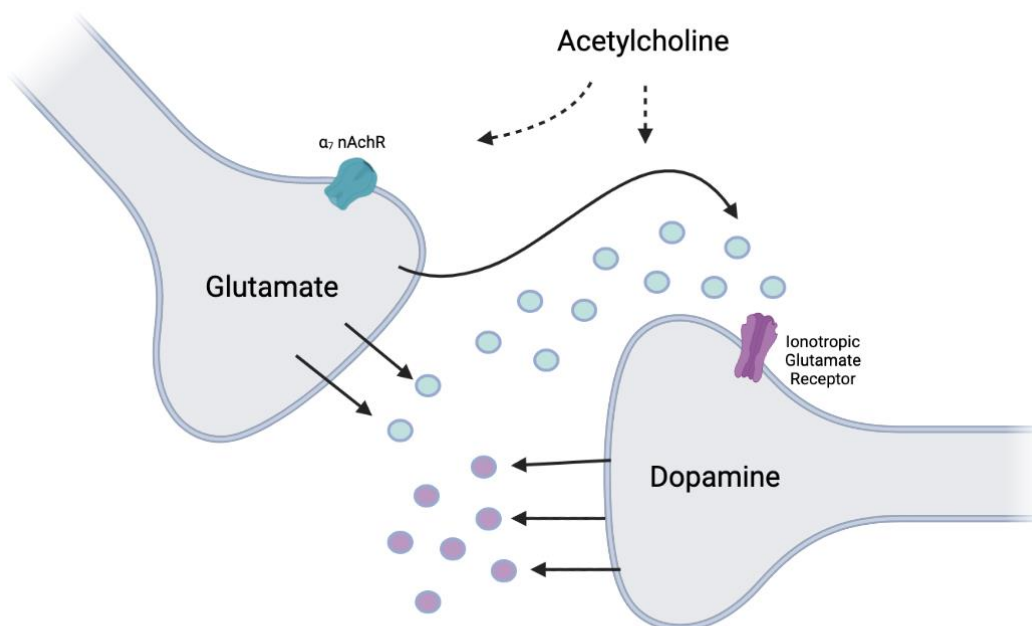


Figure 2: Presynaptic α_7 nAChRs mediate neurotransmitter release and maintenance of E/I balance in the cortex. Figure created using BioRender and adapted from (Livingstone et al., 2010).

1.2.2 *Dopamine 1 and Dopamine 2 Receptors*

Dopamine receptors are G-protein coupled receptors (GPCR) that have a wide range of neural functions including cognition, motivation, and emotional responses (Delva & Stanwood, 2021). Two receptors of interest are dopamine 1 (D1R) and dopamine 2 (D2R), which are abundantly expressed in the cortex (Delva & Stanwood, 2021). D1R can either have excitatory or inhibitory functions (Delva & Stanwood, 2021). These receptors usually activate adenylyate cyclase (AC), via $G_{\alpha s}$, to increase the concentration of cyclic adenosine monophosphate (cAMP) and activate protein kinase A (PKA). This leads to downstream phosphorylation of PKA substrates (Delva & Stanwood, 2021; Sidhu, 1998). In comparison, D2R is mainly inhibitory and inhibits the actions of AC via $G_{\alpha i}$ (Baik, 2013; Delva & Stanwood, 2021). D2R activation also has downstream effects on the protein kinase B (PKB/Akt) – glycogen synthase kinase-3 (GSK3) pathway to initiate cellular processes such as transcription, differentiation, and proliferation (Delva & Stanwood, 2021; Liu et al., 2009). Both D1R and D2R also steadily regulate the activity

of mitogen-activated protein kinase/extracellular signal-related kinase (MAPK/ERK) signaling (Chang & Karin, 2001; Delva & Stanwood, 2021). As mentioned previously, nicotine serves as a major neurotransmitter that can potentially alter dopaminergic signaling, which is crucial for proper brain development (De Long et al., 2014; Dwyer et al., 2009). However, manipulation of prefrontal dopaminergic signaling is also a hallmark of mood and anxiety disorders. Human imaging has demonstrated D1R binding is significantly decreased in the frontal cortex in individuals with mood disorders (Suhara et al., 1992). Preclinical work has reported that genetic knockdown and viral manipulation of D1R are also associated with depressive and anxiety-like phenotypes, respectively (Beyer et al., 2021; Holmes et al., 2004). Additionally, D2R antagonists have been shown to mitigate depressive behaviours by eliciting antidepressant effects, which further implicates the dopaminergic system in the pathophysiology of mood and anxiety disorders (Delva & Stanwood, 2021; Fedotova, 2012). In summary, assessing the levels of D1R and D2R will be beneficial to study the effects of nAChR-mediated dopamine release, how dopamine signaling changes in response to PNE, and how this may impact signaling cascades implicated in depression and anxiety.

1.2.3 *E/I Balance*

In addition to dopamine, an increasing number of studies have described altered E/I balance in the cortex due to glutamatergic neurons receiving less synaptic inhibition from GABAergic signaling (Fogaça & Duman, 2019). Key players involved in GABAergic neurotransmission are glutamic acid decarboxylase (GAD67) which is involved in GABA synthesis, GABA transporter type-1 (GAT-1) and parvalbumin (PV) interneurons. With regards to GABA in major depressive disorder (MDD), neuroimaging studies have reported depletions in cortical GABA concentrations as well as significant decreases in GAD67 compared to nonpsychiatric controls (Hasler et al., 2007; Karolewicz et al., 2010; Sanacora, Gueorguieva, et al., 2004; Sanacora, Mason, et al., 1999). There are also reports of GABAergic interneuron reduction in the dorsolateral PFC, which supports the idea of GABA dysfunction in MDD (Karolewicz et al., 2010; Rajkowska et al., 2007). Specifically, PV interneurons comprise 40% of GABAergic interneurons in the cortex and have been extensively studied in stress-related disorders (Fogaça & Duman, 2019).

Postmortem brain studies of individuals with MDD have confirmed decreased levels of PV in regions associated with mood and anxiety control such as the PFC and hippocampus (Knable et al., 2004; Perlman et al., 2021; Rajkowska et al., 2007). Correspondingly, GAT-1, which removes GABA from the synaptic cleft, is reduced in the medial PFC from chronic stress exposure but can be rescued upon administration of the fast-acting antidepressant ketamine (Duman et al., 2019).

Moreover, levels of excitatory glutamate neurotransmission are reportedly lower in the cortex of patients with MDD (Hasler et al., 2007; Khodoruth et al., 2022; Yildiz-Yesiloglu & Ankerst, 2006). However, glutamatergic receptors that regulate mood and affiliated functions, specifically N-methyl-D-aspartate (NMDA) and metabotropic (mGLUR) receptors, are also dysregulated in MDD and anxiety pathology (Khodoruth et al., 2022; Millan, 2006). For example, a study conducted by Feyissa et al. (2010) reported a 54% and 48% downregulation of NMDA receptor subunit 2A (NR2A) and 2B (NR2B), respectively, in the PFC of individuals living with MDD (Hashimoto, 2009). Oppositely, depressed individuals have increased cortical levels of metabotropic glutamate receptor 2/3 (mGLUR2/3; Feyissa et al., 2010; Hashimoto, 2009). Altogether, changes in these GABAergic and glutamatergic biomarkers will allow us to assess the degree of E/I imbalance in the cortex following PNE and their association with the emergence of anxiety and depressive-like molecular phenotypes.

1.2.4 *ERK1-2 and GSK3 β Signaling*

Increasing evidence also suggests that dysfunction of specific kinases sensitive to nicotine, such as ERK1-2 and GSK3 β , are involved in the pathogenesis of mood/anxiety disorders. ERK1 and ERK2 (known as ERK1-2) are activated by various upstream signaling mechanisms such as ion channels, GPCRs such as D1R and D2R, and tyrosine kinase receptors (Wortzel & Seger, 2011). ERK1/2 is activated by phosphorylation of specific threonine and tyrosine sites and subsequently translocates to the nucleus and facilitates gene transcription by activating various transcription factors (Wortzel & Seger, 2011). This signal transduction pathway has many dynamic functions in the cell, including survival, apoptosis, proliferation, and differentiation (Wortzel & Seger, 2011). Several preclinical studies have revealed increased levels of ERK1-2 activation in the

PFC and nucleus accumbens concurrent with anxiety and depressive-like phenotypes (Hudson et al., 2021; Jobson et al., 2019; Laviolette, 2021). In human postmortem analyses, examination of PFC and hippocampal tissue in depressed suicide subjects has noted decreased ERK1-2 gene expression (Dwivedi et al., 2001). Additionally, abolishment of phosphorylated ERK (pERK) is linked to reductions in anxiety whereas increased pERK has been detected in the PFC after extended stress exposure (Jobson et al., 2019; Todorovic et al., 2009; H. T. Wang et al., 2010).

Similarly, clinical and preclinical research implicates another kinase, GSK3 β , as a pathological biomarker in mood disorders (Laviolette, 2021). GSK3 β has an extensive network of substrates and is involved in a plethora of developmental functions implicated in embryonic and CNS development including neuronal differentiation, migration, and survival (J. Luo, 2012). GSK3 β is active in its basal state but becomes inhibited by phosphorylation (pGSK3 β) of specific serine residues by kinases such as ERKs, Akt and PKA (J. Luo, 2012). GSK3 β is known for its involvement in bipolar disorder but is implicated in other mood disorders like MDD (Oh et al., 2010). Preclinical research has suggested GSK3 β inhibition as a mechanism for antidepressant therapy, which is supported by decreased immobility in the forced swim test (Gould et al., 2004; Kaidanovich-Beilin et al., 2004; Oh et al., 2010). Similarly, postmortem investigations of patients with MDD have revealed elevations in GSK3 β activity and messenger ribonucleic acid (mRNA) expression in the hippocampus and ventral PFC, respectively (Karege et al., 2007; Oh et al., 2010). In summary, investigating the effects of these kinases may explain aberrations in cellular processes and neurodevelopment that contribute to the onset of mood and anxiety disorders.

1.3 Transcriptomic Signatures of Mood and Anxiety Disorders

Transcriptomic studies have majorly contributed to identifying specific genes and genetic pathways associated with anxiety and depression. Studies analyzing RNA from postmortem brain tissue of individuals with MDD have described various perturbed pathways in these disorders (Mehta et al., 2010). A study by Sequeira and colleagues (2009) observed several alterations pertaining to synaptic neurotransmission and intracellular signaling in the PFC and hippocampus of depressed suicide patients

(Sequeira et al., 2009). Specifically, they validated numerous differentially expressed (DE) genes involved in GABAergic and glutamatergic neurotransmission (Sequeira et al., 2009). Indeed, this is a common finding in transcriptome-wide association studies (TWAS) since several others have also reported alterations in GABA and glutamate signaling in MDD (Choudary et al., 2005; Klempan et al., 2009; Mehta et al., 2010; Sequeira et al., 2007). Another pathway altered in MDD transcriptomics is the ERK/MAPK pathway. In a study aiming to identify genetic markers of MDD, the comparison of rat and human postmortem PFC tissue demonstrated that 80% of convergent biomarkers were associated with alterations in the ERK signaling pathway, thus providing further support for its involvement in MDD etiology (Laviolette, 2021; Malki et al., 2015). There is also evidence of upregulation of genes encoding for proteins that facilitate transcription and translation in mood disorders, which is useful for understanding the genetic basis of molecular biomarkers and the pathophysiology of such disorders (Iwamoto et al., 2004; Mehta et al., 2010).

1.4 Clinical and Epidemiological Studies: Association Between PNE and Mood/Anxiety Disorders

The connection between maternal smoking during pregnancy and psychiatric morbidity later in life has been a topic of interest in various longitudinal cohort studies (Corrêa et al., 2022; Duko et al., 2022; Ekblad et al., 2010; Moylan et al., 2013, 2015; Tiesler & Heinrich, 2014). For example, the link between PNE and childhood internalizing behaviours was analyzed using information from the Norwegian Mother-Child Cohort Study, a prospective cohort study that recruited women who gave birth in Norway between 1999 and 2009 (Magnus et al., 2016; Moylan et al., 2015). Mothers who smoked during pregnancy reported the status of their child's internalizing behaviours at different time points following birth until 5 years of age (Moylan et al., 2015). The association between PNE and internalizing behaviours in childhood was supported, and there was a dose-dependent relationship between the number of cigarettes smoked and the increased occurrence of internalizing behaviours (Moylan et al., 2015). It was also revealed that the most detrimental developmental period to experience PNE was the first trimester of pregnancy (Moylan et al., 2015). In addition to the emergence in childhood, other reports

have shown the presentation of these phenotypes in adolescence and early adulthood as well (Corrêa et al., 2022; Ekblad et al., 2010). Interestingly, children exposed to PNE had a higher incidence of developing emotional and behavioural disorders in childhood and adolescence. They were also more likely to develop mood disorders in adulthood (Ekblad et al., 2010). Furthermore, by age 22, children who experienced PNE had a 75% increased chance of developing depression and a 45% higher chance of generalized anxiety disorder (GAD; Corrêa et al., 2022). In clinical populations, females have a higher prevalence of mood and anxiety disorders compared to males (Albert, 2015; McLean et al., 2011). Due to these previously observed sex-specific outcomes, we acknowledge there could be intrinsic sex differences that would be worthwhile to investigate in the future, but due to technical limitations, this was outside the scope of the current project. Despite the knowledge gained from clinical studies, several limitations exist. Cohort studies have been shown to have inconsistent findings that may be a result of confounding variables such as unreliable reports of smoking, socioeconomic status, maternal diet, maternal age, or other drug use (Moylan et al., 2015). Clinical studies also have an increased concentration on behavioural outcomes like ADHD, aggression, and schizophrenia in comparison to anxiety and depressive behaviours (Moylan et al., 2015). As a result, most of what is known regarding the outcomes of PNE is from preclinical studies.

1.5 Preclinical Models of Developmental Nicotine Exposure and Emergence of Mood and Anxiety Disorders

Rodent models have provided considerable value in identifying biomarkers associated with emotional disturbances in humans following developmental nicotine exposure (Dwyer et al., 2009; Hudson et al., 2021; Jobson et al., 2019; Laviolette, 2021; Polli et al., 2020; Slawecki et al., 2003; L. N. Smith et al., 2006; Vaglenova et al., 2004). Rodents that have been developmentally exposed to nicotine present a higher prevalence of anxiety and depressive behaviours compared to their control counterparts (Polli et al., 2020; Vaglenova et al., 2004). For instance, mice exposed to nicotine prenatally via maternal drinking water displayed elevated measures of anxious and compulsive behaviours in adolescence, concurrent with reductions in glutamatergic genes in the PFC

(Polli et al., 2020). This suggests a potential vulnerability of the glutamatergic system to PNE and how this may contribute to the observed behavioural phenotypes (Polli et al., 2020). Similarly, rats exposed to PNE via maternal infusion revealed higher levels of anxiety and reduced novelty-seeking behaviours, which is indicative of depression (Vaglenova et al., 2004). Along with the manifestation of abnormal behavioural outcomes, other studies of developmental nicotine exposure have identified specific biomarkers and cellular pathways implicated in mood and anxiety disorders. Jobson et al. (2019) injected rats chronically with nicotine and identified dysregulation of pyramidal neurons, altered expression of D1R, and ERK1-2 signaling in the PFC. This was accompanied by social withdrawal, cognitive deficits, anxiety, and depressive-like phenotypes (Jobson et al., 2019). Also, changes in D1R, ERK1-2 and Akt-GSK3 signaling have been reported with chronic nicotine exposure in adolescence, which further implicates the significance of these markers in the etiology of neuropsychiatric phenotypes (Hudson et al., 2021). Indeed, preclinical studies have contributed a wealth of knowledge in this field of research, but there are discrepancies due to differences in the dose, route, and timing of nicotine administrations between protocols (Vaglenova et al., 2004). Moreover, there are differences in spatiotemporal organization, developmental programming and cytoarchitecture of the brain, which makes it difficult to extrapolate findings to humans (Y. Wang et al., 2018).

1.6 Introduction to Cerebral Organoids

Due to the intricacy of the human brain, there is a need for human-based *in vitro* models to study developmental processes. However, in addition to the limitations of clinical and preclinical work, there are many technical and ethical difficulties surrounding access to fetal brain tissue to study the complex nature of prenatal development and potential environmental insults (Notaras et al., 2021; Setia & Muotri, 2019). The solution is to use a 3D, human-based model known as cerebral organoids. Cerebral organoids are a proposed model system to recapitulate aspects of brain development and human disease (Centeno et al., 2018; Kim et al., 2020). Derived from induced-pluripotent stem cells (iPSCs), or embryonic stem cells, cerebral organoids are a self-renewing and organizing system, resembling many molecular and cellular constituents within developing human

brains (Sun et al., 2021; Trujillo & Muotri, 2018). These *in vitro* systems can produce a rich diversity of cell types, form functional neural networks, and generate electrical activity (Agboola et al., 2021; Arlotta & Paşca, 2019; Chiaradia & Lancaster, 2020). The first successful venture in generating cerebral organoids was performed by Lancaster et al. (2013) to model microencephaly. Their protocol begins by forming embryoid bodies (EB) and culturing them in an induction medium to induce neuronal differentiation (Lancaster et al., 2013). This forms structures resembling ventricles and the three layers of the developing cerebral cortex: the ventricular zone (VZ), subventricular zone (SVZ), and the cortical plate (CP; Figure 3; Lancaster et al., 2013). Following neural induction, radial glia cells form ventricular-like (VL) structures, known as neural rosettes, where progenitors proliferate at the apical surface and create a scaffold (Andrews & Nowakowski, 2019). Radial glia can give rise to intermediate progenitor cells, which amplify the progenitor pool via symmetric cell divisions, and early-born neurons that migrate away from the VZ to form the CP (Andrews & Nowakowski, 2019). From here, neurons begin to populate and expand the CP in an inside-out manner, occupying the deep layers first and then migrating toward the upper layers (Andrews & Nowakowski, 2019). In addition to modelling the cytoarchitecture of the human brain, these model systems can also exemplify proteomic, epigenetic, and transcriptomic programs of the developing fetal neocortex, therefore unearthing promising applications to study neurodevelopment early in gestation (Camp et al., 2015; Notaras et al., 2021).

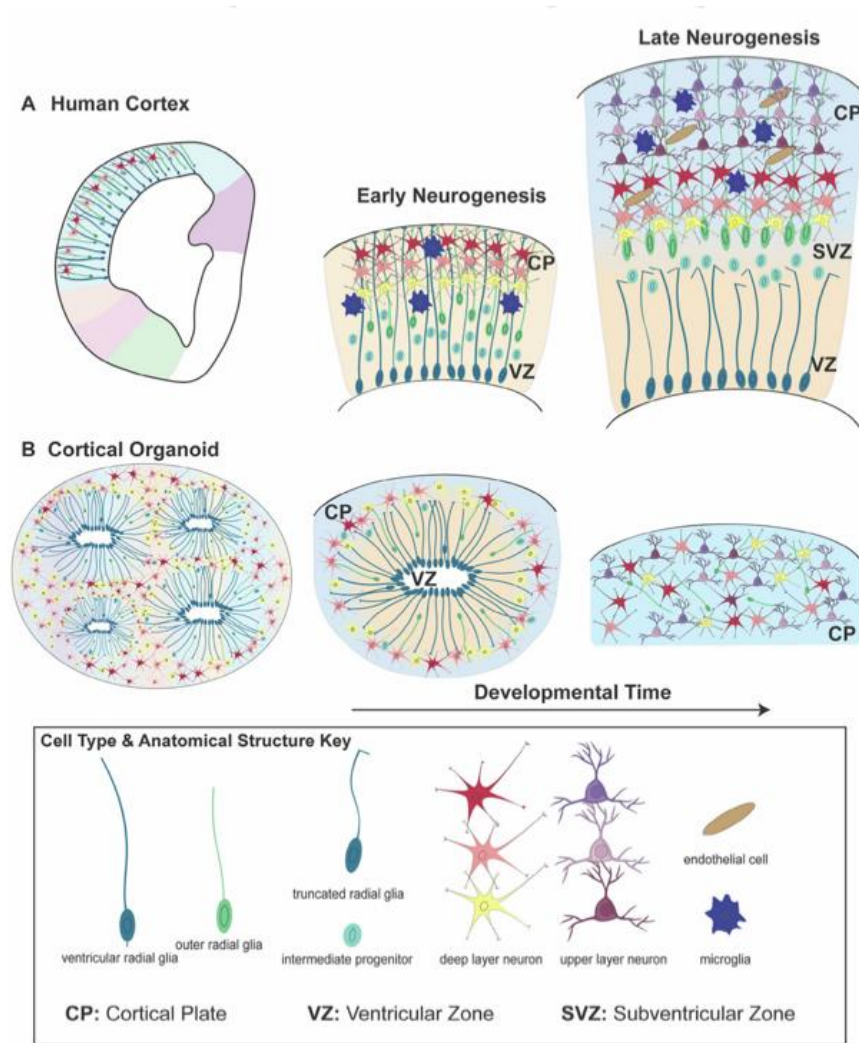


Figure 3: Cerebral organoids replicate human cortical development. Cerebral organoids contain many diverse cell types and maintain the anatomical structure as seen in human cortical development. Figure from (Andrews & Nowakowski, 2019).

An application of this experimental model is to study the effect of drug exposure on prenatal development (Figure 4). Previous organoid studies exist that have modelled the effects of PNE on neurodevelopmental processes (Notaras et al., 2021; Y. Wang et al., 2018). Wang and colleagues (2018) used an organoid-on-a-chip system to model PNE at the early stages of development. Organoids treated with 1 or 10 μM of nicotine, for 5- or 14-days displayed several aberrant neurodevelopmental events. There was evidence of premature neuronal differentiation, disrupted cortical development and brain

regionalization in the forebrain. Additionally, the effects of PNE contributed to abnormal neurite outgrowth, neuronal differentiation, and migration. This suggests neurogenesis was impaired in the early stages of development, a time equivalent to the first trimester of pregnancy. Another notable PNE study was conducted by Notaras et al., (2021). To examine the relationship between narcotic use and neuropsychiatric related risk-factors in human tissue, organoids were exposed to 10 μ M nicotine for 7 days and analyzed by reactomic, proteomic, and metabolic analyses. Their results reveal that nicotine-treated organoids were enriched in several pathways pertaining to neurodevelopment and corticogenesis. These include axon guidance, GTP signaling, robo signaling and protein translation. Likewise, wingless/integrated (Wnt) signaling, a critical pathway in neurodevelopmental programming, was dysregulated in nicotine-treated organoids alongside calcium signaling and mRNA binding. These findings suggest that PNE has the potential to provoke neurodevelopmental alterations which may contribute to future neuropsychiatric risk.

These studies have made remarkable contributions to the growing body of PNE organoid research and made advancements toward early brain development and the mechanisms underlying PNE. However, the relation between PNE and the emergence of mood and anxiety molecular phenotypes specifically is not well defined.

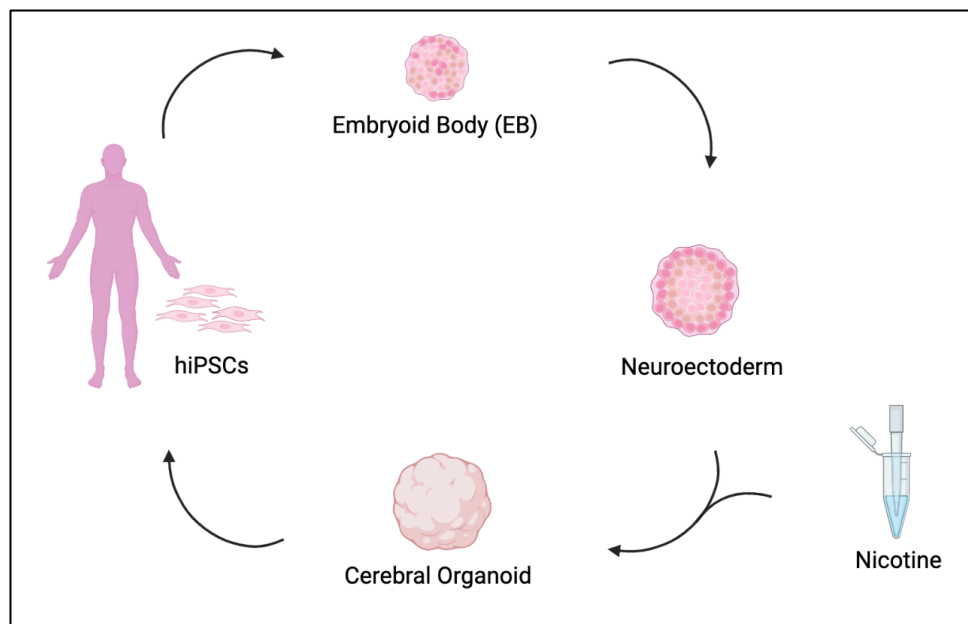


Figure 4: Process of the generation of iPSC-derived cerebral organoids to model PNE. iPSCs are derived from human fibroblasts, they form aggregates called embryoid bodies, are induced to a neural fate and develop into mature cerebral organoids. Figure made using BioRender.

1.7 Research Goal, Aims and Hypothesis

The goal of this study is to validate an *in vitro* cerebral organoid model of PNE, to characterize how nicotine exposure early in pregnancy can lead to aberrant neurodevelopmental events and the emergence of molecular biomarkers of mood and anxiety disorders. This project is comprised of three main research aims to characterize our model and explore different categories of biomolecules necessary to validate aspects of how PNE contributes to molecular phenotypes observed in mood and anxiety disorders' pathologies. These aims include:

1. The histological and molecular characterization of the PNE organoid model.
 - This aim will be accomplished by hematoxylin and eosin (H&E) staining and immunofluorescence (IF).
2. Examining protein expression of mood and anxiety molecular biomarkers following nicotine exposure.
 - This aim will be achieved by IF and Western blots.

3. Quantifying changes in gene expression following PNE.
 - This aim will be investigated by RNA Sequencing (RNA-Seq) and real-time quantitative polymerase chain reaction (qPCR).

We hypothesize that compared to vehicle (VEH) organoids, PNE will alter cortical development, dysregulate levels of molecular biomarkers of mood/anxiety disorders and alter gene expression levels. Examining these markers in tandem will validate our PNE model and illuminate how the molecular mechanisms underlying PNE can alter early human cortical brain development and dysregulate molecular pathways associated with mood and anxiety disorders.

2 Methods

2.1 Maintenance of iPSCs

2.1.1 *iPSC Thawing*

Six control iPSC lines were obtained from RUCDR Infinite Biologics (Table 1) and stored in a liquid nitrogen tank (Cryotech, YDS-50-125) until ready to thaw. To prepare culture ware for thawed cells, 6-well plates (StemCell, 38016) were coated with 1 mL Matrigel® (Corning, 354277) and warmed to 37°C for at least 1 hour before seeding. iPSCs were thawed at 37°C, transferred to a 15 mL conical tube (Falcon, 05-527-90) containing mTeSR™1 (StemCell, 85850) and centrifuged at 300 x g for 3 minutes. The supernatant was aspirated and the iPSCs were resuspended in mTeSR™1 containing 1:1000 Y-27632 of Rho-kinase inhibitor (ROK inhibitor; StemCell, 72302). To prepare the plates, Matrigel® was aspirated from each well, 1mL of mTeSR™1 was added, and an additional 1 mL of iPSC-containing medium was transferred. The iPSCs were incubated at 37°C in hypoxic conditions (4% O₂) for no more than 24 hours. The iPSCs were maintained at 4% O₂ until the organoid protocol started.

Table 1: Demographic Information of iPSC Lines from RUCDR Infinite Biologics

Alias	NIMH Sample ID	Individual ID	Sex	Race	Age (years)
CF1	MH0185865	163-416-01026-01026	F	White	24
CF2	MH0185916	163-416-01108-01108	F	White	25
CF3	MH0185905	163-416-01095-01095	F	White	33
CM1	MH0185913	163-416-01103-01103	M	White	26
CM2	MH0185983	163-416-01178-01178	M	White	29
CM3	MH0185984	163-416-01179-01179	M	White	29

2.1.2 *iPCS Medium Changes and Passaging*

Before passaging, iPSCs were observed under a microscope to assess confluency and to mark and remove regions of differentiation with a pipette tip. Cells were passaged if colonies were ~70% confluent. If cells were not ready to be passaged mTeSR™1 was aspirated, replaced with 2 mL of fresh medium and cells were incubated at 37°C. For cell passaging, the medium was aspirated from appropriate wells and 1 mL of Gentle Disassociation Reagent (StemCell, 07174) was added. The cells were incubated at room temperature for ~ 2-3 minutes until colonies began to lift. Once lifted, the Gentle Disassociation Reagent was aspirated, 1 mL of fresh mTeSR™1 was added, and cell colonies were gently detached by scraping the well with a cell scraper (StemCell, 38065). Detached cells were transferred to a 15 mL falcon and triturated 2-3 times to break up cell colonies. mTeSR™1 (1-3 mL) was added to the falcon depending on the desired split ratio (split ratios were dependent on starting iPSC confluency; Table 2). The cell-aggregate mixture (0.5 mL/well) was added to warmed Matrigel-coated plates containing fresh mTeSR™1 at the desired density and plates were incubated at 37°C until the next passage or medium change. In total, the iPSCs were maintained for ~ 2 weeks before organoid generation and the medium was changed every 24 hours. To improve the success of cortical differentiation, the iPSCs were pretreated with mTeSR™1 containing different growth factors for 4 days before starting the organoid protocol: BMP4 ([final]= 0.1 ng/mL), TFGβ1 ([final]= 0.1 ng/mL), TFGβ3 ([final]= 1 ng/mL) and activin-A ([final]= 10 ng/mL). The intended starting confluency of the cell lines was ~70%.

Table 2: Cell Confluency and Corresponding Split Ratios for iPSC Passaging

Split Ratio	Cell Confluency	Medium for Passaging 1 Well (mL)	Medium for Passaging 2 Wells (mL)
Not Split	> 50%	N/A	N/A
1:4	50-60%	1	2
1:6	65-70%	2	4
1:8	75-80%	3	6

2.2 Organoid Generation

2.2.1 *EB Formation (Day 0-5)*

Cerebral organoids were generated using the STEMdiff™ Cerebral Organoid Kit (StemCell, 08570) and the protocol was derived from Lancaster et al. 2013 (Figure 5). The EB Formation Medium was prepared (Table 3) and EB Seeding Medium was made by adding 30 μ L of ROK inhibitor to 15 mL of EB Formation Medium ([final]= 10 μ M). Regions of differentiation were marked and removed with a pipette tip, and mTeSR™1 was aspirated from the iPSC culture and replaced with 2 mL of sterile phosphate-buffered saline (PBS; StemCell, 37350). PBS was aspirated, 1 mL of Gentle Disassociation Reagent was added, and the cells were incubated for ~5 minutes at 37°C. Once lifted, iPSCs were gently resuspended by triturating 3-5 times to create a single-cell suspension and transferred to a 50 mL falcon tube (Falcon, 38010). The wells were washed with an additional 1 mL of EB Seeding Medium, added to the conical tube and centrifuged at 300 x g for 3 minutes. Following centrifugation, the supernatant was removed, 2 mL of EB Seeding Medium was added to resuspend cells and 10 μ L of cells were added to an Eppendorf containing 10 μ L of Trypan Blue (StemCell, 07050). The volume of cells required to obtain 90 cells/ μ L was calculated for each cell line using a hemocytometer and this volume was added to a 15 mL falcon containing the corresponding amount of EB Seeding Medium. Once the cells were homogenized, 100 μ L of cell suspension was added to each well of a 96-well round-bottom ultra-low attachment plate (Corning, 7007) using a multichannel pipette (9000 cells/well). The plate was incubated at 37°C and remained undisturbed for at least 24 hours. This process was repeated one at a time, for all 6 cell lines. On days 2 and 4, 100 μ L of EB Formation Medium was added to each well and the plate was incubated at 37°C until organoid induction on day 5.

2.2.2 *Induction (Day 5-7)*

Before commencing the organoid induction process, Induction Medium was prepared (Table 3) and 0.5 mL was added to each well of a 24-well ultra-low attachment plate (Corning, 3473) that was pretreated with AggreWell™ Rinsing Solution (StemCell, 07010). Using a wide bore 200 μ L pipette tip, 1-2 EBs were carefully added to each well-

containing Induction Medium. If the wells contained 2 EBs, to prevent fusion, the plate was gently rocked to ensure EBs were evenly distributed in the well. The plates were incubated at 37°C for 48 hours until organoid expansion on day 7.

2.2.3 *Expansion (Day 7-10)*

To prepare for expansion, enough Matrigel was thawed to have 16 μ L per EB and Expansion Medium was made (Table 3). Organoid Embedding Sheets (StemCell, 08579) were placed in sterile 100 mm dishes (StemCell, 38045) and 200 μ L wide bore pipette tips were used to transfer 40 μ L of medium + 1 EB from the 24-well plate to the Embedding Sheet. This was performed for 6-9 EBs at a time to prevent EBs from drying out. A standard 200 μ L pipette tip was used to remove excess medium from the EB and a cold 200 μ L tip was used to add 16 μ L of Matrigel dropwise onto each EB. To polymerize the Matrigel, the plate was placed in the incubator at 37°C for 30 minutes. Upon removing the plate from the incubator, sterile forceps were used to pick up the Organoid Embedding sheet and held over 1 well of a 6-well ultra-low adherent plate (StemCell, 27145). A chilled 1 mL pipette tip was used to draw up Expansion Medium, dig under the solidified Matrigel and wash the embedded EB's into the well. EBs were washed from the Embedding Surface until 12-16 droplets were in the well and 3 mL of Expansion Medium was used. This process was repeated for each cell line. The 6-well plates were incubated at 37°C for 3 days until organoid maturation on day 10.

2.2.4 *Maturation (Day 10+)*

To begin organoid maturation, Maturation Medium was prepared (Table 3), and all Expansion Medium was removed from wells containing organoids and replaced with 3 mL/well of Maturation Medium. The plates of organoids were placed on an orbital shaker and incubated in normoxic conditions at 37°C. Following day 10, Maturation Medium was changed every 3 days (except for days organoids received nicotine treatment) and the amount of medium added to each well was dependent on the colour of the medium on change day (pink= 3 mL, orange= 3.5-4 mL, yellow= 4-5 mL). Beginning on D48 until ~ 4 months, 1 mL of Cultrex Reduced Growth Factor Basement Membrane Extract, Type 2 (R&D Systems, 3536-005-02) was added to each fresh bottle of Maturation Medium to

support organoid development and maturation. Following the 4-month mark, the organoids received regular Maturation Medium until their final collection day.

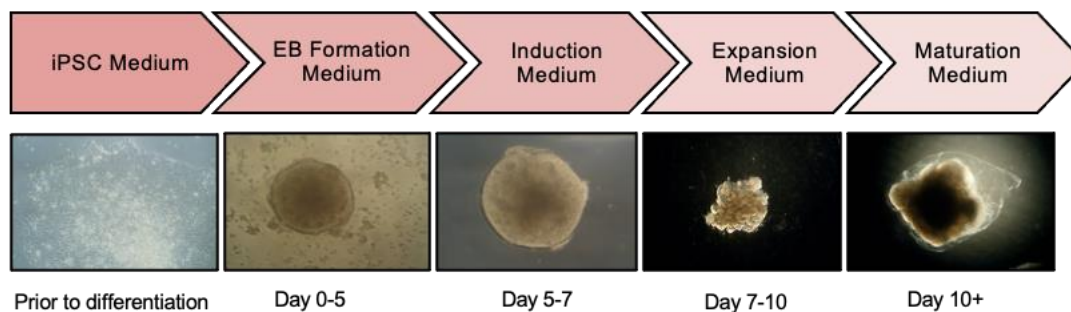


Figure 5: Description of cerebral organoid culture system and representative microscopic images. The iPSCs are maintained in culture for 2 weeks prior to organoid generation. On day 0, the organoids were cultured in an EB formation medium, and the organoids aggregated to form EBs. On day 5, the EBs were cultured in an induction medium which induced them to a neural fate. On day 7, the organoids were embedded in Matrigel and cultured in an expansion medium to allow expansion of the neuroepithelium. On day 10, the organoids were cultured in maturation medium and placed on an orbital shaker. Aside from nicotine treatment when the medium was changed daily, the maturation medium was changed every 3 days during their time in culture.

Table 3: Preparation of STEMdiff Cerebral Organoid Media

Medium	Component	Volume
EB Formation Medium (50 mL)	STEMdiff™ Cerebral Organoid Basal Medium 1	40 mL
	STEMdiff™ Cerebral Organoid Supplement A	10 mL
Induction Medium (50 mL)	STEMdiff™ Cerebral Organoid Basal Medium 1	49.5 mL
	STEMdiff™ Cerebral Organoid Supplement B	0.5 mL
Expansion Medium (25 mL)	STEMdiff™ Cerebral Organoid Basal Medium 2	24.25 mL
	STEMdiff™ Cerebral Organoid Supplement C	0.25 mL
	STEMdiff™ Cerebral Organoid Supplement D	0.5 mL
Maturation Medium (100 mL)	STEMdiff™ Cerebral Organoid Basal Medium 2	98 mL
	STEMdiff™ Cerebral Organoid Supplement E	2 mL

2.3 Antibiotic Treatment

Some cell lines experienced contamination after starting the organoid protocol. This was confirmed by a yellow, cloudy medium and by observing the wells under the microscope. The contaminated media was aspirated using a serological pipette, and the wells were

rinsed with Maturation Medium three times before using a 1000 μ L wide bore pipette to transfer the organoids to a new plate. Contaminated wells were treated with a combination of Penicillin/Streptomycin (1:200-1:1000, Gibco, 15140122), Amphotericin B (1:500-1:1000, Gibco, 15290018) and Gentamycin (1:2500-1:4000, Gibco, 15750078) for 1 week or until the wells were contamination free for 24 hours. If after 1 week the contamination did not clear, the contaminated wells were filled with a 20% bleach solution, the medium and organoids were aspirated, and the plate was discarded as biohazardous waste. The lines/conditions treated chronically with antibiotics were not used in any analysis (CF2 and CF3).

2.4 Nicotine Preparation and Organoid Treatment

Beginning on day 28, organoids were cultured in Maturation Medium with no nicotine (VEH) or a Maturation Medium treated with 0.1, 1 or 10 μ M of nicotine for 14 days. The doses and the timing of treatment were based on studies conducted by Wang et al. 2018 and Notaras et al. 2021 to mimic physiological relevancy and organoid viability. The selected doses fell within the range of average serum concentrations previously reported in pharmacokinetic studies of cigarette smoking and/or nicotine replacement therapies (Albert, 2015; DeVeugh-Geiss et al., 2010; Massadeh et al., 2009; Oncken et al., 1997; Russell et al., 1980). To prepare the nicotine, a 100 μ mol stock of the drug was created by dissolving nicotine hydrogen tartrate (Sigma, N5260) in sterile distilled water (dH₂O) and 1 mL aliquots were kept at -20°C. On each day of nicotine treatment, an aliquot was thawed in the dark at room temperature and 1:10 serial dilutions of nicotine were added to 3 falcons containing Maturation Medium to reach the desired treatment concentrations. The Maturation Medium from all wells was aspirated, VEH or nicotine-treated medium was added to each respective well and the plate was incubated at 37°C for 24 hours until the next drug treatment. Medium changes occurred daily for 14 days (the last treatment was on day 41). The organoids were collected for various histological and molecular techniques at day 42 (D42) and remained in culture until their final collection at day 180 (D180; Figure 6).

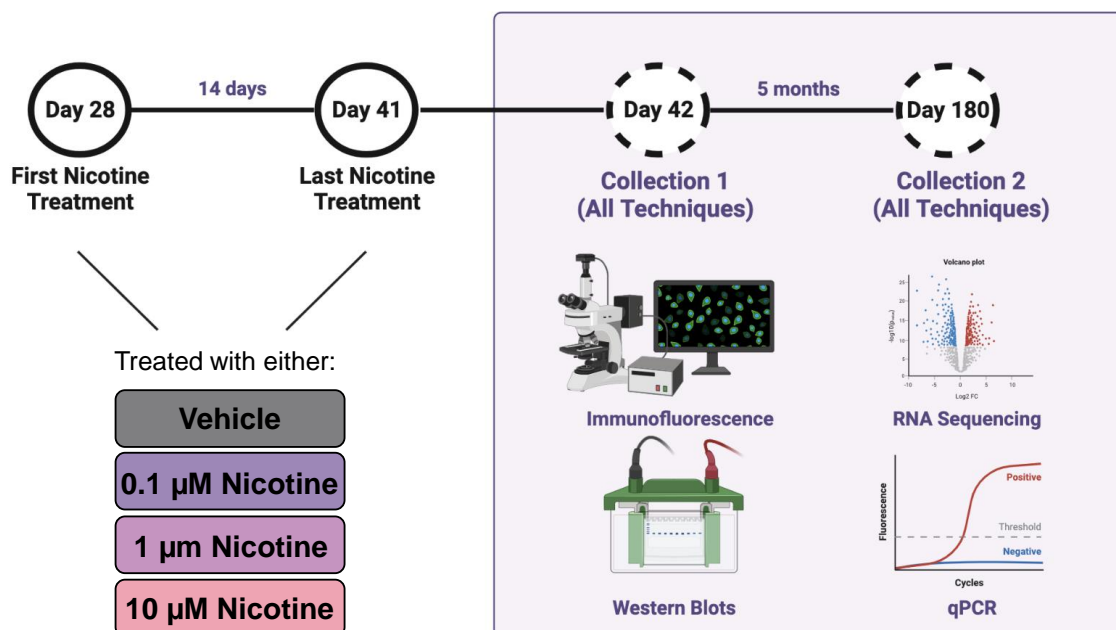


Figure 6: Details of nicotine treatment and organoid collection. Beginning on D28, the organoids were treated with VEH or one of three doses of nicotine daily, for 14 days. Following nicotine exposure on D42 and at D180 the organoids were collected for IF, western blots, RNA-Seq and qPCR. Figure made using BioRender.

2.5 Sample Preparation for IF and H&E Staining

2.5.1 Fixation

The organoids (1-2 depending on the condition) were moved from the 6-well plate with a 1 mL wide bore pipette to a fresh 50 mL conical tube containing 2-3 mL of PBS. After removing the PBS with a serological pipette, 2.5 mL of 4% paraformaldehyde solution (PFA) was added and the tubes were stored overnight at 4°C for ~16 hours.

2.5.2 Cryopreservation

The following day, the PFA was removed, and the organoids were washed 3X for 10 minutes with 3 mL of PBS with 0.1% Tween®20 (PBS-T; Sigma, P9416). After the final wash, PBS-T was removed, and 3 mL of 30% sucrose was added to the tube and stored overnight at 4°C until the embedding stage.

2.5.3 *Embedding*

When ready to embed, a 7.5% gelatin (Sigma, G2500) solution was warmed to 37°C in a water bath, the sucrose solution was removed from the tubes and replaced with enough gelatin to submerge the organoids. To ensure the gelatin was able to completely permeate the Matrigel and encapsulate the organoid, the tube was incubated for 1 hour at 37°C. The organoids were removed from the conical tube, placed in embedding moulds, and covered completely with gelatin. The blocks were flash-frozen in a slurry of dry ice and 100% ethanol and stored at -80°C once samples were completely frozen. The moulds were stored for a minimum of 24 hours before cryosectioning.

2.5.4 *Cryosectioning*

To cryosection, the gelatin blocks were removed from the freezer and warmed in the cryostat (ThermoScientific Cryostar NX50) for 20 minutes before sectioning. The cryostat temperature was set to -18°C and the thickness was adjusted to 20 µm. Slices were collected and positioned on 1:10 Poly-L-lysine (Sigma, P8920) coated Superfrost Plus Microscope Slides (Fisherbrand, 22-037-246) so there were 4 organoids per slide. Slides were labelled and kept in slide boxes at 4°C.

2.6 Immunofluorescence

2.6.1 *Blocking*

Slides were placed in Coplin staining jars (Sigma, J61899) filled with PBS-T and washed for 10 minutes at 37°C to completely remove the gelatin surrounding the organoids. To remove excess salts from the PBS-T, the slides were quickly dipped in dH₂O, laid flat and dried for ~5 minutes in the oven at 37°C. Once the slides were dry enough, an ImmEdge™ hydrophobic PAP pen (Vector, H-4000) was used to circle each organoid on the slide. For blocking, 20 µL of 5% normal donkey serum (Millipore, S30) in PBS-T was pipetted onto each organoid to completely cover them, and the slides were incubated at room temperature in humidified chambers for 1 hour.

2.6.2 Primary Antibodies

Primary antibodies were prepared in 5% donkey serum in PBS-T according to the recommended dilutions (Table 4). The blocking solution was pipetted off and replaced with 20 μ L of primary antibody solution. For negative controls, the organoids remained covered with the blocking solution and received no primary antibody. The slides were incubated overnight at 4°C in humidified chambers.

Table 4: Primary Antibodies Used in Immunofluorescence

Antibody	Host	Company	Cat. Number	Dilution
α_7 nAChR	Rabbit	Alomone Labs	ANC-007	1:50
α_4 nAChR	Mouse	Santa Cruz	sc-74519	1:50
β_2 nAChR	Goat	Abcam	ab189174	1:100
D1R	Rabbit	Abcam	ab40653	1:50
D2R	Mouse	Sigma-Aldrich	MABN53	1:200
mGLUR2/3	Rabbit	Sigma-Aldrich	06-676	1:50
GAD67	Mouse	Sigma-Aldrich	mab5406	1:50
Ki67	Rabbit	Abcam	ab15581	1:500
PROX1	Mouse	Sigma-Aldrich	mab5654	1:100
FZD9	Goat	Abcam	ab110886	1:100
FGFR1	Rabbit	Abcam	ab0646	1:200
Cl-Caspase 3	Rabbit	Cell Signaling	9661	1:200
CTIP2	Rat	Abcam	ab18465	1:100
CDH13	Goat	Novus Biologicals	AF3264	1:200
MAP2	Mouse	Sigma-Aldrich	mab3418	1:100
NR2B	Goat	Novus Biologicals	NB100-41097	1:50
GAT1	Rabbit	Rockland Immunochemicals	612-401-D56	1:100
PV	Mouse	Sigma-Aldrich	P3088	1:50

2.6.3 Secondary Antibodies

The primary antibody was poured off the slides and the slides were placed in Coplin staining jars filled with PBS-T. The slides were washed 3X for 10 minutes to remove any remaining primary antibodies. The slides were laid flat and dried in the oven at 37°C for

~5 minutes. Secondary antibodies (Invitrogen) were prepared in 5% donkey serum in PBS-T at a 1:250 dilution (Table 5) and 20 μ L was pipetted onto each organoid. Each secondary antibody had a corresponding negative control. The slides were incubated at room temperature in humidified chambers for 2 hours covered from light.

Table 5: Secondary Antibodies Used in Immunofluorescence

Antibody	Company	Cat. Number	Dilution
Alexa Fluor® D α Rb488	Invitrogen	A32790	1:250
Alexa Fluor® D α M568	Invitrogen	A10037	1:250
Alexa Fluor® D α G647	Invitrogen	A21447	1:250
Alexa Fluor® D α Rat647	Invitrogen	A78947	1:250
Alexa Fluor® D α Rat488	Invitrogen	A21208	1:250

2.6.4 *Coverslips*

The secondary antibody was poured off the slides and the slides were placed in Coplin staining jars filled with PBS-T. The slides were washed 3X for 10 minutes to remove any remaining secondary antibodies and air dried for 5-10 minutes. To completely saturate the organoid and fill the area within the hydrophobic barrier, 2-3 drops of Fluoroshield™ with 4',6-diamidino-2-phenylindole (DAPI; Sigma-Aldrich, F6057) was added to the organoids and incubated for 5 minutes at room temperature covered from light.

Coverslips (1.5 mm; Fisherbrand, 12542A) were placed over the organoids using forceps, light pressure was applied to remove air bubbles and sealed using clear nail polish. The slides were stored in a slide box at 4°C until ready to image.

2.6.5 *Confocal Microscopy*

The organoids were imaged using a Leica SP8 (D42) or Leica STELLARIS5 (D180) microscope. The 40x and 63x magnifications were used on the Leica Sp8 and STELLARIS5, respectively. Each experimental condition had 1 organoid and 2 regions of interest (ROI) were imaged per organoid. For channel setup, the 3 channels of interest (488, 568, 647) and DAPI (405) were selected, and the gates were modified to prevent photobleaching. The master gain and laser intensity were adjusted for each marker to establish a strong signal but limit oversaturation. Bidirectional X was turned on to increase scanning speed and images were taken in a 1024x1024 format at a speed of 400

Hz. Additional settings included a frame accumulation and frame average of 2. Each ROI was imaged using a Z-stack that had 6 steps ranging from 1.0-1.5 μm each. For D42, the ROIs were selected to include a ventricular-like region and the D180 ROIs were focused on the outer cortical regions. Images were scanned and saved as LIF files for later analysis.

2.6.6 *Image Analysis*

Analysis of images was conducted in a blind manner to prevent experimenter bias. Each ROI was given an alias by a third party and following analysis, the image identity was decrypted for statistical analysis. Each marker of interest was analyzed using FIJI Image J (NIH). The files were selected to be opened individually, the colour mode was selected as composite, and the stack was viewed with a hyper stack. Average intensity was chosen as the projection type and the images were split into each channel comprising the image. For each marker, the image was changed to 8-bit and auto-thresholded according to which threshold best represented the marker of interest. After the threshold was set, the image was made binary, despeckled and a watershed was used to detect and separate boundaries of overlapping cells. To select an ROI, the original DAPI image was selected. The free-hand tool was used to create an ROI that was added to the ROI manager. Then, the ROI was selected on the watershed image and the area, mean, integrated density and integrated raw density were measured and recorded in Excel. Using the analyze particle function, the size and circularity were adjusted depending on the marker of interest and bare outlines and display results were selected. The total number of particles in the results tab was recorded in Excel and the watershed images, drawing of the mask and ROIs were all saved for future reference. The images were normalized to the area by dividing the number of particles by the area ($\text{particles}/\text{mm}^3$). This process was repeated for each ROI (2 per organoid) for each marker of interest.

2.7 Hematoxylin and Eosin Staining

Following sample preparation (2.5), slides were selected under the microscope and sent off to Pathology at Robarts Research Institute (Western University, Ontario, Canada) for H&E staining. A brightfield microscope (Nikon H600L) with a 10x magnification was

used for image acquisition. The quality of the capture was 2880x2048 with a lamp brightness of 57. The auto-white balance setting was selected to ensure the colour of the sample remained unchanged against the light source. Tiling was performed with 20% stitching overlap and stitching occurred by blending. The image was focused manually as the image was captured. The images were saved as TIFF files and 1 image was taken per organoid.

2.8 Western Blot

2.8.1 *Snap Freezing*

The organoids were transferred to a 24-well plate, rinsed with Dulbecco's PBS (dPBS) and transferred to a labelled Eppendorf. Depending on the condition, 1-2 organoids were collected in separate Eppendorfs. The excess dPBS was removed using a P200 pipette, and the Eppendorf's were quickly placed on dry ice and stored at -80°C until protein extraction.

2.8.2 *Protein Extraction*

Radioimmunoprecipitation assay (RIPA) buffer was made and 200 µL was added to each Eppendorf containing an organoid (tube 1). An electric micro homogenizer (VWR, 10032-326) was used at a speed of 5.5 speed to break up the tissue and all samples were rotated at 4°C for 30 minutes. The samples were centrifuged at 15,000 rpm for 15 minutes at 4°C and all supernatant was transferred to a fresh Eppendorf (tube 2). All the supernatant except for 10 µL was transferred to another tube (tube 3) and an equal volume of 2X loading buffer was added to the supernatant. Tube 3 was quickly vortexed, boiled at 95°C for 5 minutes and stored at -20°C until ready for gel electrophoresis.

2.8.3 *Protein Quantification*

Bovine serum albumin (BSA; VWR 0332) standards (0-2000 µg) were defrosted, 10 µL was loaded into a standard clear-bottom 96-well plate by order of increasing concentration and 2 µL of lysis buffer was loaded as a blank. All BSA standards and blanks were loaded in duplicates. The rest of the wells were loaded with 2 µL of extracted protein from each organoid sample (tube 2 from protein extraction). Reagent

A/B was combined in a 50:1 ratio and 200 μL was added to each well using a multichannel pipette. The plate was wrapped in Parafilm® and incubated at 37°C for 30 minutes. A Biotek Epoch Microplate Spectrophotometer was used to analyze the plate at a wavelength of 562. Protein aliquots were created by comparing the samples to a standard curve and adding the appropriate amount of protein and 2X loading buffer to achieve a standardized concentration of 10 $\mu\text{g}/\mu\text{L}$ across all samples. The organoids treated with 10 μM did not have a high enough protein concentration, so blots were run with VEH, 0.1 and 1 μM doses only. The aliquots were stored at -20°C until the day of the experiment.

2.8.4 *Gel Electrophoresis, Blocking and Antibodies*

The cast gels were 10% and assembled into the western apparatus. A running buffer was added between the 2 plates and to the appropriate line on the chamber. The ladder was added to the first well of each gel and 29.5 μL of the sample was loaded into each well in order of cell line and treatment (e.g., CM3-V, CM3-0.1, CM3-1). The gels were run at 125V for ~1 hour 15 minutes until the blue dye from the loading buffer began to run off the gel. The gels were transferred (Bio-Rad Trans-Blot Turbo Transfer System) to a nitrocellulose membrane at 1.5A for 10 minutes. The membranes were blocked for an hour according to recommended use [BSA or milk in tris buffered saline with 0.1% Tween (TBS-T)] at room temperature, primary antibodies were prepared according to Table 6 and incubated overnight at 4°C with rocking. Following 3X washes with TBS-T, membranes were incubated in 1:10,000 secondary antibodies (Table 7) diluted in 2.5% BSA, at room temperature, for 2 hours. Membranes were washed 2X with TBS-T, 1X with TBS and stored in TBS at 4°C until ready to visualize blots.

Table 6: Primary Antibodies Used in Western Blots

Antibody	Host	Company	Cat. Number	Dilution
T-ERK1-2	Mouse	Cell Signaling	4370S	1:1000
pERK1-2	Rabbit	Cell Signaling	4370S	1:1000
T-GSK3 β	Mouse	Santa Cruz	sc-7291	1:200
pGSK β	Rabbit	Cell Signaling	8566S	1:1000
α -tubulin	Mouse	Santa Cruz	sc-8035	1:500
α -tubulin	Rabbit	Proteintech	11224-1-AP	1:500
β -actin	Mouse	Millipore Sigma	A2228	1:2000

Table 7: Secondary Antibodies Used in Western Blots

Antibody	Company	Cat. Number	Dilution
IRDye® 680RD Donkey anti-Rabbit	LI-COR	926-68073	1:10,000
IRDye® 800CW Donkey anti-Rabbit	LI-COR	926-32213	1:10,000
IRDye® 680RD Donkey anti-Mouse	LI-COR	926-68072	1:10,000
IRDye® 800CW Donkey anti-Mouse	LI-COR	926-32212	1:10,000
IRDye® 800CW Donkey anti-Goat	LI-COR	926-32214	1:10,000

2.8.5 *Blot Analysis*

Blots were scanned using a LI-COR Odyssey scanner on the high-quality membrane setting. The blot was oriented protein side down on the scanner and scanning laser intensities on the 700 and 800 channels were adjusted accordingly to capture the protein bands. The scans were saved and imported into Image Studio Lite Version 5.2. The relative band intensity was calculated and normalized to the housekeeping protein of interest on each respective membrane (α -tubulin or β -actin).

2.9 qPCR

2.9.1 *RNA Extraction*

Organoids were snap frozen (2.8.1) and stored at -80°C until RNA extraction. Trizol reagent (Invitrogen, 15596018) and an electric micro homogenizer were used to break up the tissue and the samples were incubated in 200 μL of chloroform (Sigma Aldrich, C2434) at room temperature for 3 minutes. Following centrifugation at 12,500 rpm at 4°C for 15 minutes, the supernatant was removed, placed into a sterile Eppendorf with an

equal volume of isopropanol alcohol and incubated at -20°C overnight. Following centrifugation, precipitation with 70% ethanol, and the removal of any remaining liquid, the pellet was dissolved in 20 μL DEPC-treated water (Invitrogen, AM9916) and placed on ice. To check the quality of the collection, a nanodrop 2000 spectrophotometer (ThermoFisher) was used. The nucleic acid cut-off was $>106.9 \mu\text{g}/\mu\text{L}$ and the 260/280 ratio was between 1.72-2.1. The RNA was stored long-term at -80°C until cDNA conversion.

2.9.2 *Complementary DNA (cDNA) Synthesis*

DEPC and cDNA were combined in an Eppendorf to achieve a standardized concentration of $1 \mu\text{g}/\mu\text{L}$ across all samples. A High-Capacity cDNA Reverse Transcriptase Kit (Applied Biosystems, 4368814) was used to make a master mix and 5.8 μL was added to each tube for a total reaction volume of 20 μL . The tubes were centrifuged, placed in the thermocycler (Bio-Rad C100), and run for 2.5 hours. The cDNA was diluted to 1:40 in DEPC and stored at $-20 \mu\text{L}$ until the experiment.

2.9.3 *qPCR*

Forward and reverse primers were designed using NCBI Primer Blast, and Harvard PrimerBank and sequences were validated using NIH Nucleotide Blast (Table 8). All primers were ordered from ThermoFisher, and quality was checked by analyzing the melt curves. DEPC blanks and 3 μL of cDNA were loaded into a 384 well plate (VWR, 82006-678) in triplicates. A master mix comprised of DEPC, 2.5 μM forward and reverse primer mix and SensiFAST SYBR (Meridian Bioscience, Bio-98050) was made and 5 μL was added to each well for a total reaction volume of 8 μL . The plate was sealed, run for 2 hours in the Real-Time PCR System (Bio-Rad, CFX Opus 384) and gene expression was analyzed using SYBR green fluorescence. When the plate was finished running, the quality of the run was checked by examining the cycle quantification (Cq) values and melt curves. Values with a difference of > 0.5 Cq within a triplicate were removed and a Cq average was calculated for each sample. The values obtained for all gene targets of interest were normalized to the geometric means of housekeeping genes β -actin and GAPDH. β -actin and GAPDH were determined to be suitable housekeeping genes by

using the comparative ΔC_q method. The $2^{-\Delta\Delta C_q}$ method was used to calculate the relative fold change of gene expression within the experimental samples.

Table 8: qPCR Primer Sequences

Gene	Forward Sequence (5'-3')	Reverse Sequence (5'-3')	Gene Accession #
CHRNA7	ggactcaacatgcgctgctc	ggttcttctcatccacgtcca	NM_000746.6
CHRNA2	caatgctgacggcatgtacga	cacgaacggaactcatggtg	NM_000748.3
CTIP2	ggtgcctgctatgacaagg	ggctcggacactttcctgag	NM_138576.4
D1R	gacctgtctgtactcatctcct	gtcacagttgtctatggctcag	NM_000794.5
EMX1	cgcaggtgaaggtgtggtt	tccagcttctgccgtttgt	NM_004097.3
EOMES	gtgcccacgtctacctgtg	cctgcctgtttcgtaaatgat	NM_001278182.2
FOXP1	aggagggcgagaagaagaac	tgaactcgtagatgccgttg	NM_005249.5
GAD1	gcggacccaataaccactaac	cacaaggcgactcttctcttc	NM_000817.3
GRM2	ccgcattgcacgcactcttc	ggcccagataagtgccag	NM_000839.5
GRM3	agcaatcactggagttgtcag	gcaatgagaagtgggatgttttc	NM_000840.3
ISL1	gcggagtgtaatcagtatttggga	gcatttgatcccgtacaacct	NM_002202.3
TBR1	gactcagttcatgccgtca	tgctagtaccctagccttgc	NM_006593.4

2.10 RNA Sequencing

Pooled male and female VEH (n=3) and 0.1 μ M nicotine-treated (n=3) organoids were snap frozen (2.8.1) and sent to Genome Quebec (Montreal, Quebec, Canada) for total RNA extraction, library preparation and RNA-Seq. Quality checks were performed by Genome Quebec following extraction and library preparation. The RNA integrity number (RIN) was used to assess RNA quality and all samples had RIN scores ≥ 7.0 . Paired-end reads (25 million) were sequenced on the Illumina NovaSeq platform. All raw reads were aligned and annotated with the latest ENSEMBL Homo Sapien GRCH38.p13 reference genome using STAR version 2.7.10a with recommended settings. Raw counts were generated using the Rsubread subpackage featureCounts. Lowly expressed genes were filtered out using a count per million (CPM) cutoff of 0.4 in at least 2 or more samples. Normalization and DE analysis were done using the edgeR package (Chen et al., 2016). Briefly, counts were normalized for both library size and library composition using the trimmed means of the M-values (TMM) method. Normalized counts were then fit to a gene-wise negative binomial generalized linear model, and a quasi-likelihood F test was used for DE analysis. To account for multiple testing, p-values were adjusted using Benjamini & Hochberg False Discovery Rate (FDR) correction. An FDR cut-off of < 0.05 was used to determine significance. The gprofiler2 (Kolberg et al., 2020) R interface for the web toolset g: Profiler was used to convert ENSEMBL gene IDs to gene symbols, and to perform functional enrichment analysis (over-representation analysis) on the DE genes from databases of interest. The databases included in the analysis were the Gene Ontology (GO) database, the Reactome (REAC) database, the TRANSFAC (TF) database, the human protein atlas (HPA) and the WikiPathways (WP) database. There are also three GO sub-categories: biological process (BP), cellular component (CC), and molecular function (MF). A g: SCS adjusted p-value threshold of < 0.01 was used to determine the significance of the functional enrichment analysis. To examine DE genes between VEH and 0.1 μ M nicotine organoids, a heatmap was generated using the pheatmap R package (Hu 2021). Further analysis of DE genes was completed using VarElect (<http://ve.genecards.org>). VarElect is an application that permits the analysis of your specific DE genes following sequencing and ranks genes that are found to have

variants according to specific phenotype-gene associations. To generate this list, VarElect uses information obtained from several databases such as GeneCards® (www.genecards.org), Malacards (www.malacards.org), LifeMap Discovery® (discovery.lifemapsc.com) and Pathcards (pathcards.genecards.org). The list of DE genes was imported into VarElect and 3 phenotypes of interest were individually searched: nicotine exposure, anxiety, and depression. An annotated list of DE genes associated with each phenotype was generated. This list is formed based on direct (GeneCards) and indirect links (Genecards and Malacards) between the genes and phenotype of interest. The top 20 genes for each phenotype were compared to assess which DE genes were associated across multiple phenotypes.

2.11 Statistical Analyses

Outliers were removed using Grubbs' test ($\alpha = 0.05$) and normality was assessed. All results for IF, western blot and qPCR were analyzed with one-way analysis of variance (ANOVA) or Kruskal-Wallis if appropriate. Significant ($p < 0.05$) or trending ($p < 0.1$) tests were followed up using Fisher's LSD *post hoc* test ($\alpha = 0.05$). All analyses were performed using GraphPad Prism (version 9.4.1 for Windows) and graphs are presented as mean \pm standard error of the mean (SEM). For RNA-Seq, to account for multiple testing, p-values were adjusted using Benjamini & Hochberg False Discovery Rate (FDR) correction. An FDR cut-off of < 0.05 was used to determine significance.

3 Results

Short-term Effects of PNE - D42 Results

3.1.1 *PNE Model Characterization*

To assess successful neuronal differentiation and recapitulation of features of the developing brain, we used a combination of H&E staining and IF to characterize our organoids. Histological staining with H&E (Figure 7) reveals morphological features of cerebral organoids at D42 with dark purple (hematoxylin) distinguishing cell nuclei from the extracellular matrix and cytoplasm, dyed pink (eosin). The PNE organoid model demonstrates that VEH (Figure 7A) and treatment conditions (Figure 7B-D) contain ventricular-like structures (also known as neural rosettes) which are indicative of successful neural induction and the presence of cortical tissue. These structures are characterized by a high density of H⁺ nuclei surrounding a central lumen, where neural progenitors undergo mitosis at the luminal surface to differentiate into various cell types (Figure 7E). Early on, progenitors will differentiate into neurons and divide at the ventricular zone, migrate through the intermediate zone and to the cortical plate where they comprise layers of the cortex. There are several rosettes in the VEH condition with high concentrations of densely packed cells. As we increase nicotine concentration, there is a decrease in the number and integrity of rosettes, which indicates that nicotine has an impact on rosette morphology and integrity of cortical tissue. Following H&E imaging, we noticed that 3 of the 6 lines did not develop properly, indicated by the absence of neural rosettes (CM1, CF2, CF3) and all future experiments were conducted using CM2, CM3 and CF1 cell lines.

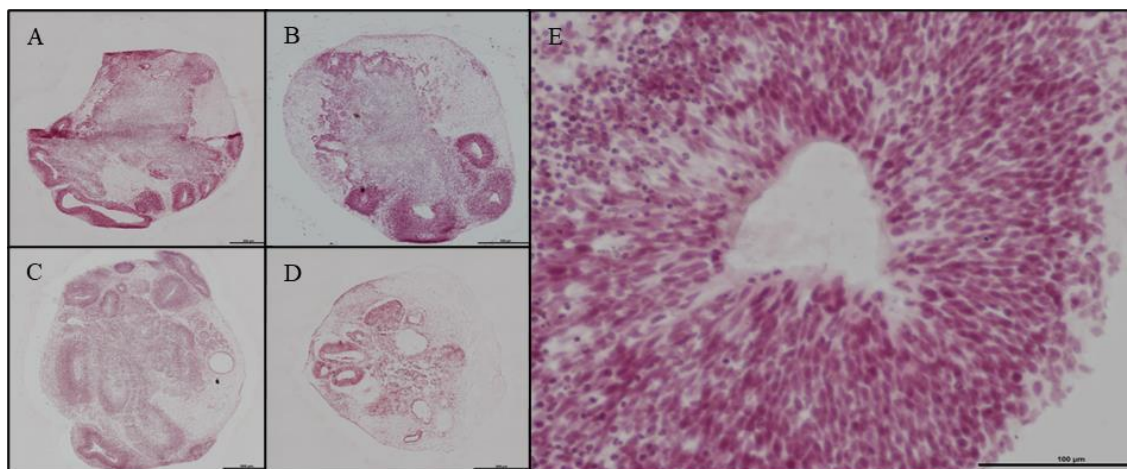


Figure 7: iPSC-derived cerebral organoids display cortical differentiation. Scale bar = 100 μm . H&E staining of VEH (A), 0.1 (B), 1 (C) and 10 μM (D) nicotine-treated organoids. Organoids displayed ventricular-like structures (E) indicative of successful cortical differentiation.

The presence of neural rosettes and successful neural induction was also confirmed by performing IF to characterize VEH organoids at D42 (Figure 8). VEH organoid cell nuclei stained positive for proliferation marker Ki67 (Figure 8A) and expression was more concentrated at the apical surface. Indeed, organoids stained positive for regional markers specific to hippocampal and cortical tissue such as Prospero homeobox 1 protein (PROX1) and frizzled-9 (FZD9; Figure 8B and 8C). Furthermore, the presence of microtubule-associated protein 2 (MAP2; Figure 8D), which stains the cytoskeleton of neurons, indicated successful neuronal induction. This was demonstrated by signs of early radial organization and increased MAP2 expression at the basal surface of the organoid rosette. Our organoids also expressed fibroblast growth factor receptor 1 (FGFR1; Figure 8E), which is vital to cell survival and migration as well as cadherin-13 (CDH13; Figure 8F) which assists with axonal growth and synapse formation over the course of development. These results exhibit that our cerebral organoids model aspects of neurogenesis, successful cortical differentiation, and developmental signatures of the developing fetal brain.

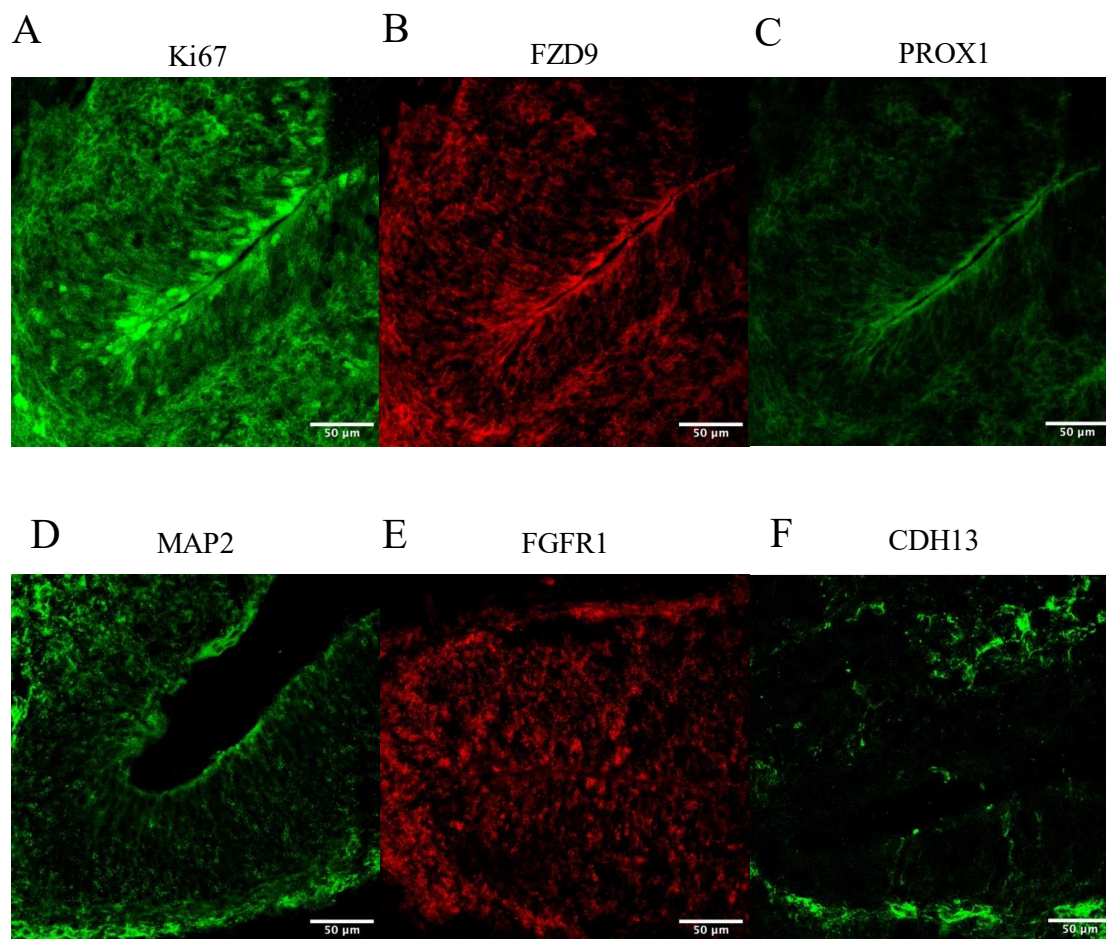


Figure 8: iPSC- derived cerebral organoids express markers specific to early brain regionalization and vital to development. Scale bar = 50 µm. **A-F** Immunofluorescent images were captured using confocal microscopy. **A-C** Staining of VEH organoids was performed for the expression of proliferation marker Ki67 (**A**) and regional markers FZD9 (**B**) and PROX1 (**C**) on D42. **D-F** VEH organoids also expressed neuronal marker MAP2 (**D**), developmental markers FGFR1 (**E**) and CDH13 (**F**).

3.1.2 *Effect of Nicotine on Characterization Markers*

Following initial characterization, to establish the presence or absence of these specific markers, we wanted to assess if nicotine had an impact on their expression. It was interesting to note that there was no difference between VEH, and nicotine-treated organoids in any of the markers from Figure 8 ($p > 0.05$; Table 9).

Table 9: Nicotine Had No Effect on the Expression of Select Brain Organoid Neurodevelopmental Characterization Markers

Marker	Function	Test	F Value	P-Value	Significance
Ki67	Proliferation	Ordinary one-way ANOVA	3.028	0.0623	Trending decrease at 0.1 μ M
FZD9	Regional	Ordinary one-way ANOVA	1.064	0.3938	ns
PROX1	Regional	Ordinary one-way ANOVA	1.065	0.3915	ns
MAP2	Neuronal	Ordinary one-way ANOVA	0.6423	0.5996	ns
FGFR1	Developmental	Ordinary one-way ANOVA	0.9742	0.4347	ns
CDH13	Developmental	Ordinary one-way ANOVA	1.271	0.3180	ns

Comparisons were made with ordinary one-way ANOVA followed by Fisher's LSD post-hoc test. Data are mean \pm SEM, n = 4-6, trending = $p < 0.1$, ns = not significant. n = 1 ROI.

However, after our 14-day treatment, there were changes in specific markers used to characterize our model of PNE (Figure 9A). Indeed, there was a significant increase in cleaved caspase 3 expression, a marker of apoptotic cell death ($H_{(3,16)} = 9.174$, $p = 0.0271$; Figure 9B). *Post hoc* analysis revealed an increase at 10 μ M ($p = 0.0114$), with no effect observed at 0.1 or 1 μ M ($p > 0.05$). We also examined deep-layer marker COUP-TF-interacting protein 2 (CTIP2), and nicotine-treated organoids had a significant increase compared to VEH ($H_{(3,16)} = 12.73$, $p = 0.0053$; Figure 9C). The *post hoc* analysis showed a similar result to cleaved caspase 3, with a significant increase at 10 μ M ($p = 0.0060$) but not at the lower doses ($p > 0.05$). These results suggest that these specific markers may be more susceptible to the influences of nicotine at higher doses, resulting in increased cell death and increased number of early-born neurons, whereas other developmental markers are less sensitive to the effects of PNE.

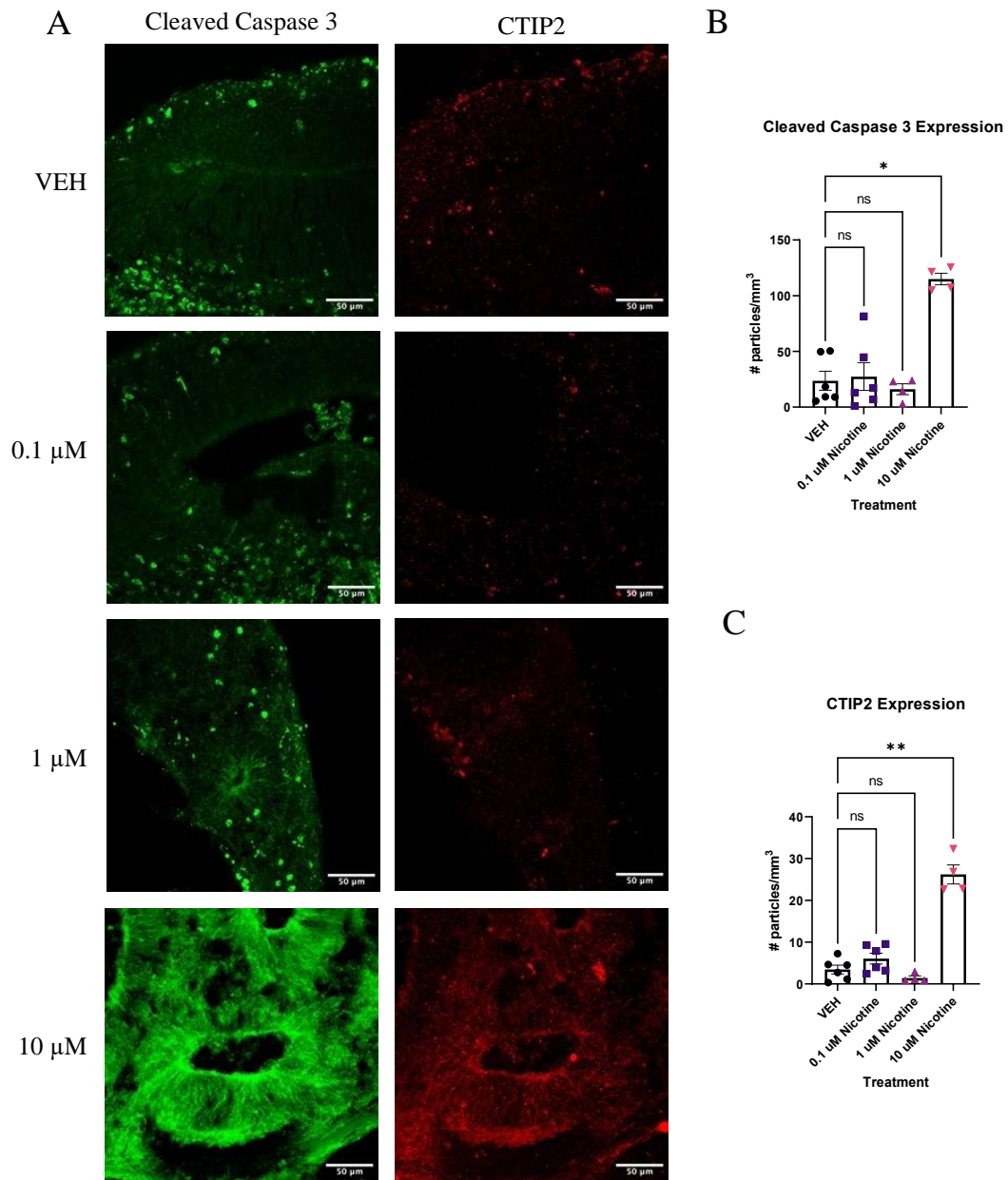


Figure 9: PNE significantly increases cell death and number of early-born neurons on D42. **A**, Immunofluorescent images captured using confocal microscopy of cleaved caspase 3 (green) and CTIP2 (red) in brain organoids treated with (0.1, 1 or 10 μ M) nicotine or without (VEH) for 14 days. Scale bar = 50 μ m. **B**, **C**, Quantification of immunofluorescent images by the number of particles per area (mm^3). **B**, Organoids treated with 10 μ M displayed a significant increase in apoptotic cell death at 10 μ M, denoted by increased expression of cleaved caspase 3. **C**, PNE significantly increased the presence of cortical layer marker CTIP2. Comparisons were made with Kruskal Wallis followed by Fisher's LSD *post hoc* test. Data are mean \pm SEM, $n = 4-6$, $**p < 0.01$, $*p < 0.05$, trending = $p < 0.1$, ns = not significant, $p > 0.05$. $n = 1$ ROI.

3.1.3 *Mood/Anxiety Molecular Biomarker Results*

3.1.3.1 *Immunofluorescence*

Developmental nicotine exposure has been shown to dysregulate markers that are present in mood and anxiety disorders. To further investigate this, we employed IF to assess the impact of PNE on these biomarkers at the protein level. To understand how nicotine may impact the expression of its target receptor, we looked at nAChR subunits that comprise the most abundant receptors in the cortex and are implicated in anxiety in depression; the α_7 , α_4 and β_2 nAChR subunits (Figure 10A). Analysis revealed that nicotine selectively altered the expression of these specific receptor subunits. One-way ANOVA revealed that PNE had no effect on α_7 at any dose ($F_{(3,19)} = 1.095$, $p = 0.3818$; Figure 10B), but there was a significant increase in α_4 ($H_{(3,15)} = 7.424$, $p = 0.0449$) and β_2 ($F_{(3,15)}$, $p = 0.0043$) nAChR subunits (Figure 10C and 10D) in nicotine treated organoids compared to VEH. Follow-up *post hoc* comparisons revealed a marked increase in α_4 at the 1 ($p = 0.0294$) and 10 μM dose ($p = 0.0205$), but not at 0.1 ($p > 0.05$). Similarly, this was also seen in β_2 at these doses ($p = 0.0477$; $p = 0.0006$; $p > 0.05$). Thus, PNE upregulates the expression of some but not all nAChRs implicated in anxiety and depression at D42.

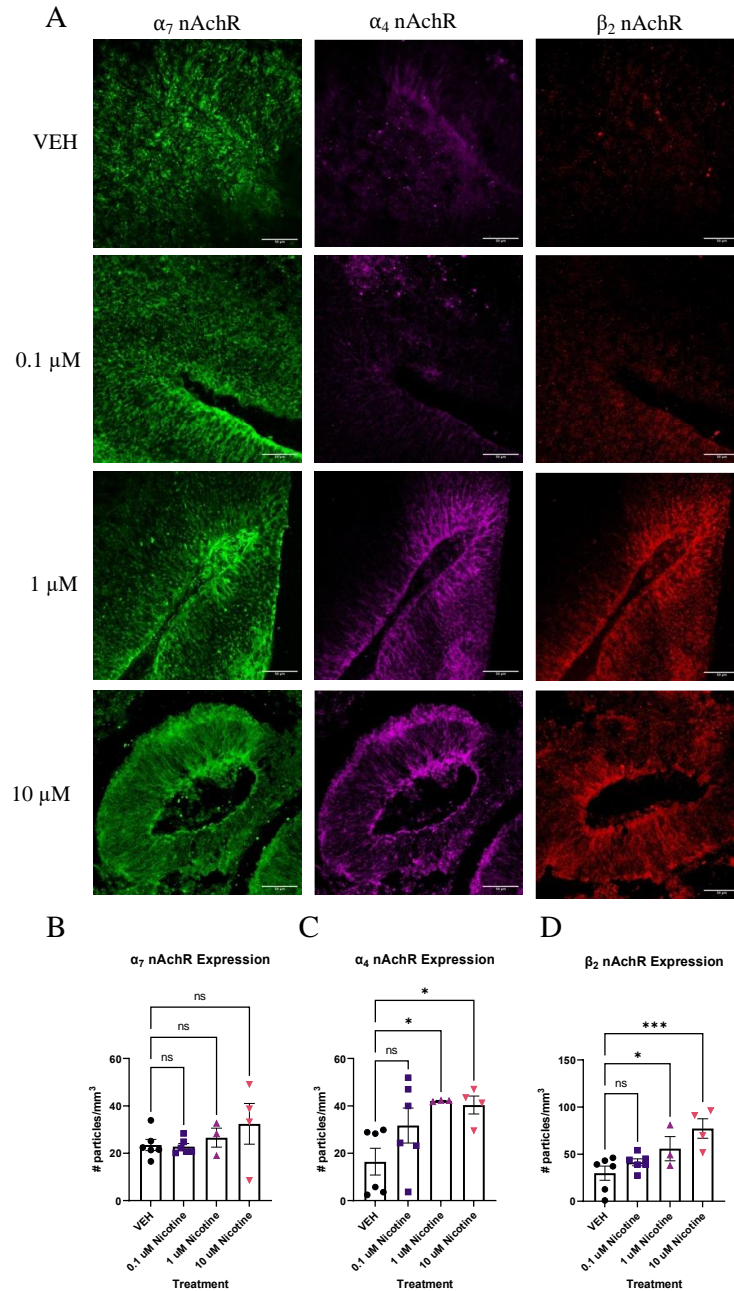


Figure 10: PNE selectively upregulates certain nAChR populations at D42. **A**, Immunofluorescent images captured using confocal microscopy of α_7 (green), α_4 (magenta) and β_2 nAChR (red) in brain organoids treated with (0.1, 1 or 10 μ M) nicotine or without (VEH) for 14 days. Scale bar = 50 μ m. **B-D** Quantification of immunofluorescent images by the number of particles per area (mm^3). PNE did not affect α_7 nAChR expression (**B**) but caused a significant increase in α_4 (**C**) and β_2 (**D**) compared to VEH organoids. Comparisons were made with one-way ANOVA or Kruskal Wallis followed by Fisher's LSD *post hoc* test. Data are mean \pm SEM, $n = 4-6$, *** $p < 0.001$, * $p < 0.05$, ns = not significant, $p > 0.05$. $n = 1$ ROI.

Since developmental nicotine exposure has been shown to disrupt dopaminergic signaling in brain regions associated with mood and anxiety control, we decided to investigate changes in D1R and D2R expression following chronic PNE (Figure 11A). Following the 14 days of drug exposure, one-way ANOVA revealed a significant decrease in D1R receptor expression ($F_{(2,13)} = 5.624$, $p = 0.0174$; Figure 11B), with *post hoc* analysis suggesting this decrease occurred at 0.1 ($p = 0.0061$) with no effect at 1 μM ($p > 0.05$). Compared to VEH, one-way ANOVA indicated PNE also significantly decreased D2R receptor expression ($F_{(2,13)} = 6.023$, $p = 0.0141$; Figure 11C). Further investigation using *post hoc* analysis exhibited that the decrease occurred at both 0.1 ($p = 0.0077$) and 1 μM ($p = 0.0178$). These results indicate that expression of these dopaminergic subtypes is influenced at lower doses of PNE and is consistent with changes in protein expression seen in mood and anxiety disorders.

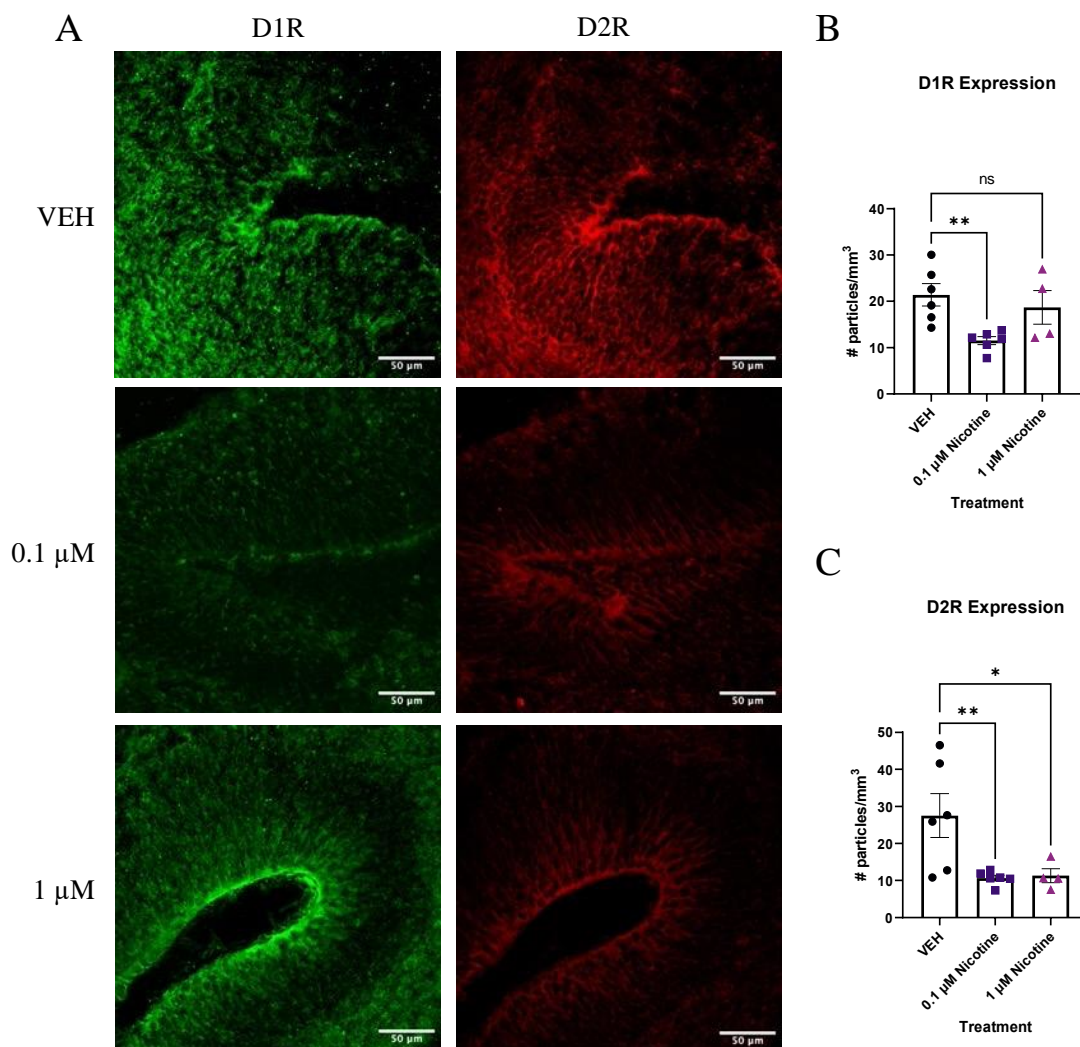


Figure 11: PNE induces significant alterations in dopaminergic receptors implicated in mood and anxiety disorders at D42. **A**, Immunofluorescent images captured using confocal microscopy of D1R (green) and D2R (red) brain organoids treated with (0.1 or 1 μ M) nicotine or without (VEH) for 14 days. Scale bar = 50 μ m. **B**, **C**, Quantification of immunofluorescent images by the number of particles per area (mm^3). Compared to VEH, organoids treated with nicotine had significantly decreased levels of D1R at 0.1 μ M (**B**) and D2R at 0.1 and 1 μ M (**C**). Comparisons were made with one-way ANOVA or Kruskal Wallis followed by Fisher's LSD *post hoc* test. Data are mean \pm SEM, $n = 4-6$, $**p < 0.01$, $*p < 0.05$, trending = $p < 0.1$, ns = not significant, $p > 0.05$. $n = 1$ ROI.

Finally, altered cortical E/I balance is a hallmark attribute of mood and anxiety disorders, so we investigated the influence of PNE on various GABAergic markers due to their role in cortical inhibition and neuron excitability (Figure 12A). One-way ANOVA analysis of IF results concluded that compared to VEH, PNE significantly decreased the expression of GABA transporter GAT-1 ($F_{(3,15)}=8.778$, $p=0.0013$; Figure 12B) with *post hoc* analysis revealing a significant decrease only at 10 ($p=0.0004$), not 1 or 0.1 μM ($p>0.05$). GABAergic alterations were also supported by a trend towards a decrease in PV interneurons in cortical regions of interest ($H_{(3,14)}=7.277$, $p=0.0502$; Figure 12C). Due to trending significance, a *post hoc* analysis was conducted and demonstrated a significant decrease in PV at 10 μM ($p=0.0350$) but not lower doses of nicotine ($p>0.05$). Finally, there was a trending decrease in levels of the GABA synthesis marker, GAD67 ($F_{(3,16)}=3.150$, $p=0.0540$; Figure 12D), which leans towards altered GABA neurotransmission in our organoids. Analogous to PV, *post hoc* comparisons were performed and revealed a significant deficit in GAD67 at 10 μM ($p=0.0157$). These results suggest that at the protein level, higher doses of nicotine have a significant effect on GABAergic markers implicated in maintaining cortical E/I balance.

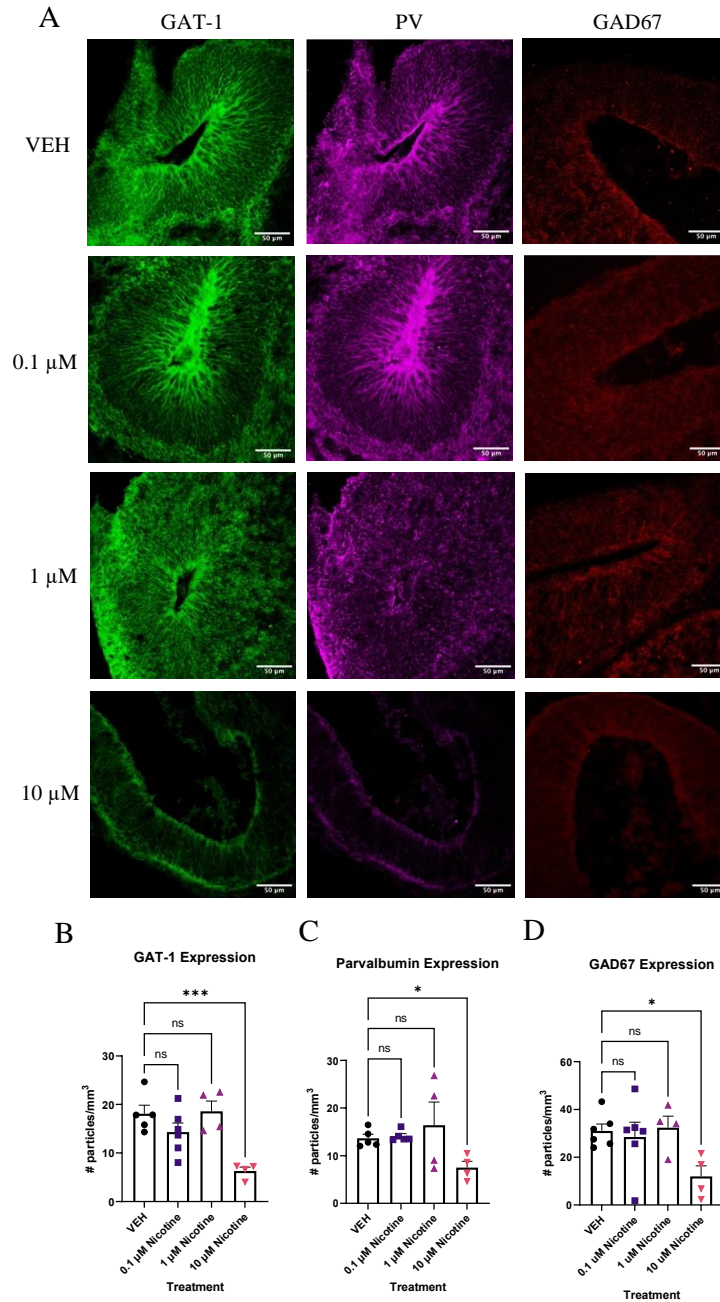


Figure 12: PNE induces significant deficits in markers vital to GABAergic synthesis, transport and signaling on D42. **A**, Immunofluorescent images captured using confocal microscopy of GABA transporter GAT-1 (green), interneuron marker PV (magenta) and GABA synthesis marker GAD67 (red) in brain organoids treated with (0.1, 1 or 10 μM) nicotine or without (VEH) for 14 days. Scale bar = 50 μm. **B-D** Quantification of immunofluorescent images by the number of particles per area (mm³). At the 10 μM dose, organoids exhibited a significant decrease in GAT-1 (**B**), PV (**C**), and GAD67 (**D**) expression compared to VEH. Comparisons were made with one-way ANOVA or Kruskal Wallis followed by Fisher's LSD *post hoc* test. Data are mean +/- SEM, n = 4-6, *** $p < 0.001$, * $p < 0.05$, trending = $p < 0.1$, ns = not significant, $p > 0.05$. n = 1 ROI.

3.1.3.2 Western Blots

In addition to investigating proteins, we sought to examine the expression of specific kinases due to their roles in nicotine exposure and mood and anxiety disorders, that could not be captured using IF. First, we looked at changes in GSK3 β due to its prominent role in neuropsychiatric phenotypes (Figure 13). One-way ANOVA indicated a trending decrease in total GSK3 β (T- GSK3 β) expression ($F_{(2,9)} = 4.058$, $p = 0.554$; Figure 13A), but no effect was seen in its phosphorylated form (pGSK3 β ; Appendix 1; $F_{(2,10)} = 2.655$, $p = 1.1189$). Due to trending significance, a *post hoc* analysis was conducted and demonstrated a significant decrease in T- GSK3 β at 1 ($p = 0.0205$) but not 0.1 μM ($p > 0.05$). Likewise, ERK1-2 dysregulation has been reported following developmental nicotine exposure concomitant with anxiety and depressive-like behaviours. There was also a trending decrease in total ERK1-2 isoform 44 (ERK1; $F_{(2,10)} = 3.550$, $p = 0.0684$; Figure 13B), but not isoform 42 (ERK2; Appendix 1; $F_{(2,10)} = 2.355$, $p = 0.1425$) or its phosphorylated forms (pERK1-2; Appendix 1; $F_{(2,10)} = 0.7249$, $p = 0.5082$ and $F_{(2,10)} = 0.9925$, $p = 0.4044$). Due to trending significance, a *post hoc* analysis was conducted and demonstrated a significant decrease in T-ERK1-2 at 0.1 ($p = 0.0456$) and 1 μM ($p = 0.0392$). These results suggest that nicotine trends towards a decrease in total kinase quantity, but not their phosphorylated counterparts.

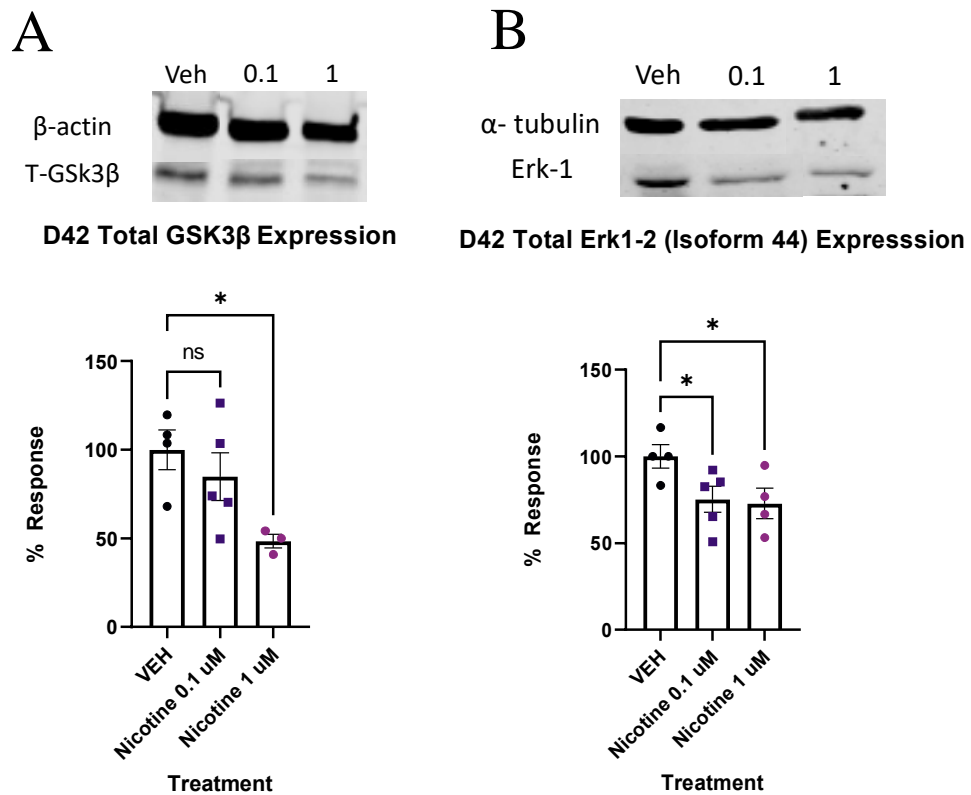


Figure 13: PNE trends towards the dysregulation of kinases implicated in mood/anxiety disorder pathology on D42. **A**, **B**, Representative western blots of whole brain organoids exposed to nicotine (0.1, or 1 μ M) or without (VEH) for 14 days. Organoids treated with nicotine demonstrated a trending decrease in total GSK3 β (**A**) and total ERK1-2 [ERK1; isoform 44] (**B**). Comparisons were made with one-way ANOVA followed by Fisher's LSD *post hoc* test. Data are mean \pm SEM, n = 3-5, *p < 0.05, trending = $p < 0.1$, ns = not significant, $p > 0.05$. n = 1 organoid.

3.1.4 *Transcriptomic Results*

3.1.4.1 *qPCR*

Following IF and western blot analysis of proteins and kinases, we wanted to consider nicotine-induced alterations at the transcriptomic level. Previously, chronic nicotine exposure has been associated with changes in markers pertaining to neural identity and forebrain development. Therefore, we evaluated changes in genes that may play a role in cortical development in conjunction with emotional and behavioural processes (Figure 14). One-way ANOVA suggests that there is a trending increase in empty spiracles homeobox 1 (EMX1; $F_{(2,14)} = 3.716$, $p = 0.0508$; Figure 14A), which is implicated in the formation of the developing cerebral cortex. Due to trending significance, a *post hoc* analysis was performed and revealed a significant increase in EMX1 at 0.1 ($p = 0.0255$) but not 1 μM ($p > 0.05$). Another gene implicated in the maturation of the cortex is forkhead-box G1 (FOXG1). One-way ANOVA also showed a trending increase in FOXG1 in nicotine organoids compared to VEH; $F_{(2,13)} = 3.582$, $p = 0.0577$; Figure 14B). Due to trending significance, a *post hoc* analysis was completed and a significant increase in FOXG1 was shown at 0.1 ($p = 0.0350$) but not 1 μM ($p > 0.05$). The final neural identify marker analyzed was ISL LIM Homeobox 1 (ISL1), a gene vital to embryonic brain development. Analysis with a one-way ANOVA demonstrated that nicotine organoids had a significant decrease in ISL1 compared to VEH ($F_{(2,14)} = 3.898$, $p = 0.0451$; Figure 14C). Follow-up with *post hoc* comparisons determined there was a significant decrease at 0.1 ($p = 0.0145$) but not 1 μM ($p > 0.05$). These results demonstrate that genes underlying cortical development are more sensitive at low doses of nicotine, which suggests that PNE may dysregulate cortical systems that are vital to emotional regulation.

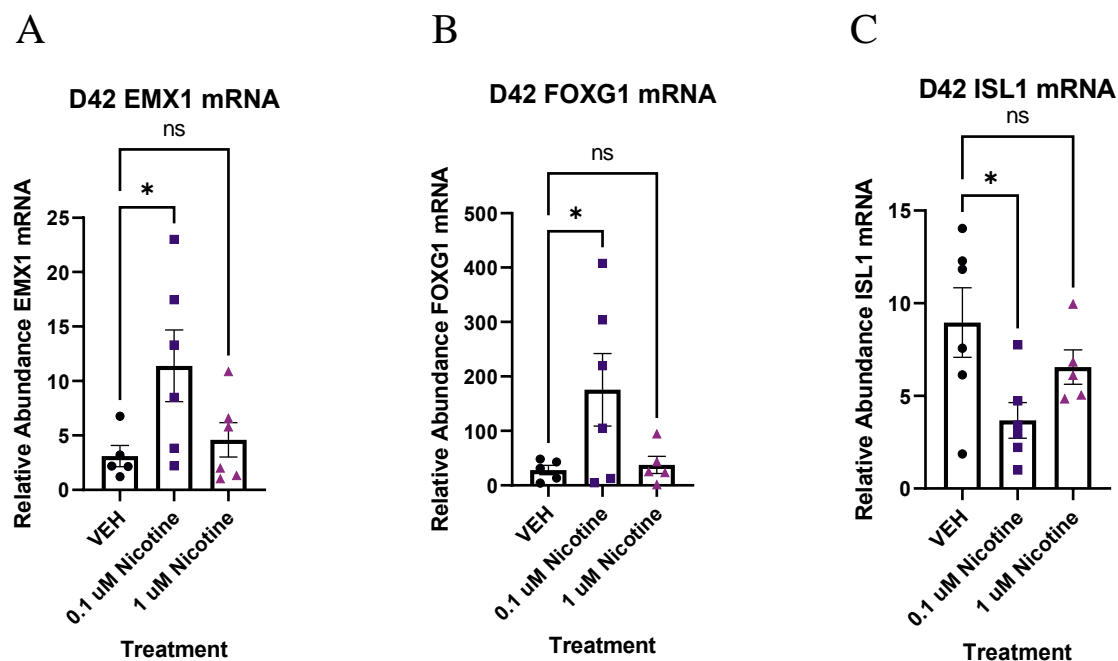


Figure 14: PNE elicits short-term changes in gene expression of various neural identity markers on D42. **A-C** Expression of relative abundance of mRNA of neural identity markers by qPCR in brain organoids exposed to nicotine (0.1, or 1 μ M) or without (VEH) for 14 days. Relative mRNA abundance was calculated by normalizing the marker of interest to the geometric means of 2 housekeeping genes, GAPDH and β -Actin. Organoids demonstrated a trending increase in cortical marker EMX1 (**A**) and forebrain marker FOXG1 (**B**). There is a significant decrease in ISL1, a maker of embryonic development (**C**). Comparisons were made with one-way ANOVA or Kruskal Wallis followed by Fisher's LSD *post hoc* test. Data are mean \pm SEM, n = 5-6, * p < 0.05, trending= p < 0.1, ns = not significant, p > 0.05. n = 1 organoid.

3.1.4.2 RNA-Seq

Both nicotine and mood/anxiety disorders have been known to cause cortical transcriptomic changes in clinical and preclinical studies. Thus, it was of great interest to see if similar DE genes and transcriptomic alterations were reported following PNE in our brain organoids (Figure 15). To gain a sense of sample variation, a multidimensional scale (MDS) plot was created (Figure 15A) and revealed that VEH and nicotine organoids separated more along the x-axis (42%) compared to the y-axis (27%). This indicates that the samples were more different from each other than they are similar. The groups clustered together nicely and separated by treatment, with VEH grouping towards

the top half of the MDS plot and nicotine organoids at the bottom half. The short-term effects of PNE were examined by quantifying the number of DE genes and it was discovered that there were 91 downregulated genes and 40 upregulated genes when comparing nicotine-treated organoids to VEH (Figure 15B). Of these DE genes, when examining the top 20 (10 most downregulated and upregulated genes sorted by log fold change), upregulated genes include NEUROG2, EOMES and the downregulated gene CYP26C1 (Table 10). There were also multiple novel transcripts within the top 20 DE genes (denoted NA in Table 10). Moreover, changes in DE gene expression were summarized using a heat map (Figure 15C), which demonstrated that relative gene expression patterns between VEH and nicotine organoids looked quite different. There appears to be a larger number of genes that are transcribed more in the VEH (red) organoids whereas the nicotine organoids have a larger number of genes that are transcribed less (blue). Alternatively, there appears to be a smaller number of genes that are transcribed less in the VEH organoids whereas the nicotine organoids have a smaller number of genes that are transcribed more.

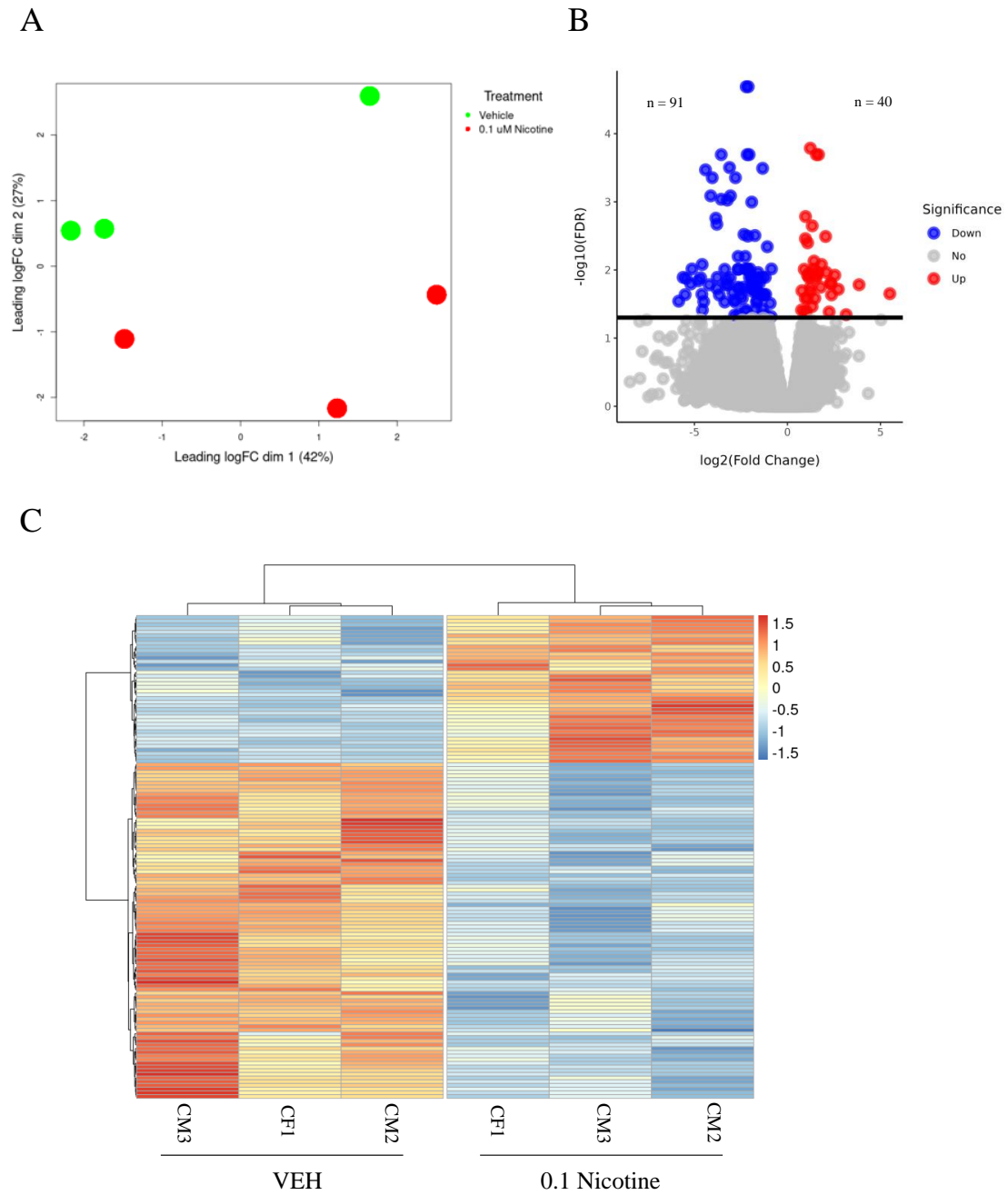


Figure 15: RNA-Seq differential gene expression of D42 VEH and 0.1 μ M nicotine-treated organoids. **A**, Multidimensional scaling (MDS) plot demonstrating the separation of VEH (green) and 0.1 μ M nicotine-treated organoids. **B**, Volcano plot illustrating the number of DE genes in VEH and 0.1 μ M treated organoids. Upregulated genes in red ($n=40$), downregulated genes in blue ($n=91$). **C**, Heatmap of all DE genes for VEH and 0.1 μ M treated organoids. Upregulated genes in red ($n=40$), downregulated genes in blue ($n=91$), $n = 3$ per group, $\text{FDR} \leq 0.05$.

Table 10: Top 20 DE Genes in VEH and Nicotine Organoids

Symbol	Gene	Log Fold Change	P-value	FDR	Significance
ENSG00000145626	UGT3A1	-5.85	1.40E-04	0.029	Down
ENSG00000250511	NA	-5.61	3.32E-05	0.013	Down
ENSG00000187553	CYP26C1	-5.50	1.01E-04	0.023	Down
ENSG00000279607	NA	-5.44	3.84E-05	0.013	Down
ENSG00000158022	TRIM63	-5.20	5.18E-05	0.016	Down
ENSG00000240990	HOXA11-AS	-5.13	1.65E-05	0.009	Down
ENSG00000248329	APELA	-4.79	4.44E-05	0.014	Down
ENSG00000174407	MIR1-1HG	-4.67	3.58E-05	0.013	Down
ENSG00000078399	HOXA9	-4.60	9.60E-05	0.023	Down
ENSG00000253293	HOXA10	-4.59	1.21E-05	0.008	Down
ENSG00000163508	EOMES	2.09	2.28E-05	0.011	Up
ENSG00000112333	NR2E1	2.24	2.29E-04	0.041	Up
ENSG00000178403	NEUROG2	2.31	4.84E-05	0.015	Up
ENSG00000087510	TFAP2C	2.35	5.21E-05	0.016	Up
ENSG00000251621	NA	2.37	1.04E-04	0.023	Up
ENSG00000286232	NA	2.55	2.79E-05	0.012	Up
ENSG00000168453	HR	2.73	7.45E-05	0.019	Up
ENSG00000280222	NA	3.16	2.55E-04	0.045	Up
ENSG00000280409	LINC01101	3.85	5.65E-05	0.016	Up
ENSG00000119614	VSX2	5.51	9.31E-05	0.022	Up

Since many genes in the organoids were differentially expressed following PNE, a functional enrichment analysis was performed to identify categories in which our DE genes were overrepresented (Figure 16). In the organoids, the category that had the highest number of counts, hence the most overrepresentation, was GO BP with 111. This was followed by GO MF with 13 counts (Figure 16A). This implies that nicotine had the greatest impact on genes that partake in biological processes and molecular functions in comparison to other categories such as GO CC, and other databases such as HPA, TF and WP.

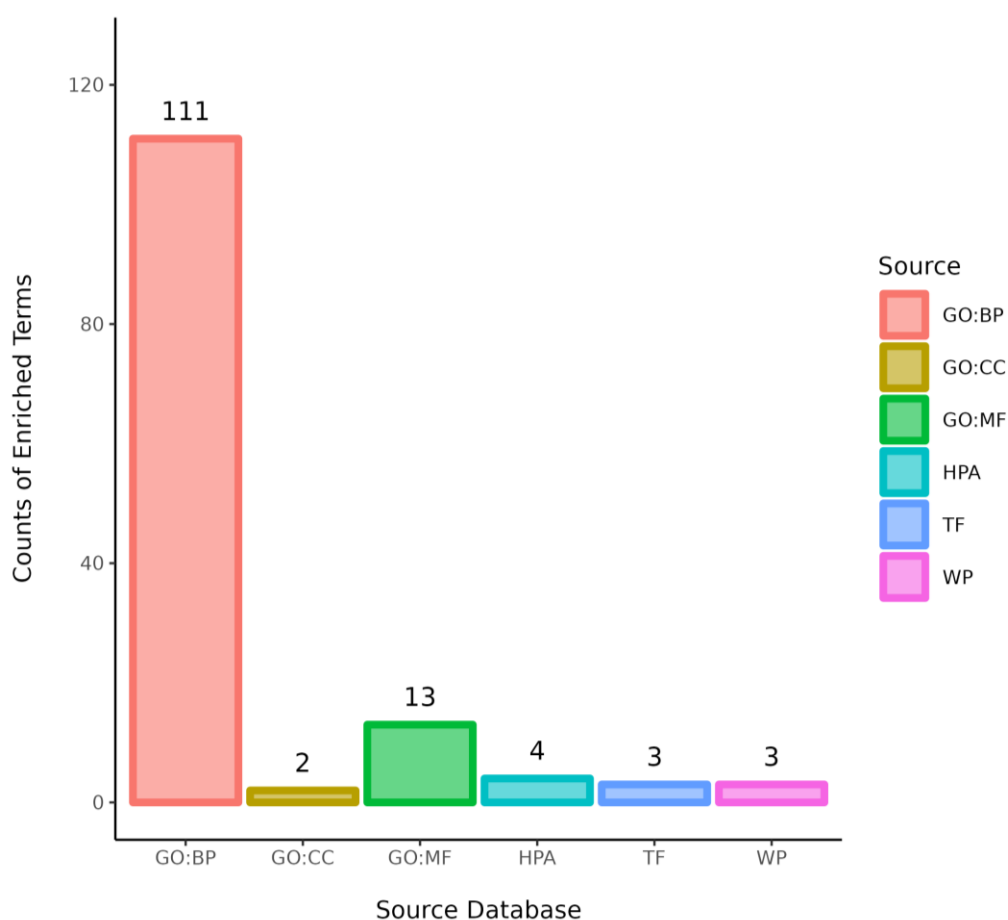
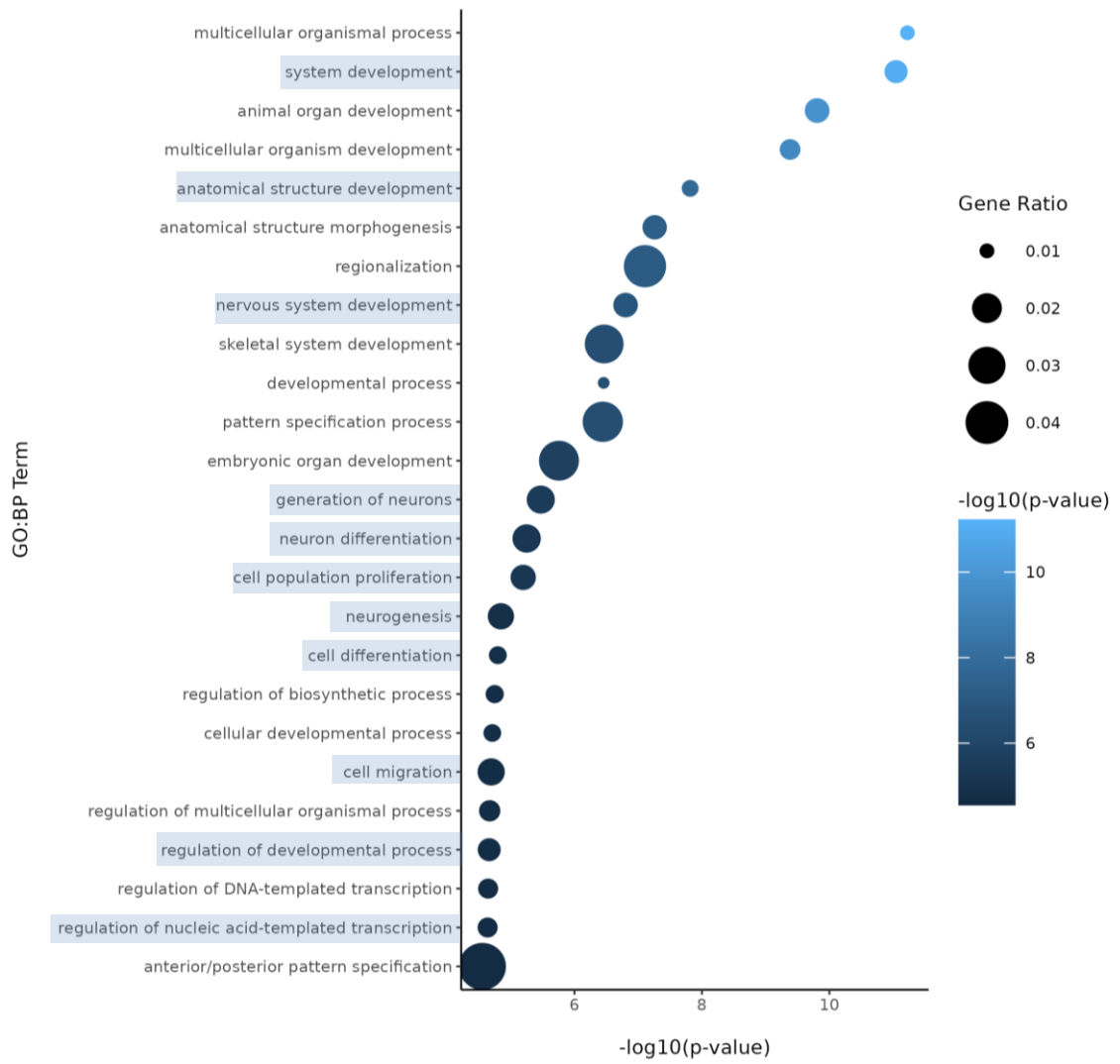


Figure 16: Functional enrichment analysis of D42 VEH and 0.1 μM nicotine-treated organoids. Overrepresented genes are categorized according to their functional characteristics quantified by the number of genes (counts) within a certain category. The categories originate from certain databases and include, from left to right, gene ontology (GO) biological processes (GO BP; 111), GO cellular component (GO CC; 2), GO molecular function (GO MF; 13), Human Protein Atlas (HPA; 4), Transfac (TF; 3) and Wikipathways (WP; 3).

To delve deeper into these classifications, GO analysis was conducted to examine specific terms that were enriched within BP and MF categories (Figure 17). The GO database defines BP as specific physiological or cellular roles carried out by the gene whereas MF describes the molecular activity of a gene but does not provide any spatial information about where these functions occur in the cell. Analysis with GO BP, which had the highest number of counts, reveals terms enriched for several developmental processes (Figure 17A). These terms involve organ ($p = 1.56e-10$), nervous system ($p = 1.58e-7$), and anatomical structural development ($p = 1.53e-8$). Likewise, a significant number of terms referring to neurogenesis ($p = 1.42e-5$) were present, including generation of neurons ($p = 3.37e-6$), neuronal differentiation ($p = 5.62e-6$), and cell migration ($p = 2.02e-5$). Several terms also included various regulatory processes like biosynthetic processes ($p = 1.78e-5$) and regulation of transcription ($p = 2.30e-5$). Like the transcription terms within BP, several terms were rereferring to transcription and DNA binding within the GO MF analysis, which further implicated the impact of PNE on gene transcription (Figure 17B). Integrin ($p = 0.011$), signaling receptor ($p = 0.026$), and transcription factor binding ($p = 2.39e-5$) were also principal terms reported in the MF analysis. Ultimately, the GO analysis elucidated that PNE significantly impacted several BPs and MFs linked to embryonic development, transcription and ultimately gene expression.

A



B

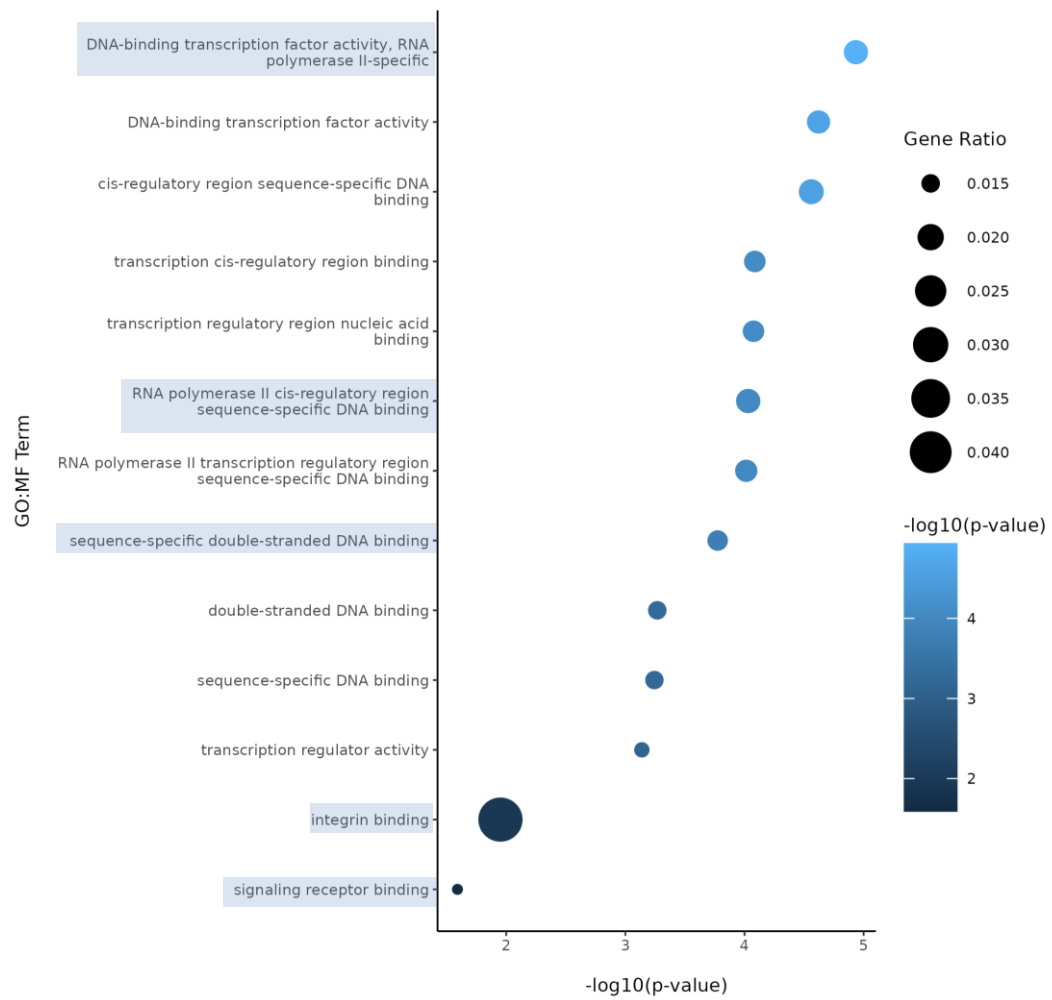


Figure 17: GO terms of overrepresented genes in D42 VEH and 0.1 μM nicotine-treated organoids. **A**, GO BP reveals that PNE elicits alterations in genes within processes such as nervous system development, neurogenesis, and other developmental processes. **B**, GO MF illustrates genes enriched in functions pertaining to DNA, signaling receptor and integrin binding activity. Circle size represents gene ratio and colour represents fold change ($-\log$ of p-value). Blue boxes represent terms of particular interest.

To follow up the GO analysis, we used VarElect to investigate the genetic overlap and phenotype-gene associations of our DE genes between 3 phenotypes of interest: nicotine exposure, anxiety, and depression (Stelzer et al., 2016; Table 11). All DE genes were imported into VarElect and ranked according to the elected phenotype. A list of the top 20 genes for each phenotype was generated. Within the list for each phenotype, 5 genes were consistent: dopamine transporter (SLC6A3), secreted phosphoprotein 1 (SPP1), nerve growth factor receptor (NGFR), histone deacetylase 9 (HDAC9) and insulin-like growth factor 2 (IGF2). These results imply that there is a shared genetic overlap between these phenotypes of interest. This may provide more insight as to how PNE and genetic variation within these genes underlies the incidence of mood and anxiety disorders.

Table 11: Common Top 20 Ranked Genes Related to Nicotine, Anxiety and Depression Phenotypes

Gene Symbol	Description	Rank (1-20) 'Nicotine'	Rank (1-20) 'Anxiety'	Rank (1-20) 'Depression'
SLC6A3	Dopamine transporter	1	1	1
SPP1	Secreted phosphoprotein 1	2	8	17
NGFR	Nerve growth factor receptor	3	13	8
HDAC9	Histone deacetylase 9	6	11	18
IGF2	Insulin-like growth factor 2	9	7	11

3.2 Long-term Effects of PNE- D180 Results

3.2.1 Mood/Anxiety Molecular Biomarker Results

3.2.1.1 Immunofluorescence

PNE has been associated with the emergence of mood and anxiety disorders later in life in children exposed to nicotine during pregnancy. Therefore, we wanted to examine not only the immediate effects of nicotine but long-term outcomes during the later stages of organoid maturation (D180; Figure 18A). Unlike the significant increase reported at D42, at D180 we saw a significant decrease in CTIP2 expression in nicotine organoids ($F_{(2,32)} = 3.476, p = 0.0431$; Figure 18B). *Post hoc* analysis stated a reduction in CTIP2 at both 0.1 ($p = 0.0444$) and 1 μ M ($p = 0.0213$) in comparison to VEH. Due to the short-term effects of PNE at D42, we also examined long-term changes in the dopaminergic receptor, D1R. One-way ANOVA also demonstrated a significant increase in D1R expression in nicotine organoids at D180 ($F_{(2,33)} = 4.349, p = 0.0211$; Figure 18C). *Post hoc* analysis identified an increase at 0.1 ($p = 0.0059$), but not 1 μ M ($p > 0.05$). In addition to alterations in dopaminergic receptors, further long-term dysregulation was also reported in glutamatergic receptors NR2B and mGLUR2/3. At D180, Kruskal-Wallis test revealed a significant upregulation in NR2B ($H_{(2,28)} = 6.136, p = 0.0465$; Figure 18D). A *post hoc* was performed and showed an increase, specifically at 0.1 ($p = 0.0333$), but not 1 μ M ($p > 0.05$). Finally, levels of mGLUR2/3 were significantly increased ($H_{(2,33)} = 11.80, p = 0.0027$; Figure 18E). *Post hoc* comparisons showed that mGLUR2/3 was elevated at both 0.1 ($p = 0.0079$) and 1 μ M ($p = 0.0013$) compared to VEH. Altogether, these results signify long-lasting changes in neuronal differentiation, dopaminergic and glutamatergic proteins that persist until later stages of development following chronic PNE.

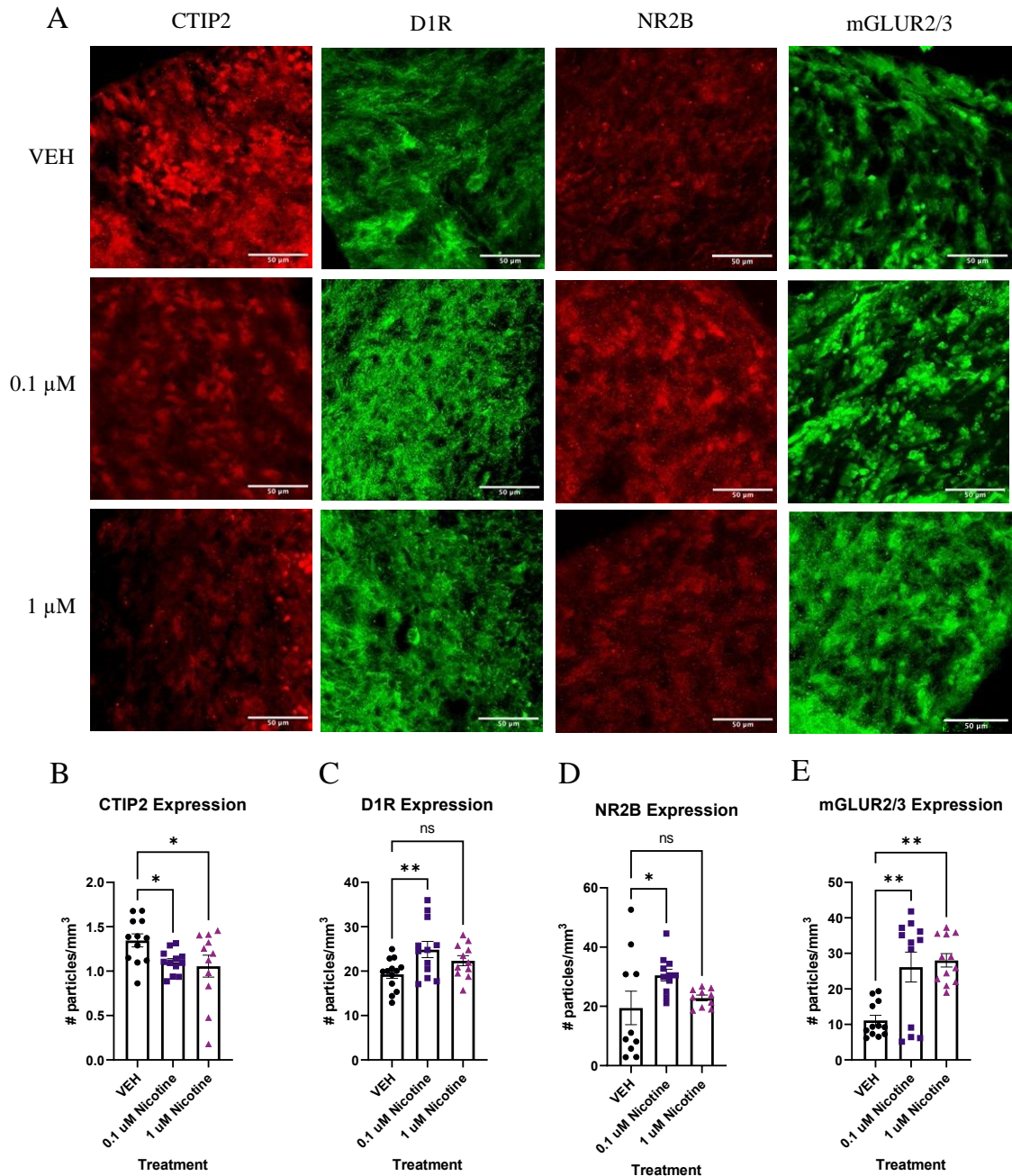


Figure 18: PNE induces long-term alterations in neuronal differentiation, dopaminergic and glutamatergic markers at D180. **A**, Immunofluorescent images captured using confocal microscopy of CTIP2 (red), D1R (green), NR2B (red) and mGLUR2/3 (green) in brain organoids treated with (0.1 or 1 μ M) nicotine or without (VEH) for 14 days. Scale bar = 50 μ m. **B-E** Quantification of immunofluorescent images by the number of particles per area (mm^3). Compared to VEH, organoids treated with nicotine had significantly decreased cortical layer marker CTIP2 levels at 0.1 and 1.0 μ M (**B**). PNE also significantly increased D1R (**C**) and glutamatergic markers NR2B (**D**) and mGLUR2/3 (**E**). Comparisons were made with one-way ANOVA or Kruskal Wallis followed by Fisher's LSD *post hoc* test. Data are mean \pm SEM, $n = 10-14$, $**p < 0.01$, $*p < 0.05$, trending = $p < 0.1$, ns = not significant, $p > 0.05$. $n = 1$ ROI.

3.2.2 *Transcriptomic Results*

3.2.2.1 *qPCR*

To complement our IF protein analysis, the last set of experiments analyzed long-term changes induced by PNE at the level of gene expression. We report that at D180, there was dysregulation in more than one neural identity marker. One-way ANOVA revealed a trend toward significantly decreased T-box brain transcription factor, a cortical pre-plate marker (TBR1; $F_{(2,14)} = 3.535$, $p = 0.0572$; Figure 19A). Due to trending significance, a *post hoc* analysis was completed and revealed a significant decrease in TBR1 at 1 ($p = 0.0207$) but not 0.1 μM ($p > 0.05$). Compared to VEH, there was also a significant decrease in neural progenitor marker EOMES (also known as TBR2; $F_{(2,13)} = 4.441$, $p = 0.0339$; Figure 19B). *Post hoc* analysis was completed and revealed a significant decrease in EOMES at 0.1 ($p = 0.0206$) and 1 μM nicotine ($p = 0.0236$). These results suggest that PNE has an enduring impact on neural and cortical development.

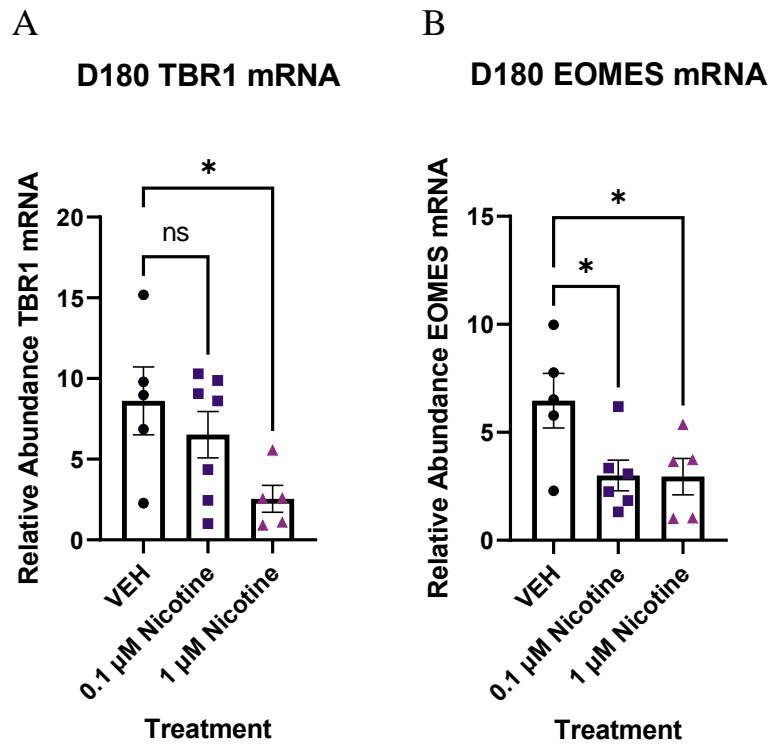


Figure 19: PNE elicits persistent, long-term changes in multiple neural identity markers at D180. **A, B,** Expression of relative abundance of mRNA of neural identity markers by qPCR in mature D180 brain organoids exposed to nicotine (0.1, or 1 μ M) or without (VEH) for 14 days. Relative mRNA abundance was calculated by normalizing the marker of interest to the geometric means of 2 housekeeping genes, GAPDH and β -actin. PNE was associated with a trending decrease in pre-plate marker TBR1 (**A**) and a significant decrease in progenitor marker EOMES (**B**). Comparisons were made with one-way ANOVA or Kruskal Wallis followed by Fisher's LSD *post hoc* test. Data are mean \pm SEM, n = 5-7, * p < 0.05, trending = p < 0.1, ns = not significant, p > 0.05. n = 1 organoid.

Lastly, we quantified any long-term changes in gene expression in glutamatergic, GABAergic, and dopaminergic markers implicated in mood and anxiety disorders (Figure 20). There was evidence of altered GABAergic and glutamatergic markers at D180, with a trending decrease in GRM2, the gene for mGLUR2 ($F_{(2,14)} = 2.796$, $p = 0.0951$; Figure 20A) and a significant decrease in GAD1, the gene for GAD67 ($F_{(2,10)} = 14.55$, $p = 0.0011$; Figure 20B). Due to trending significance in GRM2, a *post hoc* analysis was completed and revealed a significant decrease at 1 ($p = 0.0447$) but not 0.1 μM ($p > 0.05$). *Post hoc* comparisons were also performed for GAD67 and showed a significant decrease at 0.1 μM ($p = 0.0007$) compared to VEH. There was no significant effect at 1 μM ($p > 0.05$). Consistent with dopaminergic perturbations at D42, one-way ANOVA described a trending decrease in D1R at D180 compared to VEH ($F_{(2,14)} = 3.256$, $p = 0.0690$; Figure 20C). Since a trending significance was reported, *post hoc* comparisons were done and indicated a significant decrease at 1 ($p = 0.0231$) but not 0.1 μM ($p > 0.05$). These transcriptomic results signify that PNE unremittingly modifies neurotransmitter systems into later stages of neurodevelopment.

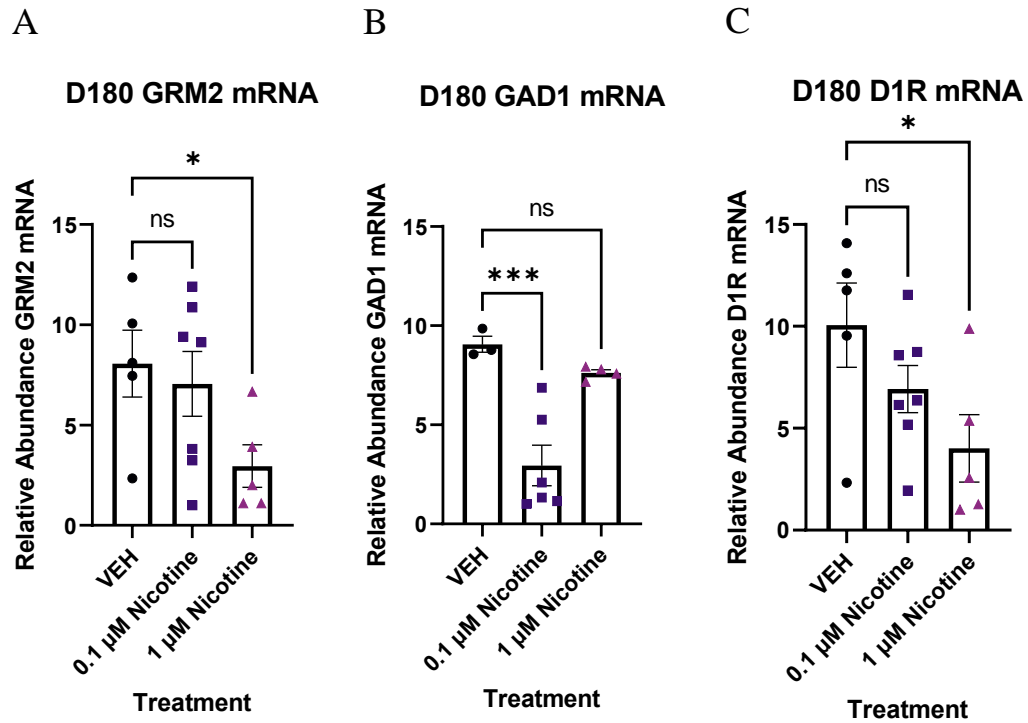


Figure 20: PNE elicits long-term changes in glutamatergic, GABAergic and dopaminergic markers implicated in mood and anxiety disorders at D180. **A-C** Expression of relative abundance of mRNA by qPCR in mature D180 brain organoids exposed to nicotine (0.1, or 1 μM) or without (VEH) for 14 days. Relative mRNA abundance was calculated by normalizing the marker of interest to the geometric means of 2 housekeeping genes, GAPDH and β -actin. **A**, PNE induced a trending, dose-dependent decrease in glutamatergic receptor GRM2. **B**, PNE significantly downregulated the expression of GABA synthesis marker GAD1. **C**, There was a significant decrease in D1R expression following PNE. Comparisons were made with one-way ANOVA or Kruskal Wallis followed by Fisher's LSD *post hoc* test. Data are mean \pm SEM, $n = 3-7$, $***p < 0.001$, $*p < 0.05$, trending = $p < 0.1$, ns = not significant, $p > 0.05$. $n = 1$ organoid.

4 Discussion

Long before the development of ENDS, nicotine has been demonstrated to disturb fetal developmental programming and result in long-lasting behavioural and emotional impairments (Wickström, 2007). Specifically, the association between developmental nicotine exposure and the emergence of mood and anxiety behaviours has been reported in various clinical and preclinical studies, including research in our lab (Hudson et al., 2021; Jobson et al., 2019; Laviolette, 2021). However, the use of cerebral organoids to explicitly model PNE presents a unique human-derived platform to build on prior research findings and bypass existing experimental limitations. Moreover, the relationship between PNE and the development of specific mood and anxiety molecular phenotypes remains elusive and has yet to be explored in a cerebral organoid model. In correspondence with previous research, chronic exposure to physiologically relevant doses of nicotine had widespread neuronal, molecular, and transcriptomic effects on our organoids (Notaras et al., 2021; Y. Wang et al., 2018). We report that chronic PNE (0.1-10 μ M) triggered apoptotic cell death and impacted the normal expression of various neural identity markers at D42 and D180. In terms of nicotine's effect on its target receptor, there was short-term upregulation of α_4 and β_2 nAChR subunits. However, PNE had no significant effect on α_7 expression. PNE also dysregulated the expression of dopaminergic receptors, with long-lasting alterations in D1R expression persisting until D180. Marked downregulation of GSK3 β and ERK1-2, kinases involved in the pathophysiology of mood and anxiety disorders, was also observed. However, this was only an immediate effect and dissipated with time. With regards to other neurotransmitter systems, PNE affected glutamatergic/GABAergic markers of interest, which implies shifted E/I balance in the cortex and remained until the later stages of organoid maturation. Finally, RNA-Seq revealed substantial transcriptomic changes in organoids treated with 0.1 μ M nicotine. Numerous BPs and MFs were differentially expressed, specifically terms concerning nervous system development, neurogenesis, and transcription activity.

4.1 PNE Dysregulates Aspects of Neurogenesis and Alters the Expression of Neural Identity Markers in the Cortex

Nicotine has previously demonstrated its capacity to impair many facets of fetal neurogenesis through nAChR-mediated signaling and underlie the manifestation of abnormal neurobehavioral outcomes. This includes changes in proliferation, neuronal differentiation, and apoptotic cell death, (Aoyama et al., 2016; Dwyer et al., 2009; A. M. Smith et al., 2010; Y. Wang et al., 2018). For instance, PNE has also been found to decrease neuron number in numerous regions including the hippocampus and cortex (A. M. Smith et al., 2010). This has been noted previously in preclinical models where PNE has disrupted the cell cycle of neural progenitors, which resulted in less cortical glutamatergic neurons, and impaired the proliferation of undifferentiated progenitors in the mouse and rat neocortex (Aoyama et al., 2016; Takarada et al., 2012). With regards to differentiation, accelerated neuronal differentiation has been reported following chronic exposure of undifferentiated neural progenitors to nicotine (Takarada et al., 2012). To further support this claim, another group, using organoid-on-a-chip technology, performed immunohistochemical and transcriptomic analysis of organoids chronically exposed to 1 and 10 μ M of nicotine (Y. Wang et al., 2018). They reported increased expression of CTIP2, an early-born neuronal marker, in nicotine-treated organoids compared to controls. This was accompanied by no change in the number of neural progenitor cells. This suggests nicotine disrupted cortical neuronal layering by the induction of premature differentiation. Finally, cleaved caspase 3, a member of the caspase family implicated in neuronal death in neural syndromes, was significantly increased in a dose-dependent manner in these organoids (Y. Wang et al., 2018). Despite nicotine's reported effect on proliferation, we report no significant change in proliferation following PNE (Appendix 3). However, this may be a result of nicotine administration outside of the main proliferation window and the timing of organoid collection (Y. Wang et al., 2018). However, Wang's descriptions of increased differentiation and apoptosis do align with our present IF findings since we report that PNE significantly increased the expression of cleaved caspase 3 and CTIP2 at D42. We did however see a significant decrease in CTIP2 by the D180 time point, which demonstrates long-term changes in neuronal development.

Apart from alterations in neurogenesis, PNE also has been found to impact the expression of various categories of neural identity markers. For example, the same study by Wang and colleagues (2018) reported differential expression of neural identity markers in their organoids following chronic PNE. They described decreased expression of preplate marker TBR1, forebrain marker FOXG1 and increased expression of hindbrain marker ISL1 (Y. Wang et al., 2018). In fact, changes in certain neural identity markers can induce behavioural deficits in the offspring. The function of cortical forebrain marker EMX1 is suggested to play a role in emotional processes (Cao & Li, 2002). A study conducted by Cao and Li (2002) determined that mice deficient in EMX1 displayed lower levels of depressive behaviours as seen by reduced immobility time in the forced swim test. These mice also experienced decreased anxiety in the light/dark box and elevated plus maze (Cao & Li, 2002). Another example is EOMES, or TBR2, a neural progenitor marker that is decreased in the PFC of mice exposed to PNE (Aoyama et al., 2016). These mice also experienced cognitive and emotional deficits in adulthood (Aoyama et al., 2016). Our qPCR data did confirm significant increases in EMX1 and FOXG1 alongside a significant decrease in ISL1 at D42. This suggests dysregulated development of neuronal populations comprising the forebrain and hindbrain. Additionally, we report significant reductions in TBR1 and EOMES present at D180 signifying long-term changes in cortical development. Overall, our qPCR results insinuate PNE-induced significant dysregulation of neurogenesis and numerous cortical markers that persist until D180. Thus, examining these alterations underlying cortical development may help to understand the impact of PNE on the behavioural dysfunctions of the offspring when these developmental pathways mature.

4.2 PNE Has Short-term Effects on α_4 and β_2 nAChR Subunit Expression, but not α_7

$\alpha_4\beta_2$ and α_7 are the most abundant nAChRs in the cortex and are implicated in various cognitive and attentional functions (Alkam & Nabeshima, 2019; Livingstone et al., 2010). Results from preclinical rodent models have revealed that chronic nicotine exposure elicits an increase in nAChR populations in the fetal cortex, as it does in adult rats (Dwyer et al., 2009). Specifically, in the rat cortex and hippocampus, chronic PNE from

gestational day 7 to 21 revealed elevated α_4 , α_7 and β_2 mRNA expression (Shacka & Robinson, 1998). This has also been seen in α_4 and α_7 mRNA of human fetuses exposed to nicotine during pregnancy (Falk et al., 2005). Our IF results revealed significantly increased α_4 and β_2 nAChR protein expression following PNE at D42. Interestingly, there was no change in α_7 expression which was unexpected due to its role in regulating cortical glutamate release (Livingstone et al., 2010). This insignificant effect in α_7 was especially surprising given our reports of immediate and long-term perturbations in GABA receptor expression in our IF and qPCR analyses. However, as mentioned previously, α_7 nAChR subunits desensitize more rapidly compared to α_4 and β_2 and have a lower affinity for nicotine. This could be a plausible explanation for differences in expression levels between the different subunits, but further research is required to further elucidate this mechanism (Dwyer et al., 2009; Fenster et al., 1999; Mcgrath-Morrow et al., 2020). Our qPCR results also indicate no changes in α_7 or β_2 subunit expression at D180 (Appendix 4). This may be a result of the receptors returning to baseline after chronic exposure. For example, *in vitro*, β_2 nAChRs levels can recover soon after nicotine washout periods (Picciotto et al., 2008). This suggests that PNE selectively upregulates α_4 and β_2 nAChR subunits early in gestation which can have functional implications in the development of mood and anxiety disorders (Saricicek et al., 2012). For instance, abnormalities in $\alpha_4\beta_2$ nAChR expression and function, specifically in the PFC and hippocampus, may contribute to these disorders due to their ability to modulate GABA release (Fogaça & Duman, 2019; Freund et al., 1988; Kutlu & Gould, 2015; Lu et al., 1992). Therefore, altered nAChR levels could lead to an imbalance in GABAergic neurotransmission, alter mood and anxiety-related brain circuitry and lay the foundation for altered E/I levels previously reported in the literature (Fogaça & Duman, 2019; Sequeira et al., 2009). In summary, to our knowledge, the specific timing that these nAChRs appear in development has yet to be identified in cerebral organoids, which further characterizes our PNE model. This newfound discovery can assist with unravelling the correlation between the temporal specificity of nicotine exposure on the circuitry of the developing fetal brain and the future emergence of mood and anxiety behaviours.

4.3 PNE Dysregulates Dopaminergic Signaling and Unremittingly Perturbs D1R Expression

In comparison to other neurotransmitter systems, the effect of PNE on dopaminergic receptors in the fetal brain is unclear. However, during a preclinical model of adolescent nicotine exposure, another critical period of neurodevelopment, rodents chronically exposed to nicotine demonstrated significantly less D1R expression levels in the PFC compared to VEH (Jobson et al., 2019; Laviolette, 2021). This was concurrent with no significant changes in D2R expression. Likewise, other animal studies have demonstrated dopaminergic hypofunction in the neocortex resulting from PNE as well as decreased dopaminergic metabolites (Ernst et al., 2001; Muneoka et al., 1997, 1999). Dopamine has been suggested to be involved in anxiety-like behaviours and is involved in the regulation of emotion, therefore this hypofrontality is also linked to the pathology of anxiety and depression (Muneoka et al., 1999; Zarrindast and Khahpai 2015). Our D42 IF findings are consistent with previous reports of decreased D1R expression following nicotine exposure. Unlike previous preclinical studies that have failed to detect differences in D2R following nicotine exposure, we also report significant decreases in D2R at D42. Interestingly, our qPCR data revealed that reductions in D1R, but not D2R (Appendix 4), persist until D180. This was concomitant with an increase in D1R protein expression. This may suggest that D1R is more vulnerable long-term to the effects of PNE in comparison to D2R and altered dopaminergic signaling persists past the point of initial exposure. Knowing that neurotransmitter systems occupy trophic roles in the development of the CNS, it is important to characterize when these receptors are susceptible to manipulation in the organoid model and in turn how they could evoke long-term neurodevelopmental consequences for the offspring (Wickström, 2007).

4.4 PNE Has Short-term Effects on Total Expression of Specific Kinases Implicated in Mood and Anxiety Disorders

In recent years, many studies have shed light on the central role of ERK1-2 and GSK β signaling in mood and anxiety-related disorders. Interestingly, we reported long-term alterations in D1R expression, and this receptor is known to interact with ERK1-2 in brain regions associated with mood and anxiety control like the PFC (Jobson et al.,

2019). Indeed, rats chronically exposed to nicotine have demonstrated reductions in D1R and increased pERK1-2 alongside anxiety and depressive phenotypes (Jobson et al., 2019). Alterations in ERK1-2 have also been noted in human postmortem and comparative transcriptomic studies (Dwivedi et al., 2001, 2009; Malki et al., 2015). For instance, the evaluation of brain tissue from depressed suicide victims reveals depletion of both MAPK and ERK1-2 in the hippocampus and PFC (Dwivedi et al., 2001, 2009). Moreover, a transcriptomic study aiming to identify genetic markers of MDD compared rat and human postmortem PFC tissue and found that 80% of convergent biomarkers were associated with alterations in the ERK signaling pathway (Malki et al., 2015). However, unlike Jobson et al. (2019) who reported no change in T-ERK1-2 and increased pERK1-2, we report no change in pERK (Appendix 1) but a decrease in T-ERK1-2 at D42. Furthermore, by D180 there were no significant differences seen in either pERK or T-ERK1-2 (Appendix 2). Reductions in total protein but no change in phosphorylation could be a result of many things including decreased gene expression, increased protein degradation or altered post-translational modifications (Chang & Karin, 2001; Roskoski, 2012; Shaul & Seger, 2007). The differences in our results from previous studies could also be a result of differing developmental periods of nicotine exposure (prenatal versus adolescence). Our evidence supports short-term alterations in T-ERK1-2 levels following PNE, but further investigation is required to assess the underlying cause for these specific modifications.

On a similar note, since the discovery of lithium as a GSK3 inhibitor, there has been much discussion surrounding its contribution to the etiology of mood disorders (Duda et al., 2020). Although many current treatment regimens for MDD operate based on the monoaminergic hypothesis of depression and indirectly enhance GSK3 β inhibition, antidepressive effects are also mediated by GSK3 β inhibitors, which further involve the kinase in MDD (Duda et al., 2020). In addition to treatment potential, studies have suggested that dysregulation of GSK3 β is a molecular biomarker of mood and anxiety disorders (Hudson et al., 2021; Laviolette, 2021). A recent preclinical study demonstrated that rats chronically exposed to nicotine during adolescence, but not adulthood, had increased expression of GSK3 β in the nucleus accumbens compared to VEH. This was also accompanied by increased ERK1-2, reductions in D1R and mood and anxiety

phenotypes (Hudson et al., 2021). This study also demonstrated that these adverse behavioural phenotypes could be mitigated through pharmacologically reversing the dysregulation of GSK3 β that occurred from nicotine exposure (Hudson et al., 2021). As seen with ERK expression, we report reduced T-GSK3 β but no change in phosphorylation at D42 (Appendix 1). These short-term alterations were also dissipated by D180 (Appendix 2). This does differ from the results of Hudson et al. 2021, but this could be a result of the differences between species, disparities in developmental programming and regional specificity of brain tissue between the experimental models. The functional roles of these kinases are not completely understood, and further research is required to comprehensively understand their involvement in nicotine-induced dysregulation and mood and anxiety phenotypes.

4.5 PNE Persistently Disrupts GABA and Glutamate Markers associated with Cortical E/I Balance

In tandem with dopaminergic alterations, other cortical biomarkers of MDD resulting from excess cholinergic signaling are hyperglutamatergia and decreased GABAergic signaling, which subsequently disrupts E/I balance (Dwyer et al., 2009; Fogaça & Duman, 2019; Hashimoto, 2009; Livingstone et al., 2010; Martin et al., 2020; Nobis et al., 2020). Increased glutamate levels have been reported in postmortem cortical tissue of individuals with MDD suggesting aberrant glutamatergic transmission underlying features of MDD (Hashimoto, 2009). In recent years, animal studies have reported antidepressant effects resulting from Ketamine, an NMDA antagonist, in reducing immobility time in the forced swim test and shock-induced behavioural changes (Chaturvedi et al., 1999; Hashimoto, 2009; Yilmaz et al., 2002). Notably, clinical studies have demonstrated the antidepressant effect of ketamine, in treatment-resistant MDD and are investigating other glutamatergic receptors (e.g., AMPA, mGLURs) as additional therapeutic targets (Hashimoto, 2009; Zarate et al., 2006). In terms of reduced inhibitory synaptic transmission, marked reductions in GABA synthesis enzymes and decreased size and density of GABAergic interneurons were found in the dorsolateral PFC of depressed individuals (Fogaça & Duman, 2019; Karolewicz et al., 2010). Likewise, a mouse model of PNE confirmed a shift towards excitation in the E/I balance, denoted by

a dose-dependent decrease in cortical GABAergic neurons (Martin et al., 2020). Similar findings of reduced GABA and receptor functioning have been described in preclinical stress models (Sanacora, Mason, et al., 1999). Our results are consistent with previously reported GABA/glutamate dysfunction in MDD. Our IF analysis exhibits GABAergic deficits, specifically decreased GAT-1, PV and GAD67 at D42 and increased expression of glutamatergic markers NR2B and mGLUR2/3 at D180. Our D180 qPCR results also reveal alterations in GRM2 and GAD1 which indicates long-lasting changes are occurring at the level of gene transcription. Nonetheless, further research is needed to acquire functional data to assess changes in neuronal firing, GABAergic and glutamatergic neurotransmission to strengthen the causal link between nicotine-related errors in E/I neurotransmission and phenotypes of mood and anxiety disorders.

4.6 Nicotine Organoids Endure Significant Transcriptomic Changes in Genes Pertaining to Nervous System Development, Neurogenesis and Transcription Regulation

Research has shown that PNE significantly impacts aspects of nervous system development such as the generation, proliferation, differentiation, and migration of neurons (Mizrak, 2019; Y. Wang et al., 2018). This has been documented in RNA-Seq of postmortem PFC tissue from fetuses of smoking mothers that revealed increased expression of genes involved in neurodevelopment (Semick et al., 2020; Sherafat et al., 2021). This exposure to nicotine underlies changes in neurotrophic factors, such as brain-derived neurotrophic factor (BDNF) and nerve growth factor (NGF) that are essential for the growth and survival of neurons (Lauterstein et al., 2016). In turn, these modifications have the capacity to influence the human genome and epigenome, which may increase the occurrence of MDD, and suggests a genetic overlap between nicotine exposure and mood disorders (Dome et al., 2010; Lauterstein et al., 2016). For example, there is evolving evidence that suggests abnormal transcriptional regulation is a crucial component of mood disorders (Hobara et al., 2010). Mainly, a theory surrounding the evolution of MDD is that chronic stress induces alterations in the transcriptional regulation of growth factors, which leads to impaired neurogenesis (Malki et al., 2015). Similar findings were reported in human postmortem brain tissue using RNA-Seq where significant DE genes were enriched in pathways relating to neurodevelopment such as

NGF, neurotrophin, and integrin signaling (Yoshino et al., 2021). There were also significant genes in specific function and disease pathways such as psychological disorders and nervous system development (Yoshino et al., 2021). Furthermore, repeated nicotine exposure can exert various epigenetic modifications such as the activity of nicotine-responsive transcription factors and inhibition of HDACs, which greatly change gene expression (Volkow, 2011). Changes in HDACs are also seen in MDD, with Hobara et al. (2010) revealing decreased HDAC9 mRNA expression in mood disorder patients compared to nonpsychiatric controls (Hobara et al., 2010). This further associates transcriptional alterations as a focal point within mood disorders. Our RNAseq results are consistent with previous findings in transcriptional PNE and MDD studies, with many of our GO BP terms representing nervous system development, neurogenesis, and regulation of developmental/transcriptional processes. As for GO MF, all the terms were related to, transcription factor activity, DNA, integrin or signaling receptor binding. This provides a better understanding of how nicotine influences these MFs that are also altered in mood and anxiety disorders. We also saw 5 overlapping DE genes between nicotine, anxiety and MDD phenotypes: SLC6A3, SPP1, NGFR, HDAC9 AND IGF2. These genes were altered following PNE but also have a role in neurodevelopment, mood and anxiety disorders or interact with genes closely related to these phenotypes (Fan et al., 2020; Hobara et al., 2010; Lauterstein et al., 2016; Y. W. Luo et al., 2015; Rafikova et al., 2021). Comprehensively, our results strengthen the genetic association between neurodevelopmental and transcriptional abnormalities resulting from PNE and the basis of mood and anxiety molecular phenotypes. Future efforts are required to fully validate and characterize novel DE transcripts, their underlying function in the cortical transcriptome and their role in neuropsychiatric disorders.

4.7 Limitations

Despite many advantages of the organoid model, there are some limitations in the current study. To begin, I had a much smaller sample size than I originally anticipated for each experiment and was unable to analyze any potential sex differences between the male and female lines. In the beginning, I was expecting to have 6 control lines to work with and have a duplicate organoid within each condition for every experiment (e.g., 2 organoids

for CM2-V etc.). However, as mentioned previously, 3 of my lines (CM1, CF2, CF3) did not differentiate properly. In 2 of these lines, this was most likely a result of chronic treatment with antibiotics following repeated bacterial/fungal contamination. I noticed after H&E staining and IF imaging, there were zero VL regions in these lines, whereas the other 3 has multiple neural rosettes. From this point forward, I decided to exclude these lines since I did not think they would be comparable to the others and would mask the potential effects of the nicotine. After this initial decrease in sample size, I had some issues with RNA extraction that resulted in many unusable samples. Luckily, I had a few extra to spare, but since we were unable to grow more organoids, I was left to work with the samples I had at the time. Future work should be focused on growing a larger number of organoids from the good lines to increase sample size and ordering replacement lines should be considered to allow for sex-specific comparisons.

Additionally, unlike the human brain which contains a vast circulatory system to distribute blood and nutrients, this model lacks meninges and vasculature, which restricts the growth and size potential of the organoids (Lancaster et al., 2013; Lancaster & Knoblich, 2014). In turn, this limits the diffusion of oxygen and availability of nutrients within the inner layers of the organoid and results in the formation of a necrotic core over time, with only healthy neurons occupying the outer layers (Lancaster, 2018).

Finally, despite normalization with controls in each experiment, there is considerable variability between organoids in the same batch and even organoids from the same cell line due to limited control of tissue heterogeneity. In our unguided protocol, this can produce organoids with a wide range of sizes and morphologies, which can influence the reliability of results (Kim et al., 2021; Lancaster et al., 2013; Lancaster & Knoblich, 2014). A way to try and mitigate the issue is by increasing the sample size and removing significant outliers. However, regardless of its benefits to support organoid growth and development, the variability may be an innate issue resulting from the Matrigel basement membrane (Kim et al., 2021).

4.8 Future Directions

Future directions for this project could be implementing additional experimental aims within this particular protocol (Lancaster et al., 2013) or increasing the specificity of the tissue using a guided method. We performed all molecular techniques at both time points apart from RNA-Seq, which was only performed immediately following PNE (D42). Considering we saw long-term differences between nicotine-treated and VEH organoids using IF and qPCR, it would be worthwhile to follow up with RNA-Seq to investigate more thorough transcriptomic changes at D180. These transcriptomic alterations could also be assessed at a more detailed level using single-cell RNA-seq. This technique would provide a richer analysis of individual cells, specific cell populations and give insight regarding tissue heterogeneity within the organoids (Guo et al., 2019). Also, to better capture alterations occurring within neurotransmitter systems affected by mood and anxiety disorders, matrix-assisted laser desorption/ionization (MALDI) can be used. MALDI mass spectrometry imaging is a label-free technique used to image the localization of biomolecules in a broad variety of samples and has been used previously to quantify changes in neurotransmitters and their metabolites like dopamine, serotonin, glutamate, and GABA (Johnson et al., 2020; Y. Wang & Hummon, 2021). To build on the plethora of structural data, data obtained from a multielectrode plate or patch clamp electrophysiology would also be beneficial to assess the function of individual neurons of network firing properties (Passaro & Stice, 2021). Utilizing these techniques in tandem to identify nicotine-related changes in neurotransmission, neuron firing and assessing their consistency with molecular markers of mood and anxiety disorders would be extremely valuable.

Other directions to elevate this project would be the use of a guided protocol to generate tissue specific to brain regions involved in mood and anxiety control, such as cortical or forebrain organoids (Kim et al., 2021; Mariani et al., 2015; Qian et al., 2016). The Lancaster protocol produces whole-brain organoids, comprised of forebrain and hindbrain tissue, which lack regional specificity (Lancaster et al., 2013). In experiments where we homogenized the whole organoid, like western blots and qPCR, it would be more comparable to other techniques like IF, where only cortical regions were analyzed.

Overall, it would be beneficial for increased regional precision and consistency between organoids (Kim et al., 2021). Moreover, a guided protocol could be taken one step further to form assembloids, which are assembled organoids from different brain regions (Miura et al., 2020). This would allow us to better understand how PNE impacts specific signaling pathways and neuronal activity between neighbouring brain regions and how this underlies neuropsychiatric syndromes (Miura et al., 2020).

4.9 Conclusions

Using cerebral organoids, my thesis aimed to validate a novel application of a human-derived *in vitro* model, to better comprehend the emergence of neurodevelopmental abnormalities and the manifestation of neuropsychiatric molecular phenotypes resulting from chronic PNE. The advent of iPSC technology coupled with molecular analyses provided a molecular framework to examine long-lasting alterations in fetal neurodevelopment, modifications in receptors/kinases vital to mood and anxiety pathophysiology and changes to the cortical transcriptome. Understanding how environmental drug exposure during pregnancy alters early cortical development and the resulting changes in biomarkers may bring awareness to the dangers of ENDS and provide a basis for the etiology of mood and anxiety disorders in human-based models. In the future, this will provide a platform for patient-specific treatments and finding appropriate and efficacious interventions to improve the outcomes of the offspring, who without choice, struggle with these neuropsychiatric disorders long-term.

References

- Adkison, S. E., O'Connor, R. J., Bansal-Travers, M., Hyland, A., Borland, R., Yong, H. H., Cummings, K. M., McNeill, A., Thrasher, J. F., Hammond, D., & Fong, G. T. (2013). Electronic nicotine delivery systems: International Tobacco Control Four-Country Survey. *American Journal of Preventive Medicine*, 44(3), 207–215. <https://doi.org/10.1016/j.amepre.2012.10.018>
- Agboola, O. S., Hu, X., Shan, Z., Wu, Y., & Lei, L. (2021). Brain organoid: a 3D technology for investigating cellular composition and interactions in human neurological development and disease models in vitro. In *Stem Cell Research and Therapy* (Vol. 12, Issue 1). BioMed Central Ltd. <https://doi.org/10.1186/s13287-021-02369-8>
- Albert, P. R. (2015). Why is depression more prevalent in women? In *Journal of Psychiatry and Neuroscience* (Vol. 40, Issue 4, pp. 219–221). Canadian Medical Association. <https://doi.org/10.1503/jpn.150205>
- Alkam, T., & Nabeshima, T. (2019). Prenatal nicotine exposure and neuronal progenitor cells. In *Neuroscience of Nicotine: Mechanisms and Treatment* (pp. 41–48). Elsevier. <https://doi.org/10.1016/B978-0-12-813035-3.00006-X>
- Andres, R. L., & Day, M. C. (2000). Perinatal complications associated with maternal tobacco use. *Seminars in Neonatology*, 5(3), 231–241. <https://doi.org/10.1053/siny.2000.0025>
- Andrews, M. G., & Nowakowski, T. J. (2019). Human brain development through the lens of cerebral organoid models. In *Brain Research* (Vol. 1725). Elsevier B.V. <https://doi.org/10.1016/j.brainres.2019.146470>
- Aoyama, Y., Toriumi, K., Mouri, A., Hattori, T., Ueda, E., Shimato, A., Sakakibara, N., Soh, Y., Mamiya, T., Nagai, T., Kim, H. C., Hiramatsu, M., Nabeshima, T., & Yamada, K. (2016). Prenatal Nicotine Exposure Impairs the Proliferation of Neuronal Progenitors, Leading to Fewer Glutamatergic Neurons in the Medial Prefrontal Cortex. *Neuropsychopharmacology*, 41(2), 578–589. <https://doi.org/10.1038/npp.2015.186>
- Arlotta, P., & Pasca, S. P. (2019). Cell diversity in the human cerebral cortex: from the embryo to brain organoids. In *Current Opinion in Neurobiology* (Vol. 56, pp. 194–198). Elsevier Ltd. <https://doi.org/10.1016/j.conb.2019.03.001>
- Baik, J. H. (2013). Dopamine signaling in reward-related behaviors. In *Frontiers in Neural Circuits* (Vol. 7, Issue OCT). Frontiers Media S.A. <https://doi.org/10.3389/fncir.2013.00152>

- Banderali, G., Martelli, A., Landi, M., Moretti, F., Betti, F., Radaelli, G., Lassandro, C., & Verduci, E. (2015). Short and long term health effects of parental tobacco smoking during pregnancy and lactation: A descriptive review. In *Journal of Translational Medicine* (Vol. 13, Issue 1). BioMed Central Ltd. <https://doi.org/10.1186/s12967-015-0690-y>
- Beyer, D. K. E., Mattukat, A., & Freund, N. (2021). Prefrontal dopamine D1 receptor manipulation influences anxiety behavior and induces neuroinflammation within the hippocampus. *International Journal of Bipolar Disorders*, 9(1). <https://doi.org/10.1186/s40345-020-00212-2>
- Blood-Siegfried, J., & Rende, E. K. (2010). The Long-Term Effects of Prenatal Nicotine Exposure on Neurologic Development. *Journal of Midwifery and Women's Health*, 55(2), 143–152. <https://doi.org/10.1016/j.jmwh.2009.05.006>
- Breland, A., McCubbin, A., & Ashford, K. (2019). Electronic nicotine delivery systems and pregnancy: Recent research on perceptions, cessation, and toxicant delivery. In *Birth Defects Research* (Vol. 111, Issue 17, pp. 1284–1293). John Wiley and Sons Inc. <https://doi.org/10.1002/bdr2.1561>
- Brook, D. W., Zhang, C., Rosenberg, G., & Brook, J. S. (2006). Maternal cigarette smoking during pregnancy and child aggressive behavior. *American Journal on Addictions*, 15(6), 450–456. <https://doi.org/10.1080/10550490600998559>
- Brooks, A. C., & Henderson, B. J. (2021). Systematic review of nicotine exposure's effects on neural stem and progenitor cells. In *Brain Sciences* (Vol. 11, Issue 2, pp. 1–18). MDPI AG. <https://doi.org/10.3390/brainsci11020172>
- Camp, J. G., Badsha, F., Florio, M., Kanton, S., Gerber, T., Wilsch-Bräuninger, M., Lewitus, E., Sykes, A., Hevers, W., Lancaster, M., Knoblich, J. A., Lachmann, R., Pääbo, S., Huttner, W. B., & Treutlein, B. (2015). Human cerebral organoids recapitulate gene expression programs of fetal neocortex development. *Proceedings of the National Academy of Sciences of the United States of America*, 112(51), 15672–15677. <https://doi.org/10.1073/pnas.1520760112>
- Cao, B. J., & Li, Y. (2002). Reduced anxiety- and depression-like behaviors in *Emx1* homozygous mutant mice. *Brain Research*, 937(1–2), 32–40. [https://doi.org/10.1016/S0006-8993\(02\)02461-7](https://doi.org/10.1016/S0006-8993(02)02461-7)
- Cardenas, V. M., Cen, R., Clemens, M. M., Moody, H. L., Ekanem, U. S., Policherla, A., Fischbach, L. A., Eswaran, H., Magann, E. F., Delongchamp, R. R., & Boysen, G. (2019). Use of electronic nicotine delivery systems (ENDS) by pregnant women I: Risk of small-for-gestational-age birth. *Tobacco Induced Diseases*, 17. <https://doi.org/10.18332/tid/106089>

- Centeno, E. G. Z., Cimarosti, H., & Bithell, A. (2018). 2D versus 3D human induced pluripotent stem cell-derived cultures for neurodegenerative disease modelling. In *Molecular Neurodegeneration* (Vol. 13, Issue 1). BioMed Central Ltd. <https://doi.org/10.1186/s13024-018-0258-4>
- Chang, L., & Karin, M. (2001). Mammalian MAP kinase signalling cascades. In *Nature* (Vol. 410). <https://doi.org/10.1038/35065000>
- Chaturvedi, H. K., Chandra, D., & Bapna, J. S. (1999). Interaction between N-methyl-D-aspartate receptor antagonists and imipramine in shock-induced depression. In *Indian Journal of Experimental Biology* (Vol. 37).
- Chiaradia, I., & Lancaster, M. A. (2020). Brain organoids for the study of human neurobiology at the interface of in vitro and in vivo. In *Nature Neuroscience* (Vol. 23, Issue 12, pp. 1496–1508). Nature Research. <https://doi.org/10.1038/s41593-020-00730-3>
- Choudary, P. V., Molnar, M., Evans, S. J., Tomita, H., Li, J. Z., Vawter, M. P., Myers, R. M., Bunney, W. E., Akil, H., Watson, S. J., & Jones, E. G. (2005). Altered cortical glutamatergic and GABAergic signal transmission with glial involvement in depression. *The Proceedings of the National Academy of Sciences*, 102(43), 15653-15658. <https://doi.org/10.1073/pnas.0507901102>
- Corrêa, M. L., da Silva, B. G. C., Wehrmeister, F. C., Horta, B. L., Gonçalves, H., Barros, F., & Menezes, A. M. B. (2022). Maternal smoking during pregnancy and children's mental health at age 22 years: Results of a birth cohort study. *Journal of Affective Disorders*, 300, 203–208. <https://doi.org/10.1016/j.jad.2021.12.125>
- De Long, N. E., Barra, N. G., Hardy, D. B., & Holloway, A. C. (2014). Is it safe to use smoking cessation therapeutics during pregnancy? In *Expert Opinion on Drug Safety* (Vol. 13, Issue 12, pp. 1721–1731). Informa Healthcare. <https://doi.org/10.1517/14740338.2014.973846>
- Delva, N. C., & Stanwood, G. D. (2021). Dysregulation of brain dopamine systems in major depressive disorder. In *Experimental Biology and Medicine* (Vol. 246, Issue 9, pp. 1084–1093). SAGE Publications Inc. <https://doi.org/10.1177/1535370221991830>
- DeVeough-Geiss, A. M., Chen, L. H., Kotler, M. L., Ramsay, L. R., & Durcan, M. J. (2010). Pharmacokinetic comparison of two nicotine transdermal systems, a 21-mg/24-hour patch and a 25-mg/16-hour patch: A randomized, open-label, single-dose, two-way crossover study in adult smokers. *Clinical Therapeutics*, 32(6), 1140–1148. <https://doi.org/10.1016/j.clinthera.2010.06.008>

- Dome, P., Lazary, J., Kalapos, M. P., & Rihmer, Z. (2010). Smoking, nicotine and neuropsychiatric disorders. In *Neuroscience and Biobehavioral Reviews* (Vol. 34, Issue 3, pp. 295–342). <https://doi.org/10.1016/j.neubiorev.2009.07.013>
- Duda, P., Hajka, D., Wójcicka, O., Rakus, D., & Gizak, A. (2020). GSK3 β : A Master Player in Depressive Disorder Pathogenesis and Treatment Responsiveness. In *Cells* (Vol. 9, Issue 3). NLM (Medline). <https://doi.org/10.3390/cells9030727>
- Duko, B., Pereira, G., Tait, R. J., Betts, K., Newnham, J., & Alati, R. (2022). Prenatal tobacco and alcohol exposures and the risk of anxiety symptoms in young adulthood: A population-based cohort study. *Psychiatry Research*, 310. <https://doi.org/10.1016/j.psychres.2022.114466>
- Duman, R. S., Sanacora, G., & Krystal, J. H. (2019). Altered Connectivity in Depression: GABA and Glutamate Neurotransmitter Deficits and Reversal by Novel Treatments. In *Neuron* (Vol. 102, Issue 1, pp. 75–90). Cell Press. <https://doi.org/10.1016/j.neuron.2019.03.013>
- Dwivedi, Y., Rizavi, H. S., Roberts, R. C., Conley, R. C., Tamminga, C. A., & Pandey, G. N. (2001). Reduced activation and expression of ERK1/2 MAP kinase in the post-mortem brain of depressed suicide subjects. In *Journal of Neurochemistry*.
- Dwivedi, Y., Rizavi, H. S., Zhang, H., Roberts, R. C., Conley, R. R., & Pandey, G. N. (2009). Aberrant extracellular signal-regulated kinase (ERK)1/2 signalling in suicide brain: Role of ERK kinase 1 (MEK1). *International Journal of Neuropsychopharmacology*, 12(10), 1337–1354. <https://doi.org/10.1017/S1461145709990575>
- Dwyer, J. B., Cardenas, A., Franke, R. M., Chen, Y. L., Bai, Y., Belluzzi, J. D., Lotfipour, S., & Leslie, F. M. (2019). Prenatal nicotine sex-dependently alters adolescent dopamine system development. *Translational Psychiatry*, 9(1). <https://doi.org/10.1038/s41398-019-0640-1>
- Dwyer, J. B., McQuown, S. C., & Leslie, F. M. (2009). The dynamic effects of nicotine on the developing brain. In *Pharmacology and Therapeutics* (Vol. 122, Issue 2, pp. 125–139). <https://doi.org/10.1016/j.pharmthera.2009.02.003>
- Ekblad, M., Gissler, M., Lehtonen, L., & Korkeila, J. (2010). Prenatal Smoking Exposure and the Risk of Psychiatric Morbidity Into Young Adulthood. *Archives of General Psychiatry*, 67(8), 841–849. <https://doi.org/10.1001/archgenpsychiatry.2010.92>

- Ekblad, M., Korkeila, J., & Lehtonen, L. (2015). Smoking during pregnancy affects foetal brain development. In *Acta Paediatrica, International Journal of Paediatrics* (Vol. 104, Issue 1, pp. 12–18). Blackwell Publishing Ltd. <https://doi.org/10.1111/apa.12791>
- England, L. J., Tong, V. T., Koblitz, A., Kish-Doto, J., Lynch, M. M., & Southwell, B. G. (2016). Perceptions of emerging tobacco products and nicotine replacement therapy among pregnant women and women planning a pregnancy. *Preventive Medicine Reports*, 4, 481–485. <https://doi.org/10.1016/j.pmedr.2016.09.002>
- Ernst, M., Moolchan, E. T., & Robinson, M. L. (2001). Behavioral and neural consequences of prenatal exposure to nicotine. *Journal of the American Academy of Child and Adolescent Psychiatry*, 40(6), 630–641. <https://doi.org/10.1097/00004583-200106000-00007>
- Falk, L., Nordberg, A., Seiger, Å., Kjældgaard, A., & Hellström-Lindahl, E. (2005). Smoking during early pregnancy affects the expression pattern of both nicotinic and muscarinic acetylcholine receptors in human first trimester brainstem and cerebellum. *Neuroscience*, 132(2), 389–397. <https://doi.org/10.1016/j.neuroscience.2004.12.049>
- Falk, L., Nordberg, A., Seiger, Å., Kjældgaard, A., & Hellström-Lindahl, E. (2002). The $\alpha 7$ nicotinic receptors in human fetal brain and spinal cord. *Journal of Neurochemistry*, 80(3), 457–465. <https://doi.org/10.1046/j.0022-3042.2001.00714.x>
- Fan, T., Hu, Y., Xin, J., Zhao, M., & Wang, J. (2020). Analyzing the genes and pathways related to major depressive disorder via a systems biology approach. *Brain and Behavior*, 10(2). <https://doi.org/10.1002/brb3.1502>
- Fedotova, J. (2012). Effects of Stimulation and Blockade of Receptor on Depression-Like Behavior in Ovariectomized Female Rats. *ISRN Pharmacology*, 2012, 1–8. <https://doi.org/10.5402/2012/305645>
- Fenster, C. P., Hicks, J. H., Beckman, M. L., Covernton, P. J. O., Quick, M. W., & Lester, R. A. J. (1999). Desensitization of Nicotinic Receptors in the Central Nervous System. *Annals of the New York Academy of Sciences*, 868(1), 620–623. <https://doi.org/10.1111/j.1749-6632.1999.tb11335.x>
- Feyissa, A. M., Chandran, A., Stockmeier, C. A., & Karolewicz, B. (2009). Reduced levels of NR2A and NR2B subunits of NMDA receptor and PSD-95 in the prefrontal cortex in major depression. *Progress in Neuro-Psychopharmacology and Biological Psychiatry*, 33(1), 70–75. <https://doi.org/10.1016/j.pnpbp.2008.10.005>

- Feyissa, A. M., Woolverton, W. L., Miguel-Hidalgo, J. J., Wang, Z., Kyle, P. B., Hasler, G., Stockmeier, C. A., Iyo, A. H., & Karolewicz, B. (2010). Elevated level of metabotropic glutamate receptor 2/3 in the prefrontal cortex in major depression. *Progress in Neuro-Psychopharmacology and Biological Psychiatry*, 34(2), 279–283. <https://doi.org/10.1016/j.pnpbp.2009.11.018>
- Fogaça, M. V., & Duman, R. S. (2019). Cortical GABAergic dysfunction in stress and depression: New insights for therapeutic interventions. In *Frontiers in Cellular Neuroscience* (Vol. 13). Frontiers Media S.A. <https://doi.org/10.3389/fncel.2019.00087>
- Freund, R. K., Jungschaffer, D. A., Collins, A. C., & Wehner, J. M. (1988). Evidence for modulation of GABAergic neurotransmission by nicotine. In *Brain Research* (Vol. 453). [https://doi.org/10.1016/0006-8993\(88\)90160-6](https://doi.org/10.1016/0006-8993(88)90160-6)
- Gould, T. D., Einat, H., Bhat, R., & Manji, H. K. (2004). AR-A014418, a selective GSK-3 inhibitor, produces antidepressant-like effects in the forced swim test. *International Journal of Neuropsychopharmacology*, 7(4), 387–390. <https://doi.org/10.1017/S1461145704004535>
- Guo, H., Tian, L., Zhang, J. Z., Kitani, T., Paik, D. T., Lee, W. H., & Wu, J. C. (2019). Single-Cell RNA Sequencing of Human Embryonic Stem Cell Differentiation Delineates Adverse Effects of Nicotine on Embryonic Development. *Stem Cell Reports*, 12(4), 772–786. <https://doi.org/10.1016/j.stemcr.2019.01.022>
- Hashimoto, K. (2009). Emerging role of glutamate in the pathophysiology of major depressive disorder. In *Brain Research Reviews* (Vol. 61, Issue 2, pp. 105–123). <https://doi.org/10.1016/j.brainresrev.2009.05.005>
- Hasler, G., Van Der Veen, J. W., Tumonis, T., Meyers, N., Shen, J., & Drevets, W. C. (2007). Reduced Prefrontal Glutamate/Glutamine and-Aminobutyric Acid Levels in Major Depression Determined Using Proton Magnetic Resonance Spectroscopy. In *Arch Gen Psychiatry* (Vol. 64). <https://doi.org/10.1001/archpsyc.64.2.193>
- Hobara, T., Uchida, S., Otsuki, K., Matsubara, T., Funato, H., Matsuo, K., Suetsugi, M., & Watanabe, Y. (2010). Altered gene expression of histone deacetylases in mood disorder patients. *Journal of Psychiatric Research*, 44(5), 263–270. <https://doi.org/10.1016/j.jpsychires.2009.08.015>
- Holmes, A., Lachowicz, J. E., & Sibley, D. R. (2004). Phenotypic analysis of dopamine receptor knockout mice; recent insights into the functional specificity of dopamine receptor subtypes. In *Neuropharmacology* (Vol. 47, Issue 8, pp. 1117–1134). <https://doi.org/10.1016/j.neuropharm.2004.07.034>

- Hu, K. (2021). Become Competent in Generating RNA-Seq Heat Maps in One Day For Novices Without Prior R Experience. *Nuclear Reprogramming*. Methods in Molecular Biology, vol 2239. Humana, New York, NY.
https://doi.org/10.1007/978-1-0716-1084-8_17
- Hudson, R., Green, M., Wright, D. J., Renard, J., Jobson, C. E. L., Jung, T., Rushlow, W., & Laviolette, S. R. (2021). Adolescent nicotine induces depressive and anxiogenic effects through ERK 1-2 and Akt-GSK-3 pathways and neuronal dysregulation in the nucleus accumbens. *Addiction Biology*, 26(2). <https://doi.org/10.1111/adb.12891>
- Huey, S. W., & Granitto, M. H. (2020). Smoke screen: The teen vaping epidemic uncovers a new concerning addiction. *Journal of the American Association of Nurse Practitioners*, 32(4), 293–298.
<https://doi.org/10.1097/JXX.0000000000000234>
- Iwamoto, K., Kakiuchi, C., Bundo, M., Ikeda, K., & Kato, T. (2004). Molecular characterization of bipolar disorder by comparing gene expression profiles of postmortem brains of major mental disorders. *Molecular Psychiatry*, 9(4), 406–416. <https://doi.org/10.1038/sj.mp.4001437>
- Jobson, C. L. M., Renard, J., Szkudlarek, H., Rosen, L. G., Pereira, B., Wright, D. J., Rushlow, W., & Laviolette, S. R. (2019). Adolescent Nicotine Exposure Induces Dysregulation of Mesocorticolimbic Activity States and Depressive and Anxiety-like Prefrontal Cortical Molecular Phenotypes Persisting into Adulthood. *Cerebral Cortex*, 29(7), 3140–3153.
<https://doi.org/10.1093/cercor/bhy179>
- Johnson, J., Sharick, J. T., Skala, M. C., & Li, L. (2020). Sample preparation strategies for high-throughput mass spectrometry imaging of primary tumor organoids. *Journal of Mass Spectrometry*, 55(4).
<https://doi.org/10.1002/jms.4452>
- Kaidanovich-Beilin, O., Milman, A., Weizman, A., Pick, C. G., & Eldar-Finkelman, H. (2004). Rapid antidepressive-like activity of specific glycogen synthase kinase-3 inhibitor and its effect on β -catenin in mouse hippocampus. *Biological Psychiatry*, 55(8), 781–784. <https://doi.org/10.1016/j.biopsych.2004.01.008>
- Karege, F., Perroud, N., Burkhardt, S., Schwald, M., Ballmann, E., La Harpe, R., & Malafosse, A. (2007). Alteration in Kinase Activity But Not in Protein Levels of Protein Kinase B and Glycogen Synthase Kinase-3 β in Ventral Prefrontal Cortex of Depressed Suicide Victims. *Biological Psychiatry*, 61(2), 240–245.
<https://doi.org/10.1016/j.biopsych.2006.04.036>

- Karolewicz, B., MacIag, D., O'Dwyer, G., Stockmeier, C. A., Feyissa, A. M., & Rajkowska, G. (2010). Reduced level of glutamic acid decarboxylase-67 kDa in the prefrontal cortex in major depression. *International Journal of Neuropsychopharmacology*, *13*(4), 411–420. <https://doi.org/10.1017/S1461145709990587>
- Khodoruth, M. A. S., Estudillo-Guerra, M. A., Pacheco-Barrios, K., Nyundo, A., Chapa-Koloffon, G., & Ouanes, S. (2022). Glutamatergic System in Depression and Its Role in Neuromodulatory Techniques Optimization. In *Frontiers in Psychiatry* (Vol. 13). Frontiers Media S.A. <https://doi.org/10.3389/fpsy.2022.886918>
- Kim, J., Koo, B. K., & Knoblich, J. A. (2020). Human organoids: model systems for human biology and medicine. In *Nature Reviews Molecular Cell Biology* (Vol. 21, Issue 10, pp. 571–584). Nature Research. <https://doi.org/10.1038/s41580-020-0259-3>
- Kim, J., Sullivan, G. J., & Park, I.-H. (2021). How well do brain organoids capture your brain? *iScience*, *24*(2). <https://doi.org/10.1016/j.isci>
- Klempan, T. A., Sequeira, A., Canetti, L., Lalovic, A., Ernst, C., Ffrench-Mullen, J., & Turecki, G. (2009). Altered expression of genes involved in ATP biosynthesis and GABAergic neurotransmission in the ventral prefrontal cortex of suicides with and without major depression. *Molecular Psychiatry*, *14*(2), 175–189. <https://doi.org/10.1038/sj.mp.4002110>
- Knable, M. B., Barci, B. M., Webster, M. J., Meador-Woodruff, J., & Torrey, E. F. (2004). Molecular abnormalities of the hippocampus in severe psychiatric illness: Postmortem findings from the Stanley Neuropathology Consortium. *Molecular Psychiatry*, *9*(6), 609–620. <https://doi.org/10.1038/sj.mp.4001471>
- Kutlu, M. G., & Gould, T. J. (2015). Nicotine modulation of fear memories and anxiety: Implications for learning and anxiety disorders. In *Biochemical Pharmacology* (Vol. 97, Issue 4, pp. 498–511). Elsevier Inc. <https://doi.org/10.1016/j.bcp.2015.07.029>
- Lancaster, M. A. (2018). Brain organoids get vascularized. In *Nature Biotechnology* (Vol. 36, Issue 5, pp. 407–408). Nature Publishing Group. <https://doi.org/10.1038/nbt.4133>
- Lancaster, M. A., & Knoblich, J. A. (2014). Generation of cerebral organoids from human pluripotent stem cells. *Nature Protocols*, *9*(10), 2329–2340. <https://doi.org/10.1038/nprot.2014.158>

- Lancaster, M. A., Renner, M., Martin, C. A., Wenzel, D., Bicknell, L. S., Hurles, M. E., Homfray, T., Penninger, J. M., Jackson, A. P., & Knoblich, J. A. (2013). Cerebral organoids model human brain development and microcephaly. *Nature*, *501*(7467), 373–379. <https://doi.org/10.1038/nature12517>
- Lauterstein, D. E., Tijerina, P. B., Corbett, K., Oksuz, B. A., Shen, S. S., Gordon, T., Klein, C. B., & Zelikoff, J. T. (2016). Frontal cortex transcriptome analysis of mice exposed to electronic cigarettes during early life stages. *International Journal of Environmental Research and Public Health*, *13*(4). <https://doi.org/10.3390/ijerph13040417>
- Lavolette, S. R. (2021). Molecular and neuronal mechanisms underlying the effects of adolescent nicotine exposure on anxiety and mood disorders. In *Neuropharmacology* (Vol. 184). Elsevier Ltd. <https://doi.org/10.1016/j.neuropharm.2020.108411>
- Liu, L., van Groen, T., Kadish, I., & Tollefsbol, T. O. (2009). DNA methylation impacts on learning and memory in aging. In *Neurobiology of Aging* (Vol. 30, Issue 4, pp. 549–560). <https://doi.org/10.1016/j.neurobiolaging.2007.07.020>
- Livingstone, P. D., Dickinson, J. A., Srinivasan, J., Kew, J. N. C., & Wonnacott, S. (2010). Glutamate-dopamine crosstalk in the rat prefrontal cortex is modulated by alpha7 nicotinic receptors and potentiated by PNU-120596. *Journal of Molecular Neuroscience*, *40*(1–2), 172–176. <https://doi.org/10.1007/s12031-009-9232-5>
- Lu, Y., Grady, S., Marks, M. J., Picciotto, M., Changeux, J.-P., & Collins, A. C. (1992). Pharmacological Characterization of Nicotinic Receptor-stimulated GABA Release From Mouse Brain Synaptosomes 1. In *the journal of pharmacology and experimental therapeutics* (Vol. 287, Issue 2).
- Luo, J. (2012). The role of GSK3beta in the development of the central nervous system. In *Frontiers in Biology* (Vol. 7, Issue 3, pp. 212–220). <https://doi.org/10.1007/s11515-012-1222-2>
- Luo, Y. W., Xu, Y., Cao, W. Y., Zhong, X. L., Duan, J., Wang, X. Q., Hu, Z. L., Li, F., Zhang, J. Y., Zhou, M., Dai, R. P., & Li, C. Q. (2015). Insulin-like growth factor 2 mitigates depressive behavior in a rat model of chronic stress. *Neuropharmacology*, *89*, 318–324. <https://doi.org/10.1016/j.neuropharm.2014.10.011>
- Magnus, P., Birke, C., Vejrurp, K., Haugan, A., Alsaker, E., Daltveit, A. K., Handal, M., Haugen, M., Høiseth, G., Knudsen, G. P., Paltiel, L., Schreuder, P., Tambs, K., Vold, L., & Stoltenberg, C. (2016). Cohort Profile Update: The Norwegian Mother and Child Cohort Study (MoBa). *International Journal of Epidemiology*, *45*(2), 382–388. <https://doi.org/10.1093/ije/dyw029>

- Mahar, I., Bagot, R. C., Davoli, M. A., Miksys, S., Tyndale, R. F., Walker, C. D., Maheu, M., Huang, S. H., Wong, T. P., & Mechawar, N. (2012). Developmental hippocampal neuroplasticity in a model of nicotine replacement therapy during pregnancy and breastfeeding. *PloS One*, 7(5).
<https://doi.org/10.1371/journal.pone.0037219>
- Malki, K., Pain, O., Tosto, M. G., Du Rietz, E., Carboni, L., & Schalkwyk, L. C. (2015). Identification of genes and gene pathways associated with major depressive disorder by integrative brain analysis of rat and human prefrontal cortex transcriptomes. *Translational Psychiatry*, 5(3).
<https://doi.org/10.1038/tp.2015.15>
- Mariani, J., Coppola, G., Zhang, P., Abyzov, A., Provini, L., Tomasini, L., Amenduni, M., Szekely, A., Palejev, D., Wilson, M., Gerstein, M., Grigorenko, E. L., Chawarska, K., Pelphrey, K. A., Howe, J. R., & Vaccarino, F. M. (2015). FOXP1-Dependent Dysregulation of GABA/Glutamate Neuron Differentiation in Autism Spectrum Disorders. *Cell*, 162(2), 375–390.
<https://doi.org/10.1016/j.cell.2015.06.034>
- Mark, K. S., Farquhar, B., Chisolm, M. S., Coleman-Cowger, V. H., & Terplan, M. (2015). Knowledge, attitudes, and practice of electronic cigarette use among pregnant women. *Journal of Addiction Medicine*, 9(4), 266–272.
<https://doi.org/10.1097/ADM.0000000000000128>
- Martin, M. M., McCarthy, D. M., Schatschneider, C., Trupiano, M. X., Jones, S. K., Kalluri, A., & Bhide, P. G. (2020). Effects of Developmental Nicotine Exposure on Frontal Cortical GABA-to-Non-GABA Neuron Ratio and Novelty-Seeking Behavior. *Cerebral Cortex*, 30(3), 1830–1842.
<https://doi.org/10.1093/cercor/bhz207>
- Massadeh, A.M., Gharaibeh, A.A., & Omari, K.W. (2009). A Single-Step Extraction Method for the Determination of Nicotine and Cotinine in Jordanian Smokers' Blood and Urine Samples by RP-HPLC and GC-MS. *Journal of Chromatographic Science*, 47. <https://doi.org/10.1093/chromsci/47.2.170>
- McCubbin, A., Fallin-Bennett, A., Barnett, J., & Ashford, K. (2017). Perceptions and use of electronic cigarettes in pregnancy. In *Health Education Research* (Vol. 32, Issue 1, pp. 22–32). Oxford University Press.
<https://doi.org/10.1093/her/cyw059>
- Mcgrath-Morrow, S. A., Gorzkowski, J., Groner, J. A., Rule, A. M., Wilson, K., Tanski, S. E., Collaco, J. M., & Klein, J. D. (2020). The Effects of Nicotine on Development. *Pediatrics*, 145(3). <https://doi.org/10.1542/peds.2019-1346>

- McLean, C. P., Asnaani, A., Litz, B. T., & Hofmann, S. G. (2011). Gender differences in anxiety disorders: Prevalence, course of illness, comorbidity and burden of illness. *Journal of Psychiatric Research*, *45*(8), 1027–1035. <https://doi.org/10.1016/j.jpsychires.2011.03.006>
- Mehta, D., Menke, A., & Binder, E. B. (2010). Gene expression studies in major depression. In *Current Psychiatry Reports* (Vol. 12, Issue 2, pp. 135–144). <https://doi.org/10.1007/s11920-010-0100-3>
- Millan, M. J. (2006). Multi-target strategies for the improved treatment of depressive states: Conceptual foundations and neuronal substrates, drug discovery and therapeutic application. In *Pharmacology and Therapeutics* (Vol. 110, Issue 2, pp. 135–370). <https://doi.org/10.1016/j.pharmthera.2005.11.006>
- Minatoya, M., Araki, A., Itoh, S., Yamazaki, K., Kobayashi, S., Miyashita, C., Sasaki, S., & Kishi, R. (2019). Prenatal tobacco exposure and ADHD symptoms at pre-school age: The Hokkaido Study on Environment and Children's Health. *Environmental Health and Preventive Medicine*, *24*(1). <https://doi.org/10.1186/s12199-019-0834-4>
- Mineur, Y. S., Einstein, E. B., Seymour, P. A., Coe, J. W., O'Neill, B. T., Rollema, H., & Picciotto, M. R. (2011). $\alpha 4\beta 2$ nicotinic acetylcholine receptor partial agonists with low intrinsic efficacy have antidepressant-like properties. *Behavioural Pharmacology*, *22*(4), 291–299. <https://doi.org/10.1097/FBP.0b013e328347546d>
- Miura, Y., Li, M. Y., Birey, F., Ikeda, K., Revah, O., Thete, M. V., Park, J. Y., Puno, A., Lee, S. H., Porteus, M. H., & Paşca, S. P. (2020). Generation of human striatal organoids and cortico-striatal assembloids from human pluripotent stem cells. *Nature Biotechnology*, *38*(12), 1421–1430. <https://doi.org/10.1038/s41587-020-00763-w>
- Mizrak, S. (2019). The Effects of High and Low Dose Nicotine Administration on Neurogenesis. *Biomedical Journal of Scientific & Technical Research*, *13*(1). <https://doi.org/10.26717/bjstr.2019.13.002343>
- Moylan, S., Gustavson, K., Øverland, S., Karevold, B. B., Jacka, F. N., Pasco, J. A., & Berk, M. (2015). The impact of maternal smoking during pregnancy on depressive and anxiety behaviors in children: The Norwegian mother and child cohort study. *BMC Medicine*, *13*(1). <https://doi.org/10.1186/s12916-014-0257-4>
- Moylan, S., Jacka, F. N., Pasco, J. A., & Berk, M. (2013). How cigarette smoking may increase the risk of anxiety symptoms and anxiety disorders: A critical review of biological pathways. *Brain and Behavior*, *3*(3), 302–326. <https://doi.org/10.1002/brb3.137>

- Muneoka, K., Nakatsu, T., Fuji, J.-I., Ogawa, T., & Takigawa, M. (1999). Prenatal Administration of Nicotine Results in Dopaminergic Alterations in the Neocortex. In *Neurotoxicology and Teratology* (Vol. 21, Issue 5). [https://doi.org/10.1016/s0892-0362\(99\)00028-8](https://doi.org/10.1016/s0892-0362(99)00028-8)
- Muneoka, K., Ogawa, T., Kamei, K., Muraoka, S.-I., Tomiyoshi, R., Mimura, Y., Kato, H., Suzuki, M. R., & Takigawa, M. (1997). Prenatal nicotine exposure affects the development of the central serotonergic system as well as the dopaminergic system in rat offspring: involvement of route of drug administrations. In *Developmental Brain Research* (Vol. 102). [https://doi.org/10.1016/s0165-3806\(97\)00092-8](https://doi.org/10.1016/s0165-3806(97)00092-8)
- Niemelä, S., Sourander, A., Surcel, H. M., Hinkka-Yli-Salomäki, S., McKeague, I. W., Cheslack-Postava, K., & Brown, A. S. (2016). Prenatal nicotine exposure and risk of schizophrenia among offspring in a national birth cohort. *American Journal of Psychiatry*, *173*(8), 799–806. <https://doi.org/10.1176/appi.ajp.2016.15060800>
- Nobis, A., Zalewski, D., & Waszkiewicz, N. (2020). Peripheral markers of depression. In *Journal of Clinical Medicine* (Vol. 9, Issue 12, pp. 1–54). MDPI. <https://doi.org/10.3390/jcm9123793>
- Notaras, M., Lodhi, A., Barrio-Alonso, E., Foord, C., Rodrick, T., Jones, D., Fang, H., Greening, D., & Colak, D. (2021). Neurodevelopmental signatures of narcotic and neuropsychiatric risk factors in 3D human-derived forebrain organoids. *Molecular Psychiatry*. <https://doi.org/10.1038/s41380-021-01189-9>
- Obisesan, O. H., Osei, A. D., Uddin, S. M. I., Dzaye, O., Cainzos-Achirica, M., Mirbolouk, M., Orimoloye, O. A., Sharma, G., Al Rifai, M., Stokes, A., Bhatnagar, A., El Shahawy, O., Benjamin, E. J., DeFilippis, A. P., & Blaha, M. J. (2020). E-Cigarette Use Patterns and High-Risk Behaviors in Pregnancy: Behavioral Risk Factor Surveillance System, 2016–2018. *American Journal of Preventive Medicine*, *59*(2), 187–195. <https://doi.org/10.1016/j.amepre.2020.02.015>
- Oh, D. H., Park, Y. C., & Kim, S. H. (2010). Increased glycogen synthase kinase-3 β mRNA level in the hippocampus of patients with major depression: A study using the Stanley neuropathology consortium integrative database. *Psychiatry Investigation*, *7*(3), 202–207. <https://doi.org/10.4306/pi.2010.7.3.202>
- Oncken, C.A., Hardardottir, H., HAtsukami, D.K., Lupo, V.R., Rodis, J.F., & Smeltzer, J.S. (1997). Effects of Transdermal Nicotine or Smoking on Nicotine Concentrations and Maternal-Fetal Hemodynamics. *Obstetrics & Gynecology*, *90*(4), 569-574. [https://doi.org/10.1016/s0029-7844\(97\)00309-8](https://doi.org/10.1016/s0029-7844(97)00309-8)

- Orzabal, M., & Ramadoss, J. (2019). Impact of electronic cigarette aerosols on pregnancy and early development. In *Current Opinion in Toxicology* (Vol. 14, pp. 14–20). Elsevier B.V. <https://doi.org/10.1016/j.cotox.2019.05.001>
- Passaro, A. P., & Stice, S. L. (2021). Electrophysiological Analysis of Brain Organoids: Current Approaches and Advancements. In *Frontiers in Neuroscience* (Vol. 14). Frontiers Media S.A. <https://doi.org/10.3389/fnins.2020.622137>
- Paterson, J. M., Neimanis, I. M., & Bain, E. (2023). Stopping Smoking During Pregnancy Are We on the Right Track? *Canadian Journal of Public Health*, 94(4), 297-299. <https://doi.org/10.1007/BF03403609>
- Perlman, G., Tanti, A., & Mechawar, N. (2021). Parvalbumin interneuron alterations in stress-related mood disorders: A systematic review. In *Neurobiology of Stress* (Vol. 15). Elsevier Inc. <https://doi.org/10.1016/j.ynstr.2021.100380>
- Philip, N. S., Carpenter, L. L., Tyrka, A. R., & Price, L. H. (2010). Nicotinic acetylcholine receptors and depression: A review of the preclinical and clinical literature. In *Psychopharmacology* (Vol. 212, Issue 1, pp. 1–12). <https://doi.org/10.1007/s00213-010-1932-6>
- Picciotto, M.R., Addy, N.A., Mineur, Y.S., & Brunzell, D.H. (2008). It's not "either/or": activation and desensitization of nicotinic acetylcholine receptors both contribute to behaviors related to nicotine addiction and mood. *Progress in Neurobiology*, 84(4), 329-342. <https://doi.org/10.1016/j.pneurobio.2007.12.005>
- Polli, F. S., Scharff, M. B., Ipsen, T. H., Aznar, S., Kohlmeier, K. A., & Andreasen, J. T. (2020). Prenatal nicotine exposure in mice induces sex-dependent anxiety-like behavior, cognitive deficits, hyperactivity, and changes in the expression of glutamate receptor associated-genes in the prefrontal cortex. *Pharmacology Biochemistry and Behavior*, 195. <https://doi.org/10.1016/j.pbb.2020.172951>
- Qian, X., Nguyen, H. N., Song, M. M., Hadiono, C., Ogden, S. C., Hammack, C., Yao, B., Hamersky, G. R., Jacob, F., Zhong, C., Yoon, K. J., Jeang, W., Lin, L., Li, Y., Thakor, J., Berg, D. A., Zhang, C., Kang, E., Chickering, M., ... Ming, G. L. (2016). Brain-Region-Specific Organoids Using Mini-bioreactors for Modeling ZIKV Exposure. *Cell*, 165(5), 1238–1254. <https://doi.org/10.1016/j.cell.2016.04.032>

- Rafikova, E., Shadrina, M., Slominsky, P., Guekht, A., Ryskov, A., Shibalev, D., & Vasilyev, V. (2021). Slc6a3 (Dat1) as a novel candidate biomarker gene for suicidal behavior. *Genes*, 12(6). <https://doi.org/10.3390/genes12060861>
- Rajkowska, G., O'Dwyer, G., Teleki, Z., Stockmeier, C. A., & Miguel-Hidalgo, J. J. (2007). GABAergic neurons immunoreactive for calcium binding proteins are reduced in the prefrontal cortex in major depression. *Neuropsychopharmacology*, 32(2), 471–482. <https://doi.org/10.1038/sj.npp.1301234>
- Regan, A. K., & Pereira, G. (2021). Patterns of combustible and electronic cigarette use during pregnancy and associated pregnancy outcomes. *Scientific Reports*, 11(1). <https://doi.org/10.1038/s41598-021-92930-5>
- Roskoski, R. (2012). ERK1/2 MAP kinases: Structure, function, and regulation. In *Pharmacological Research* (Vol. 66, Issue 2, pp. 105–143). <https://doi.org/10.1016/j.phrs.2012.04.005>
- Ross, E. J., Graham, D. L., Money, K. M., & Stanwood, G. D. (2015). Developmental consequences of fetal exposure to drugs: What we know and what we still must learn. In *Neuropsychopharmacology* (Vol. 40, Issue 1, pp. 61–87). Nature Publishing Group. <https://doi.org/10.1038/npp.2014.147>
- Ruggiero, L., Tsoh, J. Y., Everett, K., Fava, J. L., & Guise, B. J. (2000).). The transtheoretical model of smoking: comparison of pregnant and nonpregnant smokers. In *Addictive Behaviors* (Vol. 25, Issue 2). [https://doi.org/10.1016/s0306-4603\(99\)00029-5](https://doi.org/10.1016/s0306-4603(99)00029-5)
- Russell, M. A. H., Jarvis, M., Iyer, R., & Feyerabend, C. (1980). Relation of nicotine yield of cigarettes to blood nicotine concentrations in smokers. In *British Medical Journal* (Vol. 5). <https://doi.org/10.1136/bmj.280.6219.972>
- Sailer, S., Sebastiani, G., Andreu-Fernández, V., & García-Algar, O. (2019). Impact of nicotine replacement and electronic nicotine delivery systems on fetal brain development. In *International Journal of Environmental Research and Public Health* (Vol. 16, Issue 24). MDPI AG. <https://doi.org/10.3390/ijerph16245113>
- Sanacora, G., Gueorguieva, R., Epperson, ; C Neill, Wu, Y.-T., Appel, M., Rothman, D. L., Krystal, J. H., & Mason, G. F. (2005). Subtype-Specific Alterations of-Aminobutyric Acid and Glutamate in Patients With Major Depression. *Archives of General Psychiatry*, 61(7), 705-713. <https://doi.org/10.1001/archpsyc.61.7.705>

- Sanacora, G., Mason, G. F., Rothman, D. L., Behar, K. L., Hyder, F., Ognen, ;, Petroff, A. C., Berman, R. M., Charney, D. S., & Krystal, J. H. (1999). Reduced Cortical-Aminobutyric Acid Levels in Depressed Patients Determined by Proton Magnetic Resonance Spectroscopy. *Archives of General Psychiatry*, 56(11), 1043-1047. <https://doi.org/10.1001/archpsyc.56.11.1043>.
- Santomauro, D. F., Mantilla Herrera, A. M., Shadid, J., Zheng, P., Ashbaugh, C., Pigott, D. M., Abbafati, C., Adolph, C., Amlag, J. O., Aravkin, A. Y., Bang-Jensen, B. L., Bertolacci, G. J., Bloom, S. S., Castellano, R., Castro, E., Chakrabarti, S., Chattopadhyay, J., Cogen, R. M., Collins, J. K., ... Ferrari, A. J. (2021). Global prevalence and burden of depressive and anxiety disorders in 204 countries and territories in 2020 due to the COVID-19 pandemic. *The Lancet*, 398(10312), 1700–1712. [https://doi.org/10.1016/S0140-6736\(21\)02143-7](https://doi.org/10.1016/S0140-6736(21)02143-7)
- Saricicek, A., Esterlis, I., Maloney, K. H., Mineur, Y. S., Ruf, B. M., Muralidharan, A., Chen, J. I., Cosgrove, K. P., Kerestes, R., Ghose, S., Tamminga, C. A., Pittman, B., Bois, F., Tamagnan, G., Seibyl, J., Picciotto, M. R., Staley, J. K., & Bhagwagar, Z. (2012). Persistent $\beta 2^*$ -nicotinic acetylcholinergic receptor dysfunction in major depressive disorder. *American Journal of Psychiatry*, 169(8), 851–859. <https://doi.org/10.1176/appi.ajp.2012.11101546>
- Semick, S. A., Collado-Torres, L., Markunas, C. A., Shin, J. H., Deep-Soboslay, A., Tao, R., Huestis, M., Bierut, L. J., Maher, B. S., Johnson, E. O., Hyde, T. M., Weinberger, D. R., Hancock, D. B., Kleinman, J. E., & Jaffe, A. E. (2020). Developmental effects of maternal smoking during pregnancy on the human frontal cortex transcriptome HHS Public Access. *Mol Psychiatry*, 25(12), 3267–3277. <https://doi.org/10.7303/syn12299750>
- Sequeira, A., Klempan, T., Canetti, L., Ffrench-Mullen, J., Benkelfat, C., Rouleau, G. A., & Turecki, G. (2007). Patterns of gene expression in the limbic system of suicides with and without major depression. *Molecular Psychiatry*, 12(7), 640–655. <https://doi.org/10.1038/sj.mp.4001969>
- Sequeira, A., Mamdani, F., Ernst, C., Vawter, M. P., Bunney, W. E., Lebel, V., Rehal, S., Klempan, T., Gratton, A., Benkelfat, C., Rouleau, G. A., Mechawar, N., & Turecki, G. (2009). Global brain gene expression analysis links Glutamatergic and GABAergic alterations to suicide and major depression. *PLoS ONE*, 4(8). <https://doi.org/10.1371/journal.pone.0006585>
- Setia, H., & Muotri, A. R. (2019). Brain organoids as a model system for human neurodevelopment and disease. In *Seminars in Cell and Developmental Biology* (Vol. 95, pp. 93–97). Elsevier Ltd. <https://doi.org/10.1016/j.semcdb.2019.03.002>

- Shacka, J. J., & Robinson, S. E. (1998). Exposure to prenatal nicotine transiently increases neuronal nicotinic receptor subunit alpha7, alpha44 and beta2 messenger rnas in the postnatal rat brain. *Neuroscience*, 84(4), 1151-1161. [https://doi.org/10.1016/s0306-4522\(97\)00564-2](https://doi.org/10.1016/s0306-4522(97)00564-2)
- Shaul, Y. D., & Seger, R. (2007). The MEK/ERK cascade: From signaling specificity to diverse functions. In *Biochimica et Biophysica Acta - Molecular Cell Research* (Vol. 1773, Issue 8, pp. 1213–1226). <https://doi.org/10.1016/j.bbamcr.2006.10.005>
- Sherafat, Y., Bautista, M., & Fowler, C. D. (2021). Multidimensional Intersection of Nicotine, Gene Expression, and Behavior. In *Frontiers in Behavioral Neuroscience* (Vol. 15). Frontiers Media S.A. <https://doi.org/10.3389/fnbeh.2021.649129>
- Sidhu, A. (1998). Coupling of D1 and Dopamine Receptors to Multiple G Proteins Implications for Understanding the Diversity in Receptor-G Protein Coupling D1 Family of Dopamine Receptors. In *Molecular Neurobiology* (Vol. 125). <https://doi.org/10.1007/BF02740640>.
- Slawecki, C. J., Gilder, A., Roth, J., & Ehlers, C. L. (2003). Increased anxiety-like behavior in adult rats exposed to nicotine as adolescents. *Pharmacology Biochemistry and Behavior*, 75(2), 355–361. [https://doi.org/10.1016/S0091-3057\(03\)00093-5](https://doi.org/10.1016/S0091-3057(03)00093-5)
- Smith, A. M., Dwoskin, L. P., & Pauly, J. R. (2010). Early exposure to nicotine during critical periods of brain development: Mechanisms and consequences. *Journal of Pediatric Biochemistry*, 1(2), 125–141. <https://doi.org/10.3233/JPB-2010-0012>
- Smith, L. N., McDonald, C. G., Bergstrom, H. C., Brielmaier, J. M., Eppolito, A. K., Wheeler, T. L., Falco, A. M., & Smith, R. F. (2006). Long-term changes in fear conditioning and anxiety-like behavior following nicotine exposure in adult versus adolescent rats. *Pharmacology Biochemistry and Behavior*, 85(1), 91–97. <https://doi.org/10.1016/j.pbb.2006.07.014>
- Stelzer, G., Plaschkes, I., Oz-Levi, D., Alkelai, A., Olender, T., Zimmerman, S., Twik, M., Belinky, F., Fishilevich, S., Nudel, R., Guan-Golan, Y., Warshawsky, D., Dahary, D., Kohn, A., Mazor, Y., Kaplan, S., Iny Stein, T., Baris, H. N., Rappaport, N., ... Lancet, D. (2016). VarElect: The phenotype-based variation prioritizer of the GeneCards Suite. *BMC Genomics*, 17. <https://doi.org/10.1186/s12864-016-2722-2>

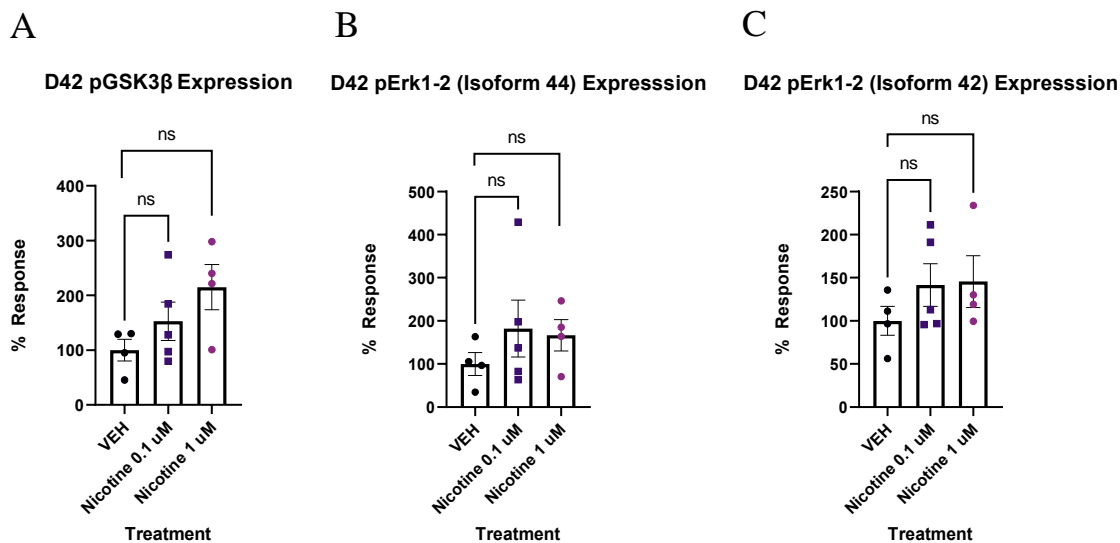
- Suhara, T., Nakayama, K., Lloue ~, Llirosi Fukuda, O., Shimizu, M., Mori, A., & Tateno, Y. (1992). Original investigations D1 dopamine receptor binding in mood disorders measured by positron emission tomography*. In *Psychopharmacology* (Vol. 106). <https://doi.org/10.1007/BF02253582>.
- Sun, N., Meng, X., Liu, Y., Song, D., Jiang, C., & Cai, J. (2021). Applications of brain organoids in neurodevelopment and neurological diseases. In *Journal of Biomedical Science* (Vol. 28, Issue 1). BioMed Central Ltd. <https://doi.org/10.1186/s12929-021-00728-4>
- Takarada, T., Nakamichi, N., Kitajima, S., Fukumori, R., Nakazato, R., Le, N. Q., Kim, Y. H., Fujikawa, K., Kou, M., & Yoneda, Y. (2012). Promoted Neuronal Differentiation after Activation of Alpha4/Beta2 Nicotinic Acetylcholine Receptors in Undifferentiated Neural Progenitors. *PLoS ONE*, 7(10). <https://doi.org/10.1371/journal.pone.0046177>
- Thapar, A., Tom Fowler, Mrcp., Rice, F., Scourfield, J., van den Bree, M., Thomas, H., Harold, G., & Hay, D. (2003). Maternal Smoking During Pregnancy and Attention Deficit Hyperactivity Disorder Symptoms in Offspring. In *Am J Psychiatry* (Vol. 160, Issue 11). <http://ajp.psychiatryonline.org>
- Tiesler, C. M. T., & Heinrich, J. (2014). Prenatal nicotine exposure and child behavioural problems. In *European Child and Adolescent Psychiatry* (Vol. 23, Issue 10, pp. 913–929). Dr. Dietrich Steinkopff Verlag GmbH and Co. KG. <https://doi.org/10.1007/s00787-014-0615-y>
- Todorovic, C., Sherrin, T., Pitts, M., Hippel, C., Rayner, M., & Spiess, J. (2009). Suppression of the MEK/ERK signaling pathway reverses depression-like behaviors of CRF 2 -Deficient mice. *Neuropsychopharmacology*, 34(6), 1416–1426. <https://doi.org/10.1038/npp.2008.178>
- Tong, V.T., Dietz, P.M., Morrow, B., D'Angelo, D.V., Farr, S.L., Rockhill, K.M., & England, L.J. (2013). Trends in Smoking Before, During and After Pregnancy-Pregnancy Risk Assessment Monitoring System, United States, 40 sites, 2000-2010. *Morbidity and Mortality Weekly Report Surveillance Summary*, 62(6).
- Trujillo, C. A., & Muotri, A. R. (2018). Brain Organoids and the Study of Neurodevelopment. In *Trends in Molecular Medicine* (Vol. 24, Issue 12, pp. 982–990). Elsevier Ltd. <https://doi.org/10.1016/j.molmed.2018.09.005>
- Vaglenova, J., Birru, S., Pandiella, N. M., & Breese, C. R. (2004). An assessment of the long-term developmental and behavioral teratogenicity of prenatal nicotine exposure. *Behavioural Brain Research*, 150(1–2), 159–170. <https://doi.org/10.1016/j.bbr.2003.07.005>

- Volkow, N. D. (2011). Epigenetics of nicotine: Another nail in the coughing. In *Science Translational Medicine* (Vol. 3, Issue 107). <https://doi.org/10.1126/scitranslmed.3003278>
- Wang, H. T., Han, F., Gao, J. L., & Shi, Y. X. (2010). Increased phosphorylation of extracellular signal-regulated kinase in the medial prefrontal cortex of the single-prolonged stress rats. *Cellular and Molecular Neurobiology*, 30(3), 437–444. <https://doi.org/10.1007/s10571-009-9468-1>
- Wang, Y., & Hummon, A. B. (2021). MS imaging of multicellular tumor spheroids and organoids as an emerging tool for personalized medicine and drug discovery. In *Journal of Biological Chemistry* (Vol. 297, Issue 4). American Society for Biochemistry and Molecular Biology Inc. <https://doi.org/10.1016/j.jbc.2021.101139>
- Wang, Y., Wang, L., Zhu, Y., & Qin, J. (2018). Human brain organoid-on-a-chip to model prenatal nicotine exposure. *Lab on a Chip*, 18(6), 851–860. <https://doi.org/10.1039/c7lc01084b>
- Whittington, J. R., Simmons, P. M., Phillips, A. M., Gammill, S. K., Cen, R., Magann, E. F., & Cardenas, V. M. (2018). The Use of Electronic Cigarettes in Pregnancy: A Review of the Literature. In *Obstetrical and gynecological survey* (Vol. 73, Issue 9). <https://doi.org/10.1097/OGX.0000000000000595>.
- Wickström, R. (2007). Effects of Nicotine During Pregnancy: Human and Experimental Evidence. In *Current Neuropharmacology* (Vol. 5). <https://doi.org/10.2174/157015907781695955>
- Wongtrakool, C., Wang, N., Hyde, D. M., Roman, J., & Spindel, E. R. (2012). Prenatal nicotine exposure alters lung function and airway geometry through $\alpha 7$ nicotinic receptors. *American Journal of Respiratory Cell and Molecular Biology*, 46(5), 695–702. <https://doi.org/10.1165/rcmb.2011-0028OC>
- Wortzel, I., & Seger, R. (2011). The ERK cascade: Distinct functions within various subcellular organelles. In *Genes and Cancer* (Vol. 2, Issue 3, pp. 195–209). SAGE Publications Inc. <https://doi.org/10.1177/1947601911407328>
- Yildiz-Yesiloglu, A., & Ankerst, D. P. (2006). Review of 1H magnetic resonance spectroscopy findings in major depressive disorder: A meta-analysis. In *Psychiatry Research - Neuroimaging* (Vol. 147, Issue 1, pp. 1–25). <https://doi.org/10.1016/j.psychresns.2005.12.004>
- Yilmaz, A., Schulz, D., Aksoy, A., & Canbeyli, R. (2002). Prolonged effect of an anesthetic dose of ketamine on behavioral despair. *Pharmacology Biochemistry and Behavior*, 71(1-2), 341-344. [https://doi.org/10.1016/s0091-3057\(01\)00693-1](https://doi.org/10.1016/s0091-3057(01)00693-1).

- Yoshino, Y., Roy, B., Kumar, N., Shahid Mukhtar, M., & Dwivedi, Y. (2021). Molecular pathology associated with altered synaptic transcriptome in the dorsolateral prefrontal cortex of depressed subjects. *Translational Psychiatry*, 11(1). <https://doi.org/10.1038/s41398-020-01159-9>
- Zarate, C. A., Singh, J. B., Carlson, P. J., Brutsche, N. E., Ameli, R., Luckenbaugh, D. A., Dennis, M. ;, Charney, S., & Manji, H. K. (2006). A Randomized Trial of an N-methyl-D-aspartate Antagonist in Treatment-Resistant Major Depression. *Archives of General Psychiatry*, 63(8), 856-864. <https://doi.org/10.1001/archpsyc.63.8.856>.
- Zarrindast, M.R., & Khakpai, F. (2015). The Modulatory Tole of Dopamine in Anxiety-like Behavior. *Archives of Iranian Medicine*, 18(9), 591-603.

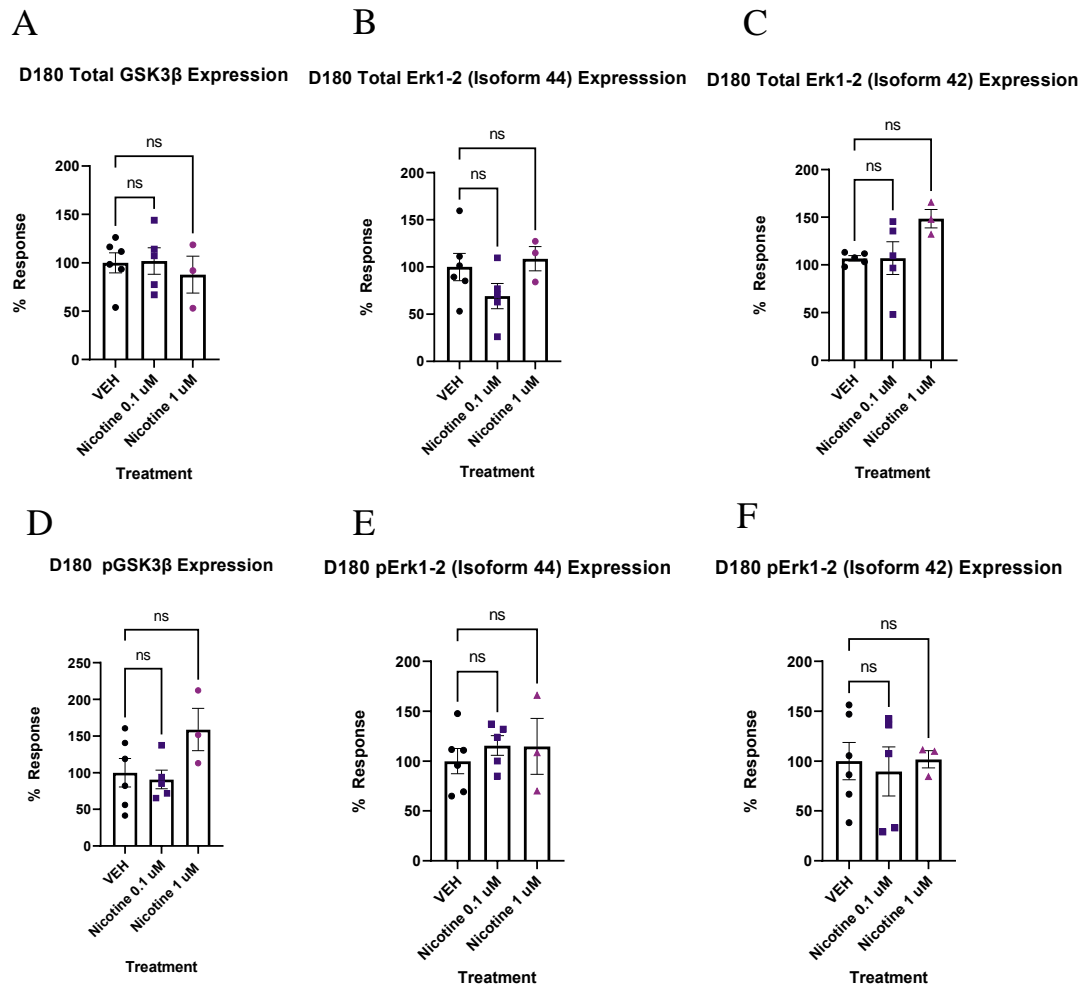
5 Appendices

5.1 Supplemental Non-Significant D42 Western Blot Results.



Appendix 1: PNE did not affect the phosphorylation of kinases implicated in mood/anxiety disorder pathology on D42. Proteins are normalized to housekeeping genes α -Tubulin or β -actin. **A-C** Percent response of whole brain organoids exposed to nicotine (0.1, or 1 μ M) or without (VEH) for 14 days. Organoids treated with nicotine demonstrated no change in pGSK3 β (A), pERK1-2 [isoform 44] (B) or pERK1-2 [isoform 42] (C). Comparisons were made with one-way ANOVA followed by Fisher's LSD *post hoc* test. Data are mean \pm SEM, n = 4-5, ns = not significant, $p > 0.05$. n = 1 organoid.

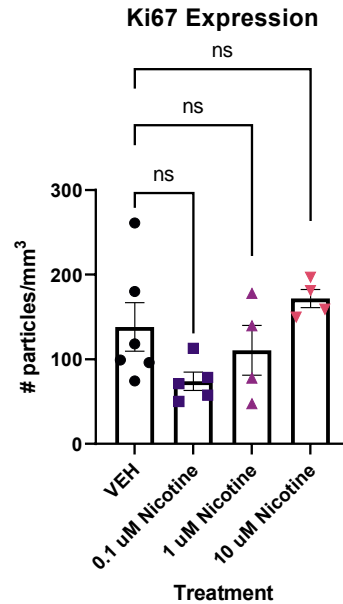
5.2 Supplemental Non-Significant D180 Western Blot Results



Appendix 2: PNE did not affect the phosphorylation of kinases implicated in mood/anxiety disorder pathology on D180. Proteins are normalized to housekeeping genes α -Tubulin or β -actin. **A-F** Percent response of whole brain organoids exposed to nicotine (0.1, or 1 μ M) or without (VEH) for 14 days. **A-C** Organoids treated with nicotine demonstrated no change in total GSK3 β (**A**), total ERK1-2 [isoform 44] (**B**) or total ERK1-2 [isoform 42] (**C**). **D-F** There was also no change in pGSK3 β (**D**), pERK1-2 [isoform 44] (**E**) or pERK1-2 [isoform 42] (**F**). Comparisons were made with one-way ANOVA followed by Fisher's LSD *post hoc* test. Data are mean \pm SEM, n = 4-5, ns = not significant, $p > 0.05$. n = 1 organoid.

5.3 Supplemental Non-Significant D42 IF Results

A



Appendix 3: PNE did not affect proliferation at D42. **A,** Immunofluorescent results of proliferation marker Ki67 in brain organoids treated with (0.1, 1 or 10 μ M) nicotine or without (VEH) for 14 days. Quantification of immunofluorescent images by the number of particles per area (mm^3). PNE did not influence Ki67 expression. Comparisons were made with one-way ANOVA or Kruskal Wallis followed by Fisher's LSD *post hoc* test. Data are mean \pm SEM, n = 4-6, ns = not significant, $p > 0.05$. n = 1 ROI.

Curriculum Vitae

Name: Emma Proud

Post-secondary Education and Degrees: University of Guelph
Guelph, Ontario, Canada
2016-2021 B.Sc.

The University of Western Ontario
London, Ontario, Canada
2021-2023 M.Sc.

Honours and Awards: University of Guelph Entrance Scholarship
2016

Dean's Honours List
2017-2020

Dean's Scholarship Undergraduate Award
2019

Canadian Graduate Scholarship Master's (CGSM)
2022-2023

Related Work Experience Teaching Assistant
The University of Western Ontario
2021-2023

Conferences:

Proud, E.K., Rodriguez-Ruiz, M. Gummerson, D., Laviolette SR. (2022). Examining the Emergence of Mood and Anxiety Molecular Phenotypes Resulting from Chronic Prenatal Nicotine Exposure in Cerebral Organoids. Joint Mental Health Research and Innovation Day, London, October 2022.

Proud, E.K., M. Rodriguez-Ruiz., Gummerson, D.M., Moreno, S.R.V., Lee, K., Hardy, D., Rushlow, W.J., and Laviolette, S.R. (2023). Examining the Emergence of Mood and Anxiety Molecular Phenotypes Resulting from Chronic Prenatal Nicotine Exposure in Cerebral Organoids. CINP World Congress of Neuropsychopharmacology, Montreal, May 2023.

Publications:

Sarikahya, M.H., Cousineau, S., De Felice, M., Lee, K., Wong, K.K.W., DeVuono, M.V., Jung, T., Rodriguez-Ruiz, M., Ng, J. H. J., Gummerson, D., **Proud, E.**, Hardy, D.B., Yeung, K.K.C., Rushlow, W., and Laviolette, S.R. (2022). Prenatal THC exposure Induces Sex-Dependent Neuropsychiatric Endophenotypes in Offspring and Long-Term Disruptions in Fatty-Acid Signaling Pathways Directly in the Mesolimbic Circuitry. *eNeuro*, 9. DOI: <https://doi.org/10.1523/ENEURO.0253-22.2022>

Sarikahya, M.H., Cousineau, S., De Felice, M., Szkudlarek, H., Wong, K., DeVuono, M.V., Lee, K., Rodriguez-Ruiz, M., Gummerson, D., **Proud, E.**, Ng, J.H.J., Hudson, R., Jung, T., Hardy, D., Yeung, K.K.C., Schmid, S., Rushlow, W., and Laviolette, S.R. Prenatal THC Exposure Induces Long-Term, Sex-Dependent Cognitive Dysfunction Associated with Lipidomic and Neuronal Pathology in the Prefrontal Cortex-Hippocampal Network. *In Review*